FOSSIL ENERGY

DOE/PC/91008-1
(DE96001298)

IMPROVED METHODS FOR WATER SHUTOFF

MASTER

Semi-Annual Report 1996

By
Randall S. Seright

August 1997

Performed Under Contract No. DE-AC22-94PC91008
Subcontract Number G4S60330

New Mexico Petroleum Recovery Research Center
New Mexico Institute of Mining and Technology
Socorro, New Mexico

National Petroleum Technology Office
U. S. DEPARTMENT OF ENERGY
Tulsa, Oklahoma

DOE/PC/91008-1
Distribution Category UC-122

Improved Methods For Water Shutoff

Semi-Annual Report

By
Randall S. Seright

August 1997

Work Performed Under Contract No. DE-AC22-94PC91008
Subcontract Number G4S60330

Prepared for
BDM-Oklahoma/
U.S. Department of Energy
Assistant Secretary for Fossil Energy

Jerry Casteel, Project Manager
National Petroleum Technology Office
P.O. Box 3628
Tulsa, OK 74101

Prepared by:
New Mexico Petroleum Recovery Research Center
New Mexico Institute of Mining Technology
Socorro, New Mexico 87801

ABSTRACT

In the United States, more than 20 billion barrels of water are produced each year during oilfield operations. Today, the cost of water disposal is typically between $0.25 and $0.50 per bbl for pipeline transport and $1.50 per bbl for trucked water. Therefore, there is a tremendous economic incentive to reduce water production if that can be accomplished without significantly sacrificing hydrocarbon production. For each 1% reduction in water production, the cost-savings to the oil industry could be between $50,000,000 and $100,000,000 per year. Reduced water production would result directly in improved oil recovery (IOR) efficiency in addition to reduced oil-production costs. A substantial positive environmental impact could also be realized if significant reductions are achieved in the amount of water produced during oilfield operations.

In an earlier project, we identified fractures (either naturally or artificially induced) as a major factor that causes excess water production and reduced oil recovery efficiency, especially during waterfloods and IOR projects. We also found fractures to be a channeling and water-production problem that has a high potential for successful treatment by gels and certain other chemical blocking agents. By analogy, these blocking materials also have a high potential for treating narrow channels behind pipe and small casing leaks. We also determined that the ability of blocking agents to reduce permeability to water much more than that to oil is critical to the success of these blocking treatments in production wells if zones are not isolated during placement of the blocking agent.

This research project has three objectives. The first objective is to identify chemical blocking agents that will (a) during placement, flow readily through fractures, small casing leaks, and narrow channels behind pipe without penetrating significantly into porous rock and without "screening out" or developing excessive pressure gradients and (b) at a predictable and controllable time, become immobile and resist breakdown upon exposure to moderate to high pressure gradients. The second objective is to identify schemes that optimize placement of the above blocking agents. The third objective is to explain why gels and other chemical blocking agents reduce permeability to one phase (e.g., water) more than that of another phase (e.g., oil or gas). We also want to identify conditions that maximize this phenomenon. This project consists of three tasks, each of which addresses one of the above objectives.

This report describes work performed during the first period of the project. In Chapter 2, we review gel placement concepts. In Chapter 3, we examine the properties of gels in fractures. In Chapter 4, the experimental results from Chapter 3 are used in a simple model to compare placement characteristics of preformed gels with those of gelants with water-like viscosities. In Chapter 5, we review some of our attempts to optimize gel placement in fractures. In Chapter 6, we investigate the mechanism responsible for polymers and gels reducing the permeability to water more than that to oil. This project will continue through September, 1998. The project is supported financially by BDM-Oklahoma, the U.S. Department of Energy, and a consortium of 15 oil companies. The first project review was held June 4 and 5 in Socorro, NM. The review was attended by 27 people representing 18 different organizations.

TABLE OF CONTENTS

TABLE OF FIGURES

LIST OF TABLES

ACKNOWLEDGMENTS

Financial support for this work is gratefully acknowledged from the United States Department of Energy, BDM-Oklahoma, ARCO, British Petroleum, Chevron, Conoco, Eniricerche, Exxon, Marathon, Norsk Hydro, Phillips Petroleum, Saga, Schlumberger-Dowell, Shell, Statoil, Texaco, and Unocal. I greatly appreciate the efforts of those individuals who contributed to this project. Dr. Jenn-Tai Liang played the major role in the work described in Chapters 6. Dr. Jill Buckley and Jostein Kolnes (of Stavanger College) participated in helpful discussions during this work. Richard Schrader performed the experimental work described in Chapters 3 and 5. John Hagstrom performed most of the experiments described in Chapter 6. I especially appreciate the thorough review of this manuscript by Julie Ruff and Mark Valenzuela.

EXECUTIVE SUMMARY

This report describes work performed during the first period of the project, "Improved Methods for Water Shutoff." This project has three general objectives. The first objective is to identify chemical blocking agents that will (a) during placement, flow readily through fractures, small casing leaks, and narrow channels behind pipe without penetrating significantly into porous rock and without "screening out" or developing excessive pressure gradients and (b) at a predictable and controllable time, become immobile and resist breakdown upon exposure to moderate to high pressure gradients. The second objective is to identify schemes that optimize placement of the above blocking agents. The third objective is to explain why gels and other chemical blocking agents reduce permeability to one phase (e.g., water) more than that of another phase (e.g., oil or gas). We also want to identify conditions that maximize this phenomenon.

Review of Gel Placement Concepts. The objective of gel treatments and similar blocking-agent treatments is to reduce channeling through fractures or high-permeability zones without significantly damaging hydrocarbon productivity. We wish to maximize gel penetration and permeability reduction in high-permeability, watered-out zones, while minimizing gel penetration and permeability reduction in less-permeable, hydrocarbon-productive zones. When practical, this objective can be met by mechanically isolating zones during the gel-placement process, so that gel injection occurs only in the high-permeability, watered-out zones. When zone isolation is not practical, we need to know when an effective gel placement can be achieved. Although we have published considerable work on this topic, many people have requested a manageable summary of our knowledge to date. Chapter 2 presents that summary.

Basic calculations using the Darcy equation reveal three important facts. First, gelants and similar fluid blocking agents can penetrate a significant distance into all open zones. Second, an acceptable gelant placement is much easier to achieve in linear flow than in radial flow. Third, if flow is radial, then hydrocarbon-productive zones must be protected during gelant placement. These facts mean that excess channeling and water production problems can be treated much more readily if they are caused by linear-flow phenomena, such as vertical fractures, fractured systems, or flow behind pipe. Even so, placement of blocking agents is very important in linear flow as well as in radial flow. When flow is radial (e.g., unfractured wells), field engineers would be well-advised not to apply blocking-agent treatments unless hydrocarbon productive zones are protected during placement of the blocking agent. A strong need exists for the development of new ideas to optimize placement of gels and other blocking agents, both in linear and radial systems.

Gel Properties in Fractures and Tubes. Chapter 3 examines the placement properties of preformed gels when used as blocking agents for conformance control in fractures. Results of new experiments are reported that characterize how gel extrusion through fractures and tubes is affected by fracture or tube conductivity, fracture or tube length, gel age, and gel velocity. Our work focused on a gel that contained 0.5% HPAM (Allied Colloids Alcoflood 935), 0.0417% Cr(III)-acetate, and 1% NaCl at 105°F.

We found that during gel extrusion through short (0.5 to 15 ft) fractures and tubes at high velocities, pressure gradients were insensitive to flow rate. Gels exhibited shear-thinning behavior in short fractures and tubes that correlated with the gel superficial velocity and the fracture width or tube diameter. In short fractures or tubes with sufficiently small opening sizes, gels dehydrated during extrusion, thus reducing the rate of gel propagation. This effect was more pronounced as the opening size decreased. The delay in gel propagation in short tubes was insensitive to velocity and gel age. Gel resistance factors in fractures increased rapidly with increased gel age during the first 24 hours but increased more gradually during the next 200 hours. Pressure gradients became more erratic with increasing gel age.

The behavior of Cr(III)-acetate-HPAM, resorcinol-formaldehyde, Cr(III)-xanthan, Cr-redox-HE-100, and hydroquinone-hexamethylenetetramine-HPAM gels in short tubes was qualitatively consistent with that in short fractures. For different types of gels, the delay in gel propagation in short tubes did not correlate with gel rigidity or pressure gradient. In 0.03-inch-ID, 100-ft-long tubes, resistance factors decreased substantially with increased length along the tube. This behavior was quite different from that in short fractures or tubes. Therefore, we are presently uncertain whether gel extrusion through long tubes can adequately imitate gel extrusion through long fractures.

Placement of Preformed Gels Versus Water-Like Gelants. In Chapter 4, the results from our experiments are used during a modeling study to compare the placement of preformed gels with those of gelants with a water-like viscosity. We found that the gel-dehydration effect can aid gel placement by minimizing the degree of gel penetration (i.e., the distance of gel penetration into a given fracture pathway divided by that for the most-conductive fracture pathway between an injector-producer pair). For preformed gels, the degree of penetration was insensitive to the fracture length ratio (i.e., the length of a less-conductive fracture divided by the length of the most-conductive fracture in the system). In contrast, for gelants with a water-like viscosity, the degree of penetration decreased dramatically with increased fracture length ratio. For fracture length ratios below 2, preformed gels may have a placement advantage over water-like gelants. In most field applications, fracture length ratios will be less than 3.

Schemes to Optimize Gel Placement in Fractures. In Chapter 5, we review some of our attempts to optimize gel placement in fractures. We investigated several schemes, including (1) injection of mechanically degraded Cr(III)-acetate-HPAM gels, (2) injection of mechanically degraded Cr(III)-acetate-HPAM gels, followed by injection of a $CrCl_3$ solution, (3) injection of a partially crosslinked hydroquinone-hexamethylenetetramine-HPAM gel, followed by a $CrCl_3$ solution, (4) injection of an HPAM water-in-oil emulsion, preceded or followed by a $CrCl_3$ solution, (5) injection of a gelant with a water-like viscosity, followed by a water postflush before gelation, and (6) injection of a preformed gel, followed by a pyrophosphate solution. Although none of these schemes proved to be successful, our efforts to date must be regarded as preliminary.

Disproportionate Permeability Reduction. The ability of blocking agents to reduce the permeability to water much more than to oil is critical to the success of water-shutoff treatments in production wells if zones cannot be isolated. Results from the literature and our own

experimental work have shown that many polymers and gels exhibit this disproportionate permeability reduction. In our previous studies, we extensively examined the possible mechanisms for this disproportionate permeability reduction. Although we still do not have a plausible explanation for this phenomenon, many interesting leads have been generated during the course of the study. Our previous studies ruled out gravity and lubrication effects as possible mechanisms. Also, gel shrinking and swelling are unlikely to be responsible for this phenomenon. Our experimental results indicate that wettability may play a role; however, its effects are unclear. In Chapter 6, we continue our study of the disproportionate permeability reduction.

Based on a micromodel study by Dawe and Zhang, we proposed that the competition between capillary forces and gel elasticity might contribute to disproportionate permeability reduction. Results from oil/water experiments showed that lowering the oil-water interfacial tension from 42.5 dyne/cm to 8 dyne/cm did not result in a lower permeability to oil. This finding does not support the theory that capillary forces and gel elasticity contribute to disproportionate permeability reduction. However, we suspect that the addition of an oil-soluble surfactant may have changed the surface properties of both the water and the oil phases. To eliminate this complication, we are searching for a third phase with significantly different surface properties than those of Soltrol 130.

In a small glass tube (3 cm × 0.5 cm × 0.05 cm), an aqueous gel reduced the permeability to water more than that to oil. During oil injection, we observed that oil droplets forced their way through an aqueous gel. The gel acted as an elastic material, creating just enough room for the oil droplets to squeeze through. During water injection, most of the water flowed through the pathways created by oil, except the pathways were more constricted due to the lack of capillary effects. These findings are consistent with the micromodel results of Dawe and Zhang. We plan to expand our visualization studies of the disproportionate permeability reduction using these small glass tubes.

A hydroquinone-hexamethylenetetramine-HPAM gel (with gelation reaction quenched after two days at 110°C) reduced the permeability to oil more than to water in Berea sandstone. However, the reverse disproportionate permeability reduction diminished when a more rigid HMT-HPAM gel (with gelation reaction quenched after eight days at 110°C) was used. We do not know why this occurred. More work will be needed to understand this unusual phenomenon.

Based on results from core experiments using an oil-based gel, we proposed that disproportionate permeability reduction might be caused by oil and water following segregated pathways on a microscopic scale. We speculate that if this theory is valid, a simultaneous injection of oil and an aqueous gelant during placement should enhance disproportionate permeability reduction. However, simultaneous injection of oil with an aqueous gel using gelant/oil volume ratios of 50/50 or 30/70 did not enhance the disproportionate permeability reduction. These findings do not support the segregated-oil-and-water-pathway theory. We suspect that the volume fraction of oil used during placement might be too high. Experiments are being conducted using higher gelant/oil volume ratios.

For Berea sandstone, the disproportionate permeability reduction was more pronounced in high-permeability (793-md) rock than in low-permeability (95-md) rock. However, the disproportionate permeability reduction was more pronounced in a 24-md limestone core than in a 95-md sandstone core. Also, for the limestone core, the residual resistance factors both for water and for oil were significantly lower than those in the sandstone cores. Perhaps, the limestone interfered with the gelation process to a greater extent than the sandstone. To eliminate the interference due to mineralogical differences, we are using artificial porous media (e.g., fused glass-bead cores) to study the effect of rock permeability on the disproportionate permeability reduction.

Results from a core experiment using an aqueous gel indicated that polymer was produced during multiple cycles of water/oil injection after treatment. However, the polymer concentrations in the brine effluent were too low to be responsible for the strong non-Newtonian behavior observed during brine injection after treatment. For a given fluid velocity, F_{rrw} decreased as the amount of polymer remaining in the porous medium decreased.

1. INTRODUCTION

In the United States, more than 20 billion barrels of water are produced each year during oilfield operations. Today, the cost of water disposal is typically between $0.25 and $0.50 per bbl for pipeline transport and $1.50 per bbl for trucked water. Therefore, there is a tremendous economic incentive to reduce water production if that can be accomplished without significantly sacrificing hydrocarbon production. For each 1% reduction in water production, the cost-savings to the oil industry could be between $50,000,000 and $100,000,000 per year. Reduced water production would result directly in improved oil recovery (IOR) efficiency in addition to reduced oil-production costs. A substantial positive environmental impact could also be realized if significant reductions are achieved in the amount of water produced during oilfield operations.

In an earlier project, we identified fractures (either naturally or artificially induced) as a major factor that causes excess water production and reduced oil recovery efficiency, especially during waterfloods and IOR projects. We also found fractures to be a channeling and water-production problem that has a high potential for successful treatment by gels and certain other chemical blocking agents. By analogy, these blocking materials also have a high potential for treating narrow channels behind pipe and small casing leaks. We also determined that the ability of blocking agents to reduce permeability to water much more than that to oil is critical to the success of these blocking treatments in production wells if zones are not isolated during placement of the blocking agent.

Objectives

This project has three general objectives. The first objective is to identify chemical blocking agents that will (a) during placement, flow readily through fractures, small casing leaks, and narrow channels behind pipe without penetrating significantly into porous rock and without "screening out" or developing excessive pressure gradients and (b) at a predictable and controllable time, become immobile and resist breakdown upon exposure to moderate to high pressure gradients. The second objective is to identify schemes that optimize placement of the above blocking agents. The third objective is to explain why gels and other chemical blocking agents reduce permeability to one phase (e.g., water) more than that of another phase (e.g., oil or gas). We also want to identify conditions that maximize this phenomenon.

Report Content

This report describes work performed during the first period of the project. In Chapter 2, we review gel placement concepts. In Chapter 3, we examine the properties of gels in fractures. In Chapter 4, the experimental results from Chapter 3 are used in a simple model to compare placement characteristics of preformed gels with those of gelants with water-like viscosities. In Chapter 5, we review some of our attempts to optimize gel placement in fractures. In Chapter 6, we investigate the mechanism responsible for polymers and gels reducing the permeability to water more than that to oil.

2. A REVIEW OF GEL PLACEMENT CONCEPTS

The objective of gel treatments and similar blocking-agent treatments is to reduce channeling through fractures or high-permeability zones without significantly damaging hydrocarbon productivity. We wish to maximize gel penetration and permeability reduction in high-permeability, watered-out zones, while minimizing gel penetration and permeability reduction in less-permeable, hydrocarbon-productive zones. When practical, this objective can be met by mechanically isolating zones during the gel-placement process, so that gel injection occurs only in the high-permeability, watered-out zones. When zone isolation is not practical, we need to know when an effective gel placement can be achieved. Although we have performed and published considerable work on this topic, many people have requested a manageable summary of our knowledge to date. This chapter presents that summary. Detailed documentation of each concept can be found in the references.

Linear Versus Radial Flow

Basic calculations using the Darcy equation reveal three important facts.[1] First, gelants and similar fluid blocking agents can penetrate a significant distance into all open zones. Second, an acceptable gelant placement is much easier to achieve in linear flow than in radial flow. Third, if flow is radial, then hydrocarbon-productive zones must be protected during gelant placement.

The above statements can be understood by comparing calculations for linear versus radial parallel corefloods (see Fig. 1). In each set of corefloods, assume that Core 1 is 10 times more permeable than Core 2 (i.e., $k_1/k_2=10$) and both cores have the same porosity. Initially, all cores are filled with water.

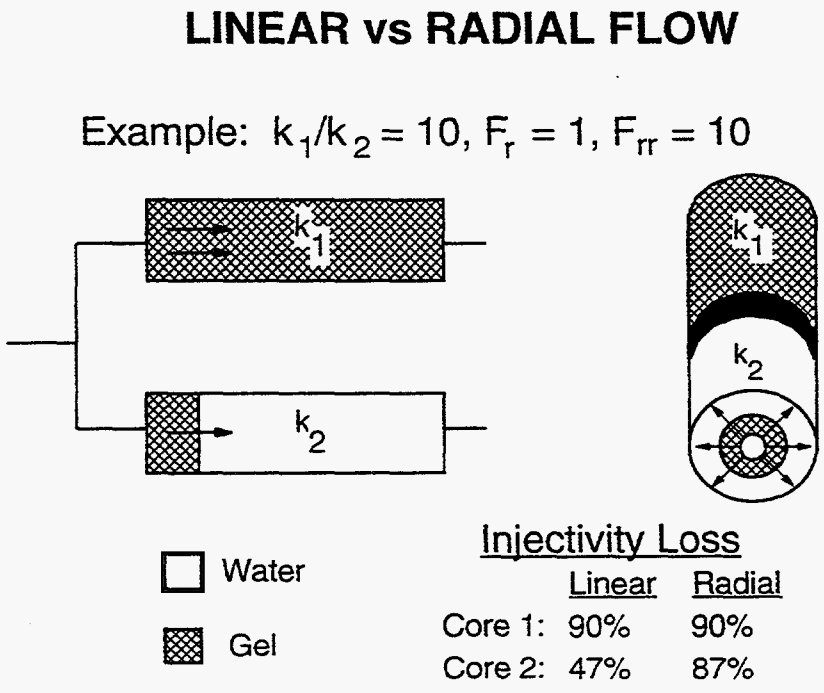

Fig. 1. Linear versus radial parallel corefloods.

A gelant—with a water-like viscosity, i.e., the resistance factor, F_r, is equal to 1—is injected simultaneously into Cores 1 and 2 until Core 1 is filled. For the parallel linear corefloods, the gelant fills the first 10% of the pore space in Core 2. For the radial floods, the volume of gelant entering Core 2 is also 10% of the volume that enters Core 1; however, because the radius of the gelant front varies with the square root of the volume injected, the final gelant radius in Core 2 is approximately 1/3 (i.e., $\approx \sqrt{1/10}$) that in Core 1.

After the gelant is placed, flow is stopped to promote gelation. Wherever the gel forms, the permeability to water is reduced by a factor of 10 (i.e., the residual resistance factor, F_{rr}, is equal to 10). Next, water injection is resumed, and the final water injectivity is determined for each core. In both the linear and radial corefloods, Core 1 is completely filled with gel, so it experiences a 90% injectivity loss. For the linear case, a 47% injectivity loss is calculated for Core 2 (using the Darcy equation for flow in series).[1] Since a much larger injectivity loss occurs in the high-permeability core, the gel treatment significantly improves the injection profile. However, the damage to Core 2 is significant.

In the radial system, calculations (again, using the Darcy equation for flow in series)[1] reveal that Core 2 experiences an 87% injectivity loss. Therefore, in radial flow, the gel treatment causes approximately a 90% injectivity loss in both cores without significantly improving the injection profile. These simple calculations illustrate two of the three important facts that are revealed by the Darcy equation: an acceptable gelant placement is much easier to achieve in linear flow (e.g., vertically fractured wells) than in radial flow (e.g., wells without fractures), and if flow is radial, then hydrocarbon-productive zones must be protected during gelant placement.

In Unfractured Wells (Radial Flow), Is Protection of Oil Zones Needed During Gelant Placement in Heterogeneous Reservoirs? (Yes.)

A common misconception is that protection of hydrocarbon productive zones is not needed during gelant placement if the reservoir is heterogeneous. For radial-flow systems, this concept can be easily disproved. Consider an unfractured water injection well in a reservoir (40-acre, 5-spot pattern, with unit mobility ratio) with seven non-communicating layers. The wellbore radius, r_w, is 0.33 ft, and all layers have the same thickness. The permeabilities and porosities of the layers are listed in Table 1. The porosities (ϕ, in percent) are related to permeabilities (k, in md) by Eq. 1.

$$\phi = 4\log_{10}(k) + 10 \qquad (1)$$

For this reservoir, the Dykstra-Parsons coefficient of permeability variation is approximately 0.9. This value indicates an extremely high degree of reservoir heterogeneity.[2,3]

A gelant is injected that has the same viscosity and mobility as water. For a given radius of penetration into the most-permeable layer, a gelant of this type penetrates the minimum distance into less-permeable zones.[1,4] Assume that the gelant is injected to reach a radius, r_{p1}, of 50 ft in the most-permeable zone (Layer 1, or the 640-md layer). Zones are not isolated, so the gelant also penetrates into the other layers. Table 1 lists the radii of gelant penetration in the different layers (r_{pi}). These values can be calculated easily using Eq. 2.

Table 1. For Radial Flow, Reservoir Heterogeneity Does Not Ensure an Effective Gel Placement

				Fraction of original injectivity retained		
Layer	k, md	ϕ, %	Radius of gelant penetration, ft	F_{rr}=2	F_{rr}=10	F_{rr}=100
1	640	21.2	50.0	0.75	0.25	0.029
2	320	20.0	36.4	0.76	0.26	0.031
3	160	18.8	26.5	0.77	0.28	0.033
4	80	17.6	19.4	0.79	0.29	0.036
5	40	16.4	14.2	0.80	0.31	0.039
6	20	15.2	10.4	0.81	0.33	0.042
7	10	14.0	7.7	0.83	0.35	0.046

$$\frac{r_{p1}^2 - r_w^2}{r_{pi}^2 - r_w^2} = \frac{k_1 \phi_i}{k_i \phi_1} \qquad (2)$$

where the subscript, i, refers to a given less-permeable layer of interest. Note that the radius of gelant penetration into the 10-md layer is 7.7 ft. Thus, the gelant penetrates a significant distance into all layers, including the least-permeable layer.

After gelant injection, the well is shut in during gelation. After gelation, water injection is resumed. Wherever the gel forms, the permeability to water is reduced by the residual resistance factor, F_{rr}. This causes some injectivity loss in all layers that contain gel. We are interested in the relative injectivity that is retained in each of the layers after the gel treatment, (i.e., final water injectivity divided by initial water injectivity). Table 1 lists these values for gel F_{rr} values of 2, 10, and 100 (corresponding to weak, moderate, and strong gels, respectively). In all three cases, the gel treatment causes almost as much injectivity loss in the high-permeability zones as in the low-permeability zones. In other words, the gel treatment does not significantly improve the flow profile. In these examples, the residual resistance factor was assumed to be independent of permeability. For polymers and weak gels, residual resistance factors usually increase with decreasing permeability,[5-9] potentially leading to gel treatments that damage low-permeability zones more than high-permeability zones.

In summary, extreme reservoir heterogeneity does not eliminate the need to protect hydrocarbon-productive zones during gelant placement in unfractured injection wells (where flow is radial). A more detailed discussion of this point can be found in Ref. 2.

Are Field Results Consistent with Calculations Using the Darcy Equation? (Yes.)

As shown above, basic calculations indicate that flow profiles are not expected to be improved by gel treatments in unfractured wells (i.e., radial flow) if zones are not protected during gelant placement. During the past ten years, we have actively sought field examples that contradict this prediction.[10-12] We have found no definitive contradictions. Those that claim contradictions fall into four categories.[10-13] In the first category, wells with fractures were incorrectly assumed not to have fractures. Often, the actual injectivities or productivities for the wells (i.e., the left side of Eq. 3, $q/\Delta p$, in BPD/psi) were five or more times greater than the injectivities or productivities calculated using the Darcy equation for radial flow (i.e., the right side of Eq. 3).

$$\frac{q}{\Delta p} >> \frac{\Sigma kh}{141.2\mu \ln(r_e/r_w)} \qquad (3)$$

The high injectivity or productivity values suggest that the wells experienced a problem with fractures or formation parting. Since vertical fractures allow extensive crossflow in the formation, flow profiles taken at the wellbore were usually meaningless.

In the second category, the wells experienced a serious problem with flow behind pipe. This type of problem can usually be diagnosed using temperature surveys (especially for liquids) or noise surveys (especially for gases).[14] As was the case when vertical fractures were present, flow profiles taken at the wellbore were usually meaningless.

In the third category, too much faith was placed in the resolution of the tools and methods used to measure flow profiles.[11] In the wells selected for these field tests, at least two distinct zones should be present that are separated by an impermeable barrier. These zones should be separated by a sufficient distance (10 feet or more) to ensure that injection profiles can clearly distinguish flow into the different zones. Also, depending on the circumstances of their use,[14] one should recognize that the profiling tools (e.g., spinners or radio-tracer profiling tools) have limits on their accuracy (e.g., ±10-20%).

In the fourth category, unsupported conclusions were drawn about the effects of gel treatments based exclusively on overly optimistic interpretations of oil production decline curves.[11-13]

Certainly, it would be valuable to find well-documented field cases that contradict the predictions from the Darcy equation. These cases could reveal important new principles that could be exploited to optimize gel placement. However, in the absence of these cases, field engineers would be well-advised not to apply gel treatments in wells with radial flow unless hydrocarbon productive zones are protected during gelant placement. For those who remain skeptical of the Darcy predictions, you are challenged to find a convincing counter example.

Do Hall Plots Indicate Selectivity During Gelant Placement? (No.)

Hall plots are often used as a diagnostic method during gelant injection in field applications. In a Hall plot, the term, $\Sigma p_{tf}\Delta t$, is plotted versus the cumulative injection volume, where p_{tf} is the flowing wellhead pressure and Δt is the time increment.[15] Under steady-state or pseudo-steady-state conditions, the Hall plot should give a straight line with a slope,

$$m_H = \frac{141.2\mu\left[\ln(r_e / r_w) + s\right]}{kh} \qquad (4)$$

where m_H has units of psi-D/B, μ is viscosity in cp, r_e is external drainage radius in ft, s is skin factor, k is permeability in md, and h is formation thickness in ft. This slope, m_H, gives the reciprocal of injectivity. Thus, Hall plots indicated changes in injectivity for wells. Furthermore, these injectivities reflect values that are averaged over all open zones. The Hall plot reveals nothing about whether a gelant or other injected fluid is penetrating selectively into one zone more than another.[10] This point is made in Figs. 2 and 3 for unfractured and fractured wells, respectively. A more detailed discussion of this point can be found in Ref. 10.

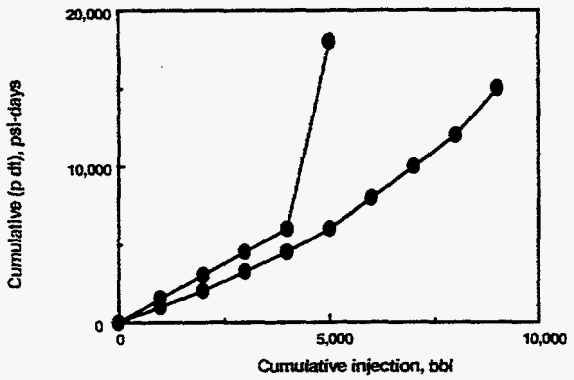

An increasing slope could result from:

- plugging the high-k zones more than the low-k zones,
- plugging the low-k zones more than the high-k zones,
- plugging all zones to the same extent (most likely scenario).

Fig. 2. Hall plots for wells with radial flow.

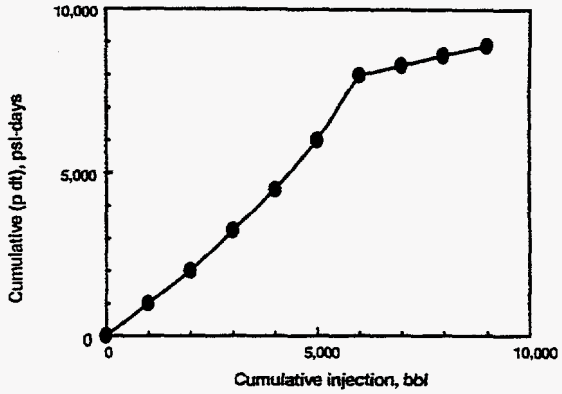

A decreasing slope could result from:

- opening or fracturing into previously unswept zones,
- re-opening a fracture that the gel had recently sealed,
- opening a fracture that cuts through all zones.

Fig. 3. Hall plots for fractured wells.

In summary, Hall plots may be a useful indicator of the overall pressure or rate of pressure increase in a well. However, they do not indicate whether the blocking agent is being placed in a beneficial or harmful manner.

Is Gel Placement Important in Wells or Reservoirs with Fractures? (Yes.)

Calculations using the Darcy equation reveal that an acceptable gel placement is much easier to achieve in linear flow (e.g., wells with fractures) than in radial flow (e.g., wells without fractures). However, this fact does not mean that gel placement is unimportant in fractured wells. Fig. 4 shows idealized placement locations for gels in fractures. First, consider a production well where water channels through a fracture. In the ideal gel placement, the fracture is plugged far from the wellbore, but the fracture remains open near the well (upper left part of Fig. 4). Then, water channeling can be reduced while maintaining a high productivity for the well. If the gel plugs the near-wellbore portion of the fracture (lower left part of Fig. 4), water channeling may be reduced, but the productivity of the well could be lowered to an unacceptable value.

In vertical fractures that cut through multiple zones, we might want to exploit gravity and density differences to place gel in the lower part of a fracture, thereby reducing water influx from the lower zones while leaving the upper part of the fracture open to oil flow (center part of Fig. 4). In contrast, gel placement in the upper part of the fracture could be detrimental.

The amount of gelant that leaks off from a fracture face is also important (right side of Fig. 4). Ideally, the distance of gelant leakoff from the fracture face should be very small. If the leakoff distance is too great, the near-wellbore region could be plugged, and the gel treatment could do more harm than good. A basic principle of fluid displacement in porous media is that the efficiency of the displacement increases with increasing viscosity of the injected fluid.[1,3] This principle suggests that other factors being equal in a fractured system, the distance of gelant leakoff will be greater for a high-viscosity gelant than for a low-viscosity gelant. For gel treatments, this principle presents a potential problem for viscous gelants—that too much gelant

may leak off from the fracture into the formation rock. Leakoff associated with the use of viscous gelants could compromise the effectiveness of a treatment unless it is controlled.

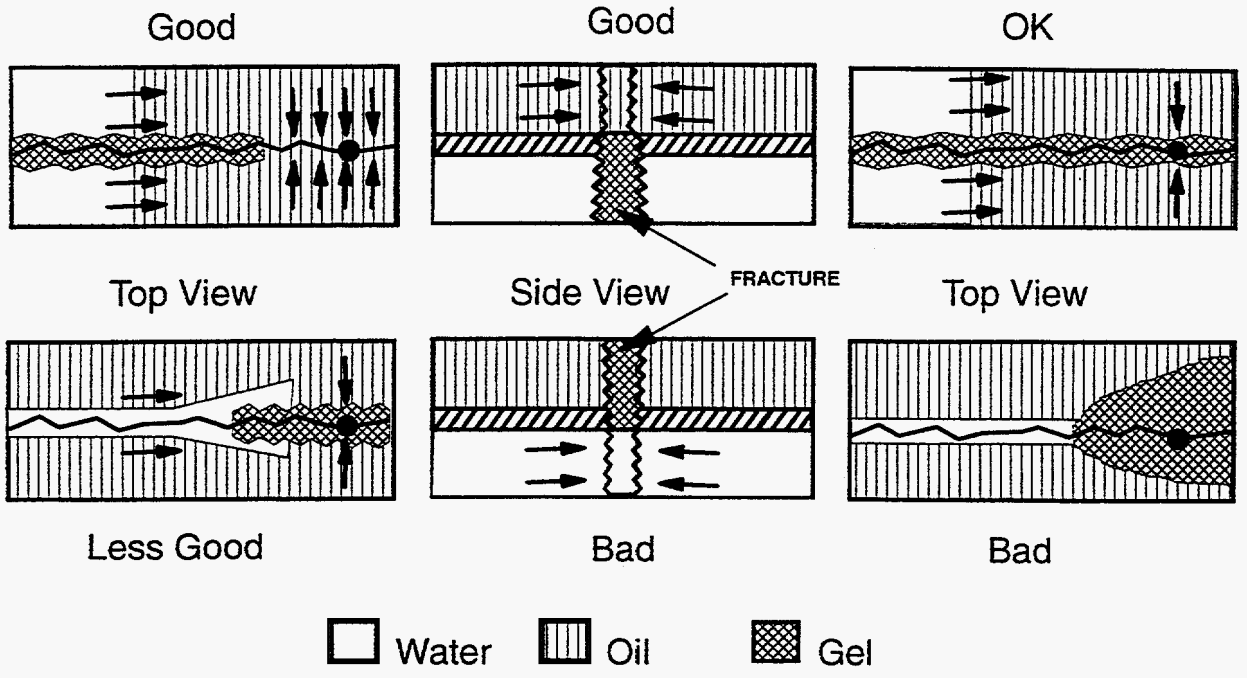

Fig. 4. Idealized locations for gels in fractures.

Thus, gel placement is extremely important in fractured wells and reservoirs. This topic is one of our major research areas. It will be discussed in more detail in Chapters 3, 4, and 5. Our previous work in this area is described in Refs. 16 and 17.

Can Relative-Permeability Effects Be Exploited to Prevent Gelants from Entering Oil Zones? (No.)

A common misconception was that water-based gelants enter zones with high water saturations much more readily than zones with high oil saturations. If correct, very few waterfloods would work because water must enter and displace hydrocarbons from the oil zones. In part, this misconception occurs because people recognize that the relative permeability to water is very low at high oil saturations. However, this view fails to consider that a "shock front" forms between an oil bank and the water bank, which was injected to displace the oil. At this shock front, the water saturation increases sharply from low to high values.[18] Of course, the relative permeability to water is greatest at high water saturations.

We examined the relative distances of penetration of water-based gelants into oil versus water zones as a function of permeability contrast (1 to 1,000), water or oil saturation (0.2 to 0.8), oil/water viscosity ratio (0.1 to 100), endpoint water relative permeabilities ranging from 0.1 to 0.7, and in fractured and unfractured wells.[18] These conditions cover most known field and laboratory applications. Straightforward applications of fractional-flow theory and material balance calculations demonstrated that gelants can penetrate significantly into all open zones in

production wells—not just those with high water saturations (Fig. 5). Ref. 18 demonstrates that except for reservoirs with high oil/water viscosity ratios (i.e., 100 or greater), the relative distances of gelant penetration into different zones will be quite similar to those determined from simple calculations using the Darcy equation.

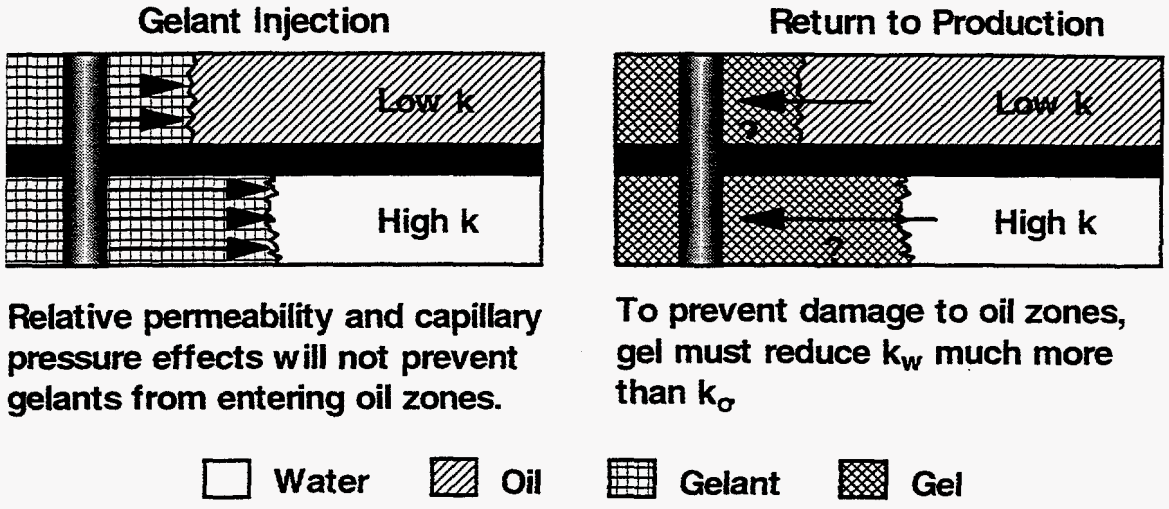

Fig. 5. Placement of gelants in production wells.

Can Capillary-Pressure Effects Be Exploited to Prevent Water-Based Gelants from Entering Oil Zones? (In field applications—no. In oil-wet laboratory cores—sometimes.)

Another common misconception is that capillary pressure effects will prevent water-based gelants from entering oil zones. This concept is disproved in Ref. 2. In water-wet reservoirs, capillary pressure will actually enhance imbibition of the aqueous gelant into the oil zones. In oil-wet laboratory cores, capillary pressure can inhibit gelants from entering the porous rock if the injection pressures are low.[2] However, in virtually all field applications, the pressure drop between the wellbore and the formation will be much greater than the capillary pressure. Therefore, in field applications, capillary pressure will not prevent gelants from penetrating significant distances into oil zones.[2]

Since Some Polymers and Gels Can Reduce k_w Much More than k_o or k_g, Where Will This Property Be Most Useful? (Wells and reservoirs where vertical fractures cut through both water and hydrocarbon zones.)

A special property that was reported for some polymers and gels is an ability to reduce permeability to water much more than that to oil or gas.[19-27] In Ref. 18, we demonstrated that this property is of value only when zones with high hydrocarbon saturation are distinct from the offending water-producing zones. In other words, this "disproportionate permeability reduction" will not mitigate water production from a reservoir that has effectively only one zone. Even if the polymer or gel can significantly reduce permeability to water without affecting the permeability to oil, the average fractional flow of water and oil from that zone must remain the same. If the polymer or gel near a production well allows oil to pass but not water, the water saturation will increase near the gel bank, thus, decreasing the relative permeability to oil until

the fractional water and oil flows match the values that existed before the polymer or gel treatment.[18] Therefore, unless a particular zone is at its irreducible water saturation, a polymer or gel treatment will always cause some loss of oil productivity (i.e., B/D-psi), even if the polymer or gel reduces k_w without affecting k_o. This loss of oil productivity necessarily will be in direct proportion to the loss of water productivity caused in that particular zone.[18]

The ability of polymers and gels to reduce k_w much more than k_o is most useful when zones of high-oil saturation are being produced along with zones of high-water saturation. If a particular zone produces only oil and the polymer or gel does not affect k_o, no reduction in oil productivity will occur. In contrast, for zones that produce only water, water productivity will be reduced in direct proportion to the reduction in k_w.

For the credible experimental data reported to date, polymers and gels may reduce k_w more than k_o, however, they always reduce k_o to some extent. In the best cases, Zaitoun and Kohler[24] reported that adsorbed polymers significantly reduced k_w at any given water saturation, while the oil relative-permeability curve was basically unaffected by the polymer. However, the polymer increased the irreducible water saturation, thus lowering the endpoint relative permeability to oil. Therefore, for all practical purposes in zones with high oil saturations, the polymer treatment reduces the effective permeability to oil.

In radial flow, how much reduction in k_o can be tolerated? This question is addressed in Fig. 6.

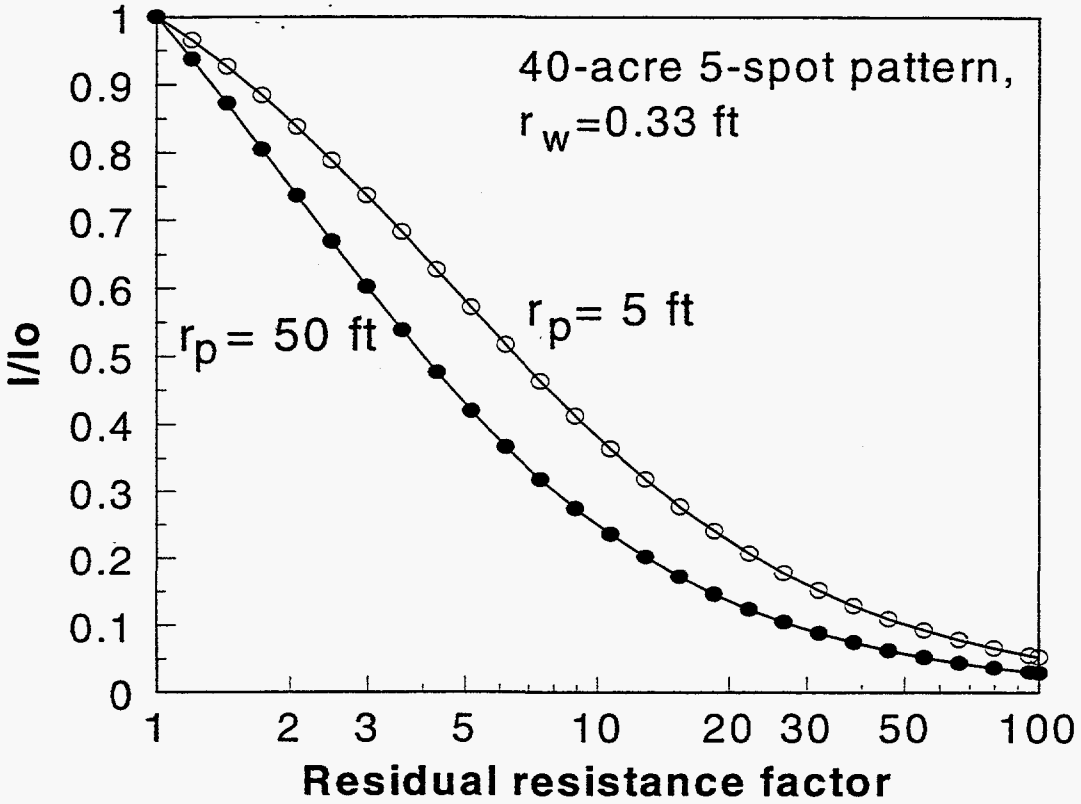

Fig. 6. Fraction of original injectivity or productivity retained (I/Io) versus residual resistance factor. Radial flow (unfractured well).

Fig. 6 plots the fraction of original injectivity or productivity retained (I/I_o) after a polymer or gel treatment as a function of the residual resistance factor (i.e., the permeability reduction provided by the polymer or gel). Fig. 6 applies to a waterflooded reservoir with a 40-acre, 5-spot pattern with a unit-mobility displacement. The wellbore radius was 0.33 ft. Two cases of radii of gelant penetration, r_p, are presented—5 ft and 50 ft. A comparison of these two curves reveals that for a given residual resistance factor, the injectivity or productivity losses are not strongly dependent on the radius of gelant penetration.

For radial flow, Fig. 6 reveals that relatively small residual resistance factors can cause significant injectivity or productivity losses. For example, for a gel radius of 50 ft, a F_{rr} value of 2 causes a 27% loss in I/I_o, while a F_{rr} value of 10 causes a 75% loss. Both of these losses might be considered unacceptable if these are oil zones. Thus, in unfractured wells, hydrocarbon residual resistance factors (F_{rro}) must be small. (Depending on the rock and the gelant system, these low F_{rro} values may be difficult to obtain in a predictable and controllable manner.[28])

The disproportionate permeability reduction may be of greater value in treating production wells where vertical fractures cut through both water and hydrocarbon zones[25] (see Fig. 7). When a gelant is injected into a fractured production well, hopefully, it will propagate a large distance down the length of the fracture while leaking off a very short distance into the porous rock. Assume that the gelant leaks off 0.2 ft into both the oil and water zones. Also, assume that the gel reduces k_o by a factor of 50 while reducing k_w by a factor of 50,000. (We are aware of a gel with these properties.[25]) Upon first consideration, a F_{rro} value of 50 might appear to be prohibitively high. However, because of the short distance of leakoff in this example (0.2 ft), the gel only adds the equivalent of 10 feet of additional rock that the oil must flow through to enter the fracture (i.e., 0.2 ft x 50). In contrast, for the water zone, the water must flow through the equivalent of 10,000 ft of additional rock to enter the fracture (i.e., 0.2 ft x 50,000). Thus, the gel can substantially reduce water production without significantly affecting oil productivity.

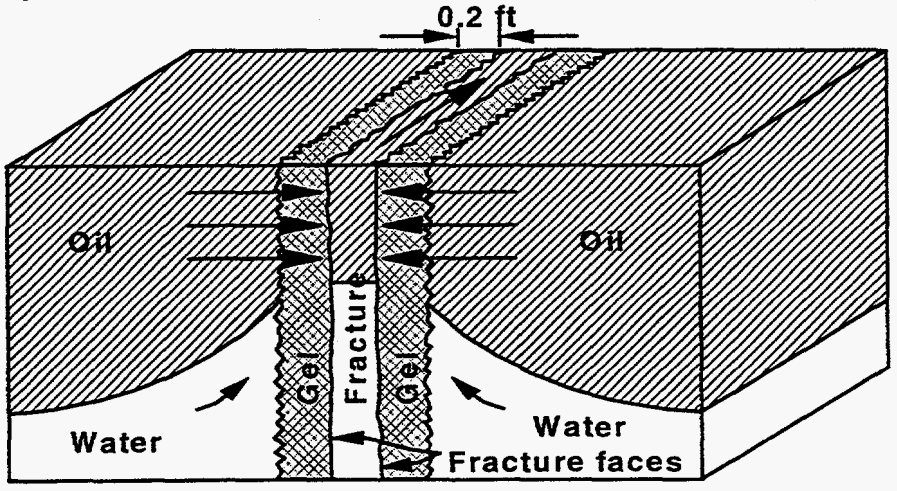

Equivalent resistance to flow added by the gel
In oil zone: 0.2 ft x 50 = 10 ft.
In water zone: 0.2 ft x 50,000 = 10,000 ft.

Fig. 7. Gel restricting water entry into a fracture.

Can Gel Treatments Effectively Mitigate Three-Dimensional Coning? (No, except in rare circumstances.)

When gel treatments are applied to treat coning problems, a common misconception is that the gelant will only enter the water zones at the bottom of the well. In reality, this situation will occur only if the oil is extremely viscous and/or the aqueous gelant is injected at an extremely low rate (to exploit gravity during gelant placement).[17,18,25] In the majority of field applications to date, the crude oils were not particularly viscous, and gelant injection rates were relatively high.[10,12] For the reasons explained in the previous section, in three-dimensional (3-D) coning applications, one must be concerned about damage that polymer or gel treatments cause to hydrocarbon-productive zones.

Even if a polymer or gel reduces k_w without affecting k_o, gel treatments have limited utility in treating 3-D coning problems. Extensive numerical studies using a variety of coning models indicate that gel treatments can only provide improvement if the desired production rate is less than 1.5 to 5 times the pretreatment critical rate.[25] This circumstance rarely occurs.

Can Gel Treatments Effectively Mitigate "Two-Dimensional Coning" in Fractured Wells? (Yes, with the proper gel placement and gel properties.)

In contrast to the very limited potential of polymers and gels in treating 3-D coning, these treatments have much greater potential for "two-dimensional coning" where vertical fractures cause water from an underlying aquifer to be sucked up into a well.[18,25] Whereas gel treatments will only raise the critical rate by factors from 1.5 to 5 in unfractured wells, they can raise the critical rate by more than a factor of 100 in fractured wells (see Fig. 8).

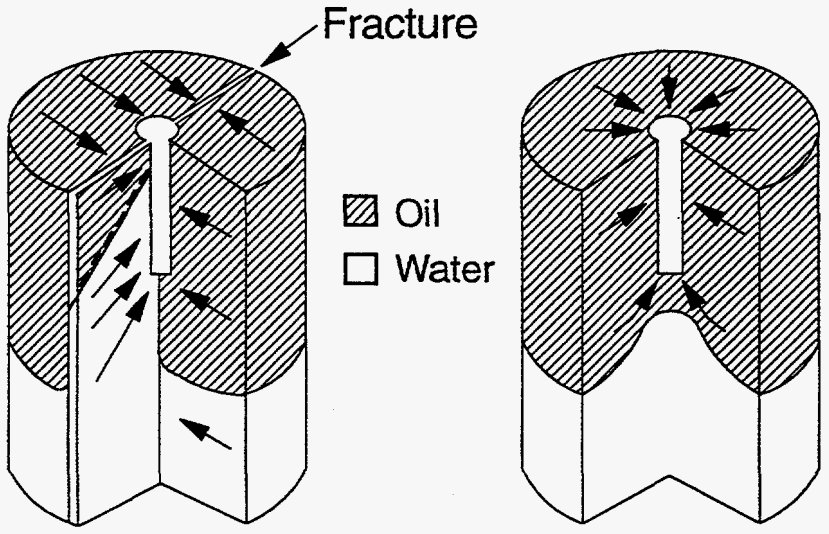

Blocking agents could increase the critical rate:

- by a factor of 1.5 to 5 in unfractured wells,
- by a factor of 100 in fractured wells.

Fig. 8. Reduced coning in fractured versus unfractured wells.

In Radial-Flow Systems, Can the Rheology of Existing Non-Newtonian Polymer Solutions Provide a Better Placement Than That for Gelants with Water-Like Viscosities? (No.)

A basic principle of fluid displacement is that the efficiency of the displacement increases with decreasing mobility (or increasing viscosity) of the displacing phase.[1,3] This is also a basic principle of polymer flooding. For a given distance of viscous-fluid penetration into a high-permeability zone, the distance of penetration into less-permeable zones becomes greater with increased viscosity or resistance factor (F_r) of the injected fluid.[1] This concept is illustrated in Fig. 9 for a gelant displacing water in a radial system with non-communicating zones. The y-axis in Fig. 9 plots the radial distance of gelant penetration in a low-permeability zone (Layer 2) when the gelant reaches 50 ft in the most-permeable zone (Layer 1). This quantity is plotted versus the permeability contrast, k_1/k_2. Fig. 9 shows that at any given permeability contrast, the degree of gelant penetration (i.e., the distance of penetration in a low-permeability zone relative to that in the most-permeability zone) is greater for a gelant with F_r=100 than for a gelant with F_r=1.

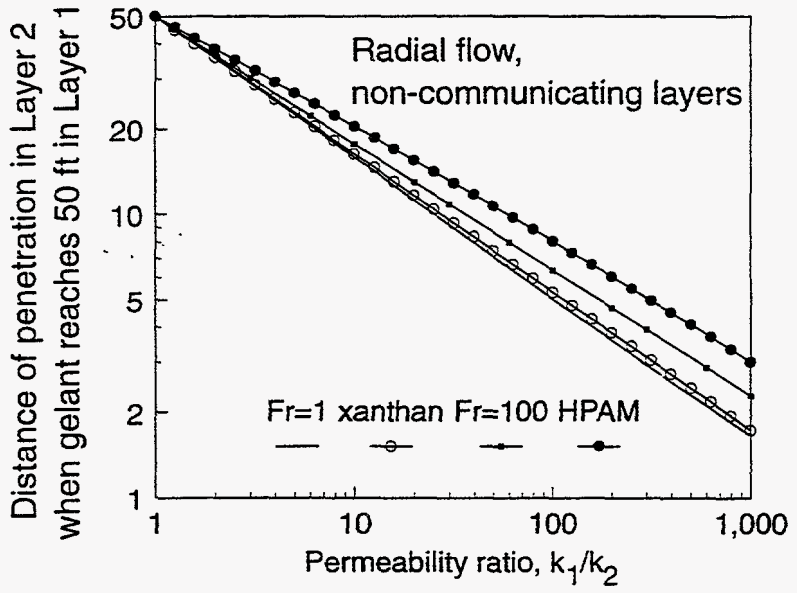

Fig. 9. Effect of rheology on gelant placement in radial flow.

Fig. 9 also shows that for any given permeability contrast, a gelant with F_r=1 provides a lower degree of penetration than non-Newtonian polyacrylamide or xanthan solutions. (Fig. 10 illustrates the non-Newtonian rheology of polyacrylamide and xanthan solutions.) In Refs. 4 and 29, we examined whether the non-Newtonian rheology of existing polymeric gelants can be exploited to optimize gel placement. In Ref. 4, we considered eight different rheological models that have been used to describe the behavior of polyacrylamide and polysaccharide solutions in porous media. We considered shear-thinning models, shear-thickening models, and models that showed combined shear-thinning and shear-thickening behavior. All of the models were examined during simulation of placement behavior in parallel linear corefloods, parallel radial corefloods, fractured wells, and wells without fractures. The analysis revealed that in radial flow,

for all models tested, the rheology of existing polymeric gelants will not allow a placement that is superior to that for a gelant with a water-like viscosity or resistance factor (i.e., F_r=1).

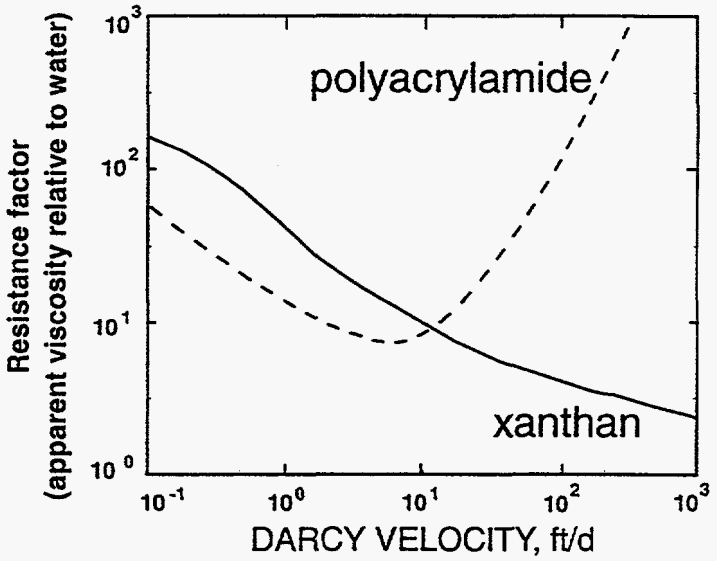

Fig. 10. Rheology of xanthan and polyacrylamide solutions in porous media.

During water injection after gel placement, an apparent non-Newtonian behavior can be observed.[8,9,29] An analysis of this behavior that has been reported to date does not suggest that it will eliminate the need to protect hydrocarbon-productive zones during gelant placement.[11,29]

Are Gel Treatments Fundamentally Different from Polymer Floods? (Yes.)

The distinction between a blocking agent (e.g., a gel) and a mobility-control agent (e.g., a polymer solution) is an important concept to understand (see Fig. 11). A mobility-control agent should penetrate as much as possible into the less-permeable zones so that oil can be displaced from poorly swept zones. In contrast, we wish to minimize penetration of blocking agents into the less-permeable, oil-productive zones. Any blocking agent that enters the less-permeable zones can hinder subsequent injected fluids (e.g., water, CO_2, steam) from entering and displacing oil from those zones.[13]

Important distinctions also exist between polymer solutions that are used in mobility-control applications and gelants and gels that are used in blocking applications. Published laboratory results consistently show three characteristics of gelants and gels in porous rock.[8,9,17,29-31] First, early in the gelation process, gelants flow freely through porous media, like uncrosslinked polymer solutions. Second, after gel aggregates grow to approach the size of pore throats, they become trapped and no longer flow at any significant rate. Third, the transition between these two conditions occurs over a relatively short time period. These facts further emphasize that gel treatments are not polymer floods. Gels, crosslinked polymers, gel aggregates, and the so-called "colloidal dispersion gels" (1) are not simply viscous polymer solutions, (2) do not propagate through porous rock like polymer solutions, and (3) do not enter and plug the most-permeable zones first and plug progressively less-permeable zones later.[13] Thus, one cannot simply add a small amount of crosslinker to a polymer solution and expect it to act like a super polymer flood.

One should be concerned if a vendor uses traditional polymer-flooding arguments or simulations to argue the benefits of a gel treatment.

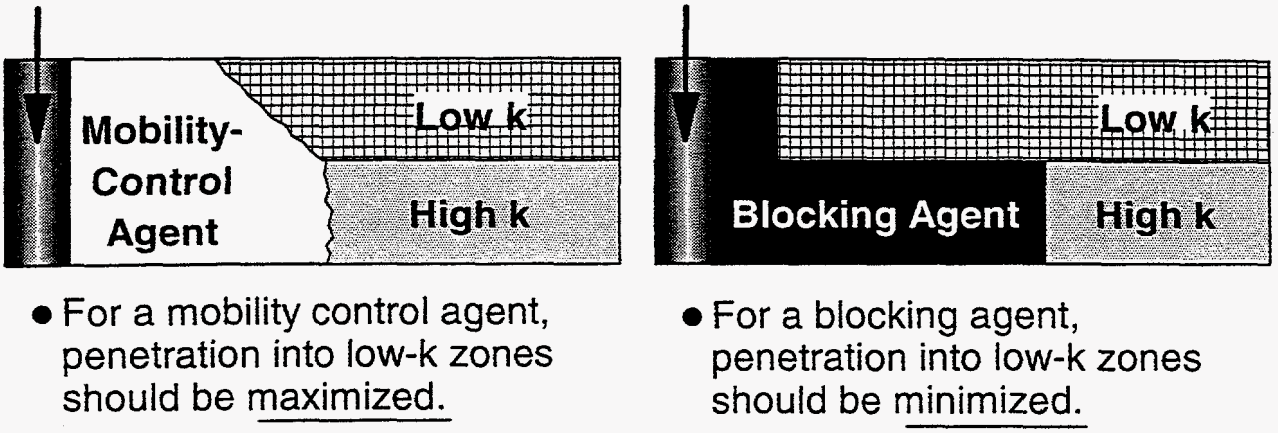

Fig. 11. Distinction between a mobility-control agent and a blocking agent.

Since Chemical Propagation and Retention Rates Vary with Permeability, Can These Differences Be Exploited to Eliminate the Need to Protect Hydrocarbon-Productive Zones During Gelant Placement? (No, based on evidence to date. However, this may be possible in the future, depending on research progress.)

For many years, people have recognized that polymer and gel resistance factors, residual resistance factors, and chemical retention values in porous media increase with decreasing permeability.[5-9] Fig. 12 provides example data that were reported by Vela *et al.*[5] for polyacrylamide solutions.

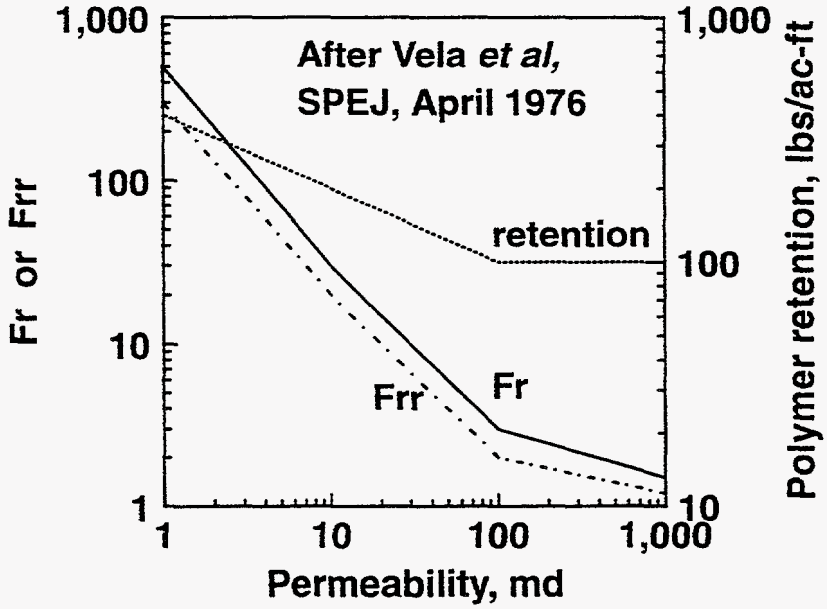

Fig. 12. Resistance factors (Fr), residual resistance factors (Frr), and retention values for polyacrylamide solutions in sandstone.[5]

Since resistance factors and retention values increase with decreasing permeability, can this behavior be exploited to minimize polymer or gelant penetration into low-permeability zones? Also, once the polymer or gelant has been placed, will the treatment ultimately improve the flow profile? Using data such as those in Fig. 12, calculations can be performed to answer these questions. Table 2 summarizes the results from calculations made using Fig. 12 and the methods described in Ref. 1. These calculations reveal that the permeability dependence of the resistance factor and retention values does, indeed, reduce the degree of penetration, $(r_{p2}-r_w)/(r_{p1}-r_w)$. With these factors taken into account, the degree of penetration was 0.082. For comparison, if F_r=4 and the retention was the same in both layers, the degree of penetration would have been 0.311. The last column in Table 2 reveals that in spite of the apparently favorable placement properties, the treatment caused a much greater injectivity loss in the low-permeability layer than in the high-permeability layer. This result occurred because the residual resistance factor was much greater in the low-permeability rock than in the high-permeability rock.

Table 2. Results of Placement Calculations Using the Data of Vela *et al.*[5]

Layer	k, md	F_r	F_{rr}	retention, lbs/ac-ft	$\frac{r_{p2}-r_w}{r_{p1}-r_w}$	injectivity retained
1	137	4	2.4	75	---	68%
2	12	51	45	772	0.082	32%

Other researchers[32-35] have suggested promising new concepts that may help to limit the distance of polymer penetration or permeability reduction in less-permeable zones. Certainly, these ideas should be pursued and encouraged. However, we must remember that the effectiveness of a given blocking agent depends on its permeability-reduction properties, as well as its placement properties. Whenever a promising new concept is suggested, simple screening calculations (like those illustrated in Table 2) should be performed to confirm that the idea can actually improve flow profiles. Additional work in this area can be found in Refs. 1, 4, 8, 9, 11, and 29.

Can Diffusion Be Exploited to Dilute the Gelant Bank in Low-Permeability Zones Enough to Prevent Gelation, While Allowing an Effective Gel Plug to Form in High-Permeability Zones? (Only if the gelant banks are extremely small-- < 1 ft.)

In concept, diffusion and dispersion could dilute gelants enough to prevent gelation in less-permeable, oil-productive zones while still allowing a gel plug to form in watered-out, high-permeability streaks. Whether or not a chemical bank can be diluted enough by diffusion to prevent gelation depends on at least four factors: 1) the size of the chemical bank, 2) the diffusion coefficient, 3) the gelation time, and 4) the extent of dilution required to prevent gelation.

Diffusion coefficients (D) are typically on the order of 10^{-5} cm^2/s for low-molecular-weight chemicals in water.[34] These chemicals include gelants such as acrylamide monomer, phenol, and formaldehyde. Diffusion coefficients are typically on the order of 10^{-8} cm^2/s for high-molecular-weight polymeric gelants such as polyacrylamide or xanthan.[37] For low-molecular-weight species in a viscous polymer solution (e.g., $Cr_2O_7^{-2}$ in water with 0.2% polyacrylamide), the

diffusion coefficient should have some intermediate value—varying inversely with the viscosity of the solution.[38]

Gelation times range from a few minutes to several days for most formulations that have been considered for near-wellbore gel treatments. In general, the gelation time decreases with increasing concentrations of the gelling agents.[39,40] Also, some minimum concentration of the proper reactants must be present in order for gelation to occur. In most field applications of gel treatments, the concentrations of reactants that are injected are well above the minimum levels required for gelation. Thus, significant dilution (often by a factor of two or more) is required in order to prevent gelation.

To be conservative, we assume that the gelation reaction is stopped by only a ten percent dilution of the reactants. Thus, the reader should bear in mind that the reductions in gel-bank size that are forecast due to dilution by diffusion will be overly optimistic. By overestimating the impact of diffusion in our analysis, we increase confidence in our major conclusion from this study. That is, in field applications in unfractured wells, diffusion will not usually cause enough dilution to prevent gelation in the less-permeable zones.

In field applications of gel treatments, wells are commonly shut-in for some time after injection of the gelant to allow the gel to form. During the time prior to gelation, diffusion acts to dilute the chemical banks. The size of the mixing zone, L_m, created by diffusion alone (no dispersion) during this time can be approximated using Eq. 5,

$$L_m \approx 3.62\sqrt{Dt_g} \qquad (5)$$

where t_g is gelation time. The mixing zone given by Eq. 5 extends from the point where the gelant has been diluted to 90 percent of the original concentration to the point where the gelant has been diluted to 10 percent of the original concentration.[36] Fig. 13 illustrates a typical concentration profile that results when diffusion or dispersion smears an interface that was originally sharp. Fig. 13 also illustrates the size of the mixing zone that is given by Eq. 5.

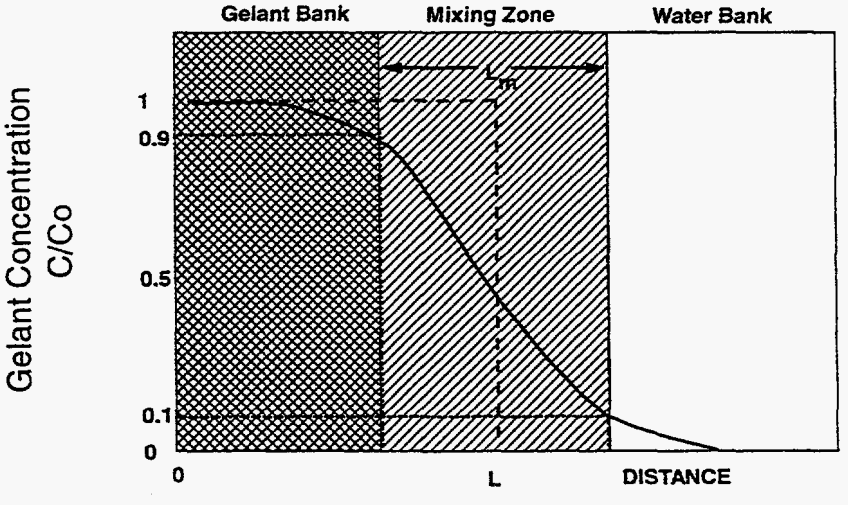

Fig. 13. Concentration profile at the interface between the gelant and water banks.

If the gelation reaction is stopped by a ten percent dilution of the reactants, then diffusion will reduce the gel bank size by the distance $L_m/2$. Fig. 14 provides values of $L_m/2$ as a function of time and diffusion coefficient. A key point illustrated by Fig. 14 is that diffusion will not create a large mixing zone in the period associated with typical gelation times. Even for relatively large diffusion coefficients (10^{-5} cm^2/s), $L_m/2$ is only about 0.2 ft (5 cm) after ten days. Considering the depths of penetration for gelants in typical field applications (see Fig. 9), diffusion is not likely to have a significant impact in unfractured wells. However, in fractured wells where the gelant leaks off a very short distance from the fracture faces, diffusion could have an important impact.

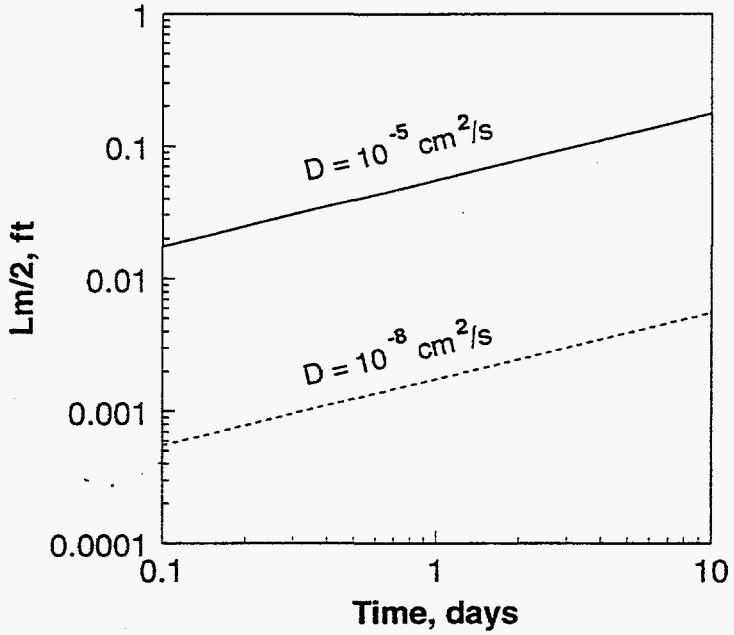

Fig. 14. Length of mixing zone caused by diffusion.

Diffusion can significantly affect results from parallel laboratory corefloods. Consider injection of a 1-cp gelant to displace water from two one-foot-long cores that are being flooded in parallel. Assume that one core is ten times more permeable than the other and both cores have the same porosity. When the gelant reaches the outlet of the most-permeable core, the gelant will have penetrated 0.1 ft into the less-permeable core. Over the course of one day, most of the gelant in the less-permeable core could be diluted if the diffusion coefficient is 10^{-5} cm^2/s. Therefore, diffusion during gel placement in parallel laboratory corefloods can mislead one to conclude that zone isolation is not needed during gel placement in field projects.

Can Dispersion Be Exploited to Dilute the Gelant Bank in Low-Permeability Zones Enough to Prevent Gelation, While Allowing an Effective Gel Plug to Form in High-Permeability Zones? (No.)

During injection of a gelant to miscibly displace water, both diffusion and dispersion will occur. While diffusion is the transport of mass because of spatial concentration differences, dispersion is mixing caused by variations in the velocity within each flow channel and from one channel to another.[41] In flow through reservoirs, dispersion usually is much more important than

diffusion.[41] The size of the mixing zone (again, between the 90%-10% concentration levels) created by dispersion can be estimated using Eq. 6,

$$L_m \approx 3.62\sqrt{\alpha L} \qquad (6)$$

where α is the dispersivity of the porous medium and L is the distance traveled by the fluid front. Laboratory values for α commonly are in the range from 0.001 to 0.05 ft.[38,41,42] However, field dispersivity values are usually significantly greater than laboratory values because of the greater heterogeneity experienced on the larger scale.[41]

Ref. 42 presents a detailed examination of the impact of dispersion and diffusion on gelant placement. From that analysis, we concluded that dispersion will dilute gelant banks in high-permeability zones by approximately the same factor as in low-permeability zones. Therefore, dispersion is unlikely to aid gelant placement.

In Systems Without the Potential for Crossflow, Can a More Selective Gel Placement Be Achieved by Injecting a Water-Like Gelant Followed by a Water Postflush? (No.)

Additional mixing and thinning of gelant banks can be induced by injecting water to displace gelants away from the wellbore prior to gelation. In this section, the discussion will focus on displacement of a water-like gelant (F_r=1) by injection of water. The next section will discuss the case where water displaces a viscous gelant.

If water is injected to displace a water-like gelant, the mobility ratio for the displacement is unity. In radial flow, injection of a water postflush will thin the gelant bank, even in the absence of diffusion and dispersion (see Fig. 15). However, this thinning is not large, and it occurs to about the same proportion in all zones. This point is illustrated in Fig. 16. The situation represented in Fig. 16 is as follows. First, a water-like gelant is injected into a radial, multilayer reservoir until the gelant propagates to a radius of 50 ft in the most-permeable layer (Layer 1). (The wellbore radius is 0.5 ft, and all layers have the same porosity.) At this time the length of the gelant bank (bank radius minus the wellbore radius) will be 49.5 ft, 15.3 ft, 4.5 ft, and 1.2 ft in layers that have permeabilities that are 1, 10, 100, and 1000 times less than that in the most-permeable layer, respectively. After injection of the gelant, water is injected to displace the gelant away from the wellbore. Fig. 16 plots the length of the gelant bank in a given zone (Layer 2, where the permeability ratio, k_1/k_2, is specified in the figure) as a function of radius of the water postflush in the most-permeable zone. Fig. 16 reveals that a water postflush out to 50 ft in the most-permeable zone reduces the length of the gelant bank in all zones by roughly a factor of two.

Ref. 42 presents a detailed examination of the impact of bank thinning, dispersion, and diffusion on gelant placement when a water postflush displaces a water-like gelant away from the wellbore before gelation. From that analysis, we concluded that a water postflush prior to gelation can significantly increase injectivity in a radial geometry. Unfortunately, injectivity increases by approximately the same proportion in all zones. Also, diffusion and dispersion can reduce the size of a gel bank during a water postflush. However, the bank size is reduced by about the same proportion in all zones. Thus, a water postflush usually does not help to eliminate the need to protect hydrocarbon-productive zones during gel placement.

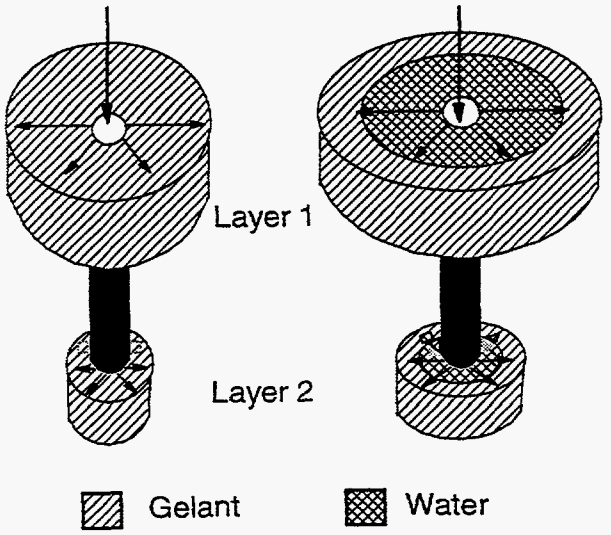

Fig. 15. Illustration of a water postflush.

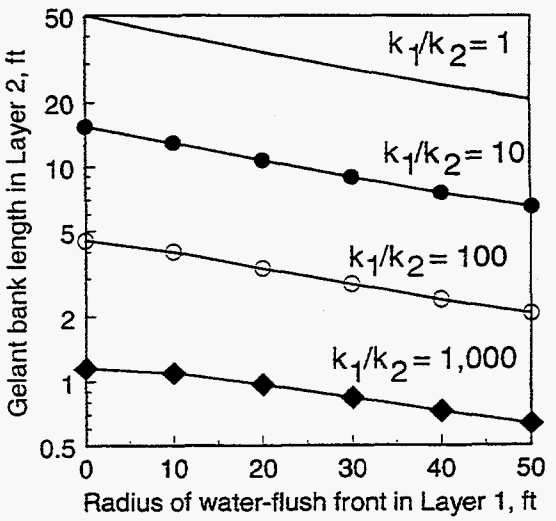

Fig. 16. Thinning of the gelant bank.

When Using Viscous Gelants, Can Viscous Fingering by a Water *Postflush Reliably Break Through the Gelant Bank in Low-Permeability Zones Before That in High-Permeability Zones? (No.)*

When a viscous gelant is used, a water postflush prior to gelation will tend to form viscous fingers through a gelant (see Fig. 17). When compared to the most-permeable zone, the size of the gelant bank is smaller in the less-permeable zones, so viscous fingers have a shorter distance to travel to achieve breakthrough. However, the viscous fingers will propagate much more rapidly in the most-permeable zone.

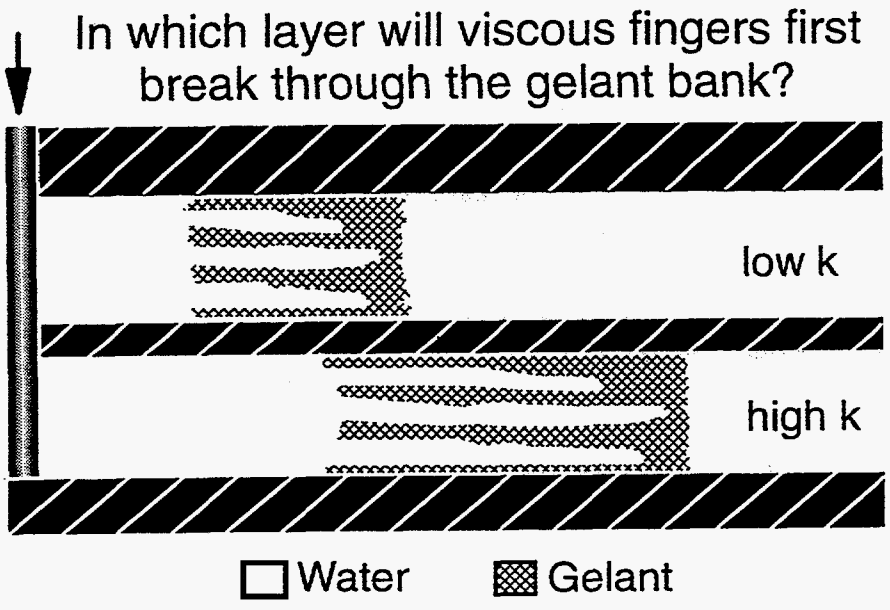

Fig. 17. Use of a water postflush to displace a viscous gelant.

Ref. 42 describes a detailed theoretical and experimental investigation to answer the above question. That study found that in reservoirs with non-communicating layers, the viscous fingers break through the gelant banks in the high-permeability zones, on average, at about the same time as in the less-permeable zones. Therefore, viscous fingering generally will not eliminate the need to protect hydrocarbon-productive zones during gel placement.

Can Worm-Holing by a Degrading Postflush Reliably Break Through the Gel Bank in Low-Permeability Zones Before That in High-Permeability Zones? (No.)

If a gel-degrading fluid (e.g., acid, bleach, enzymes, oxidizers) is injected after the gel forms, worm holes will form through the gel for most practical injection rates.[43] Since worm-holing phenomena scale the same as viscous fingering, the analogous arguments made above apply to worm-holing, as well as viscous fingering.[43] In particular, in reservoirs with non-communicating layers, a degrading postflush will not reliably break through a gel bank in low-permeability zones before that in high-permeability zones.

In Systems with the Potential for Crossflow, Can a More Selective Gel Placement Be Achieved by Injecting a Gelant Followed by a Mobility-Matched Postflush? (Yes, under limited circumstances.)

In unfractured wells, when viscous gelants are injected to displace water or relatively light oils, placement characteristics are always less desirable if crossflow can occur than if crossflow cannot occur.[2,44] This point is illustrated in Fig. 18, which shows the results from five visualization experiments where various xanthan solutions were injected to displace water from a two-layer bead pack. One layer was 11.2 times more permeable than the other layer, and no restrictions to vertical flow existed between the layers.

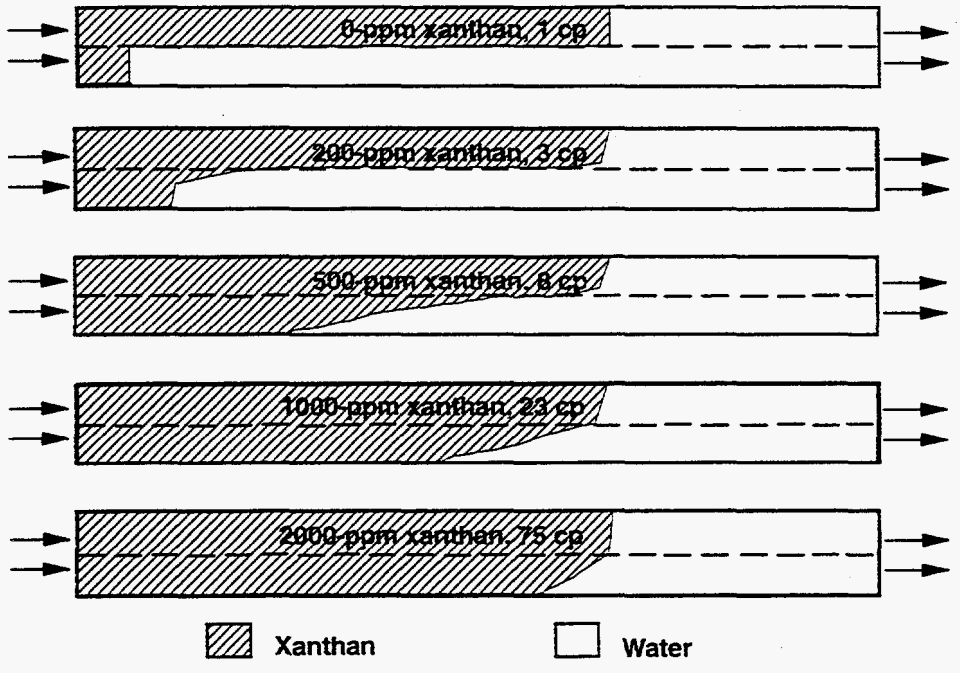

Fig. 18. Crossflow in a two-layer bead pack; xanthan solutions displacing water; k_1/k_2=11.2

Fig. 18 demonstrates that the degree of crossflow into the less-permeable layer increased with increased viscosity of the displacing fluid (xanthan solution). When the polymer/water viscosity ratio was greater than the permeability ratio (i.e., as for the 1,000-ppm and 2,000-ppm xanthan solutions), the average velocity for the polymer fronts was approximately equal in both layers. These finding were consistent with theoretical predictions.[45,46] This behavior is excellent for a traditional polymer flood, but not for a gel treatment. As mentioned earlier, for blocking-agent applications, the distance of gelant penetration into the less-permeable zones should be minimized.

Fig. 19 illustrates the behavior seen when water was injected after placement of a 2,000-ppm xanthan solution in the two-layer bead pack. Viscous fingering occurred rapidly and almost exclusively in the high-permeability zones. More detail on this topic can be found in Refs. 2 and 44.

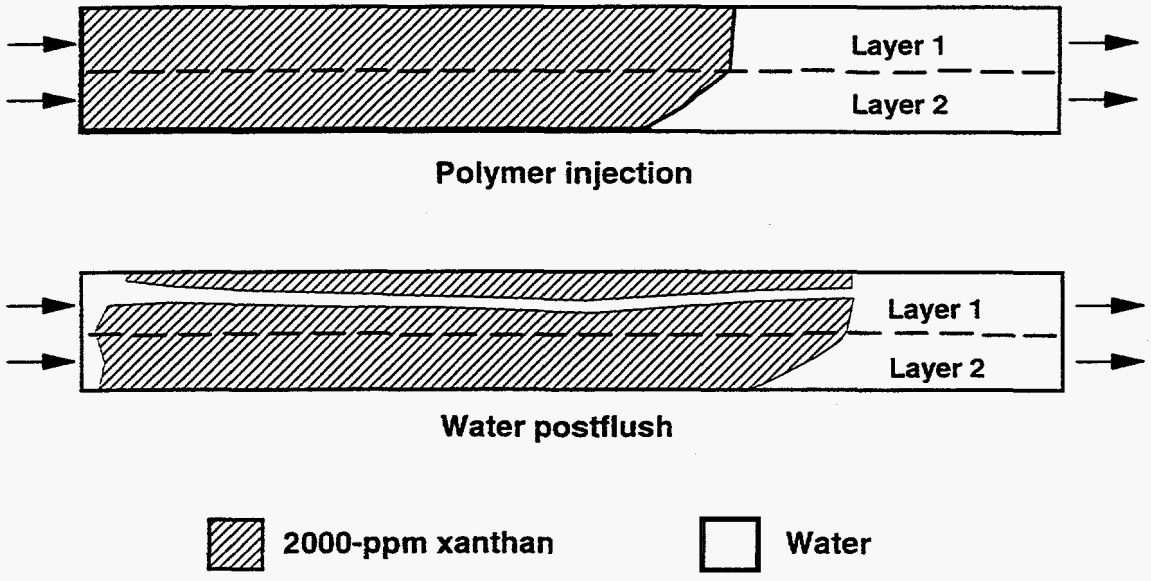

Fig. 19. Fingering through a viscous polymer bank in a two-layer bead pack; k_1/k_2=11.2.

In concept, a desirable gel placement could be achieved in reservoirs where crossflow can occur.[2,44,47,48] The basic idea for this placement scheme is illustrated in Fig. 20. During waterflood operations, assume that injected water has reached a production well by following a high-permeability pathway. Presumably, considerable mobile oil remains in less-permeable strata. For the first step of the gel treatment, a gelant with a water-like viscosity is injected (Fig. 20a). Because of the low viscosity of the gelant, penetration into the less-permeable zones is minimized.[1,44] Second, water is injected to displace the water-like gelant away from the wellbore (Fig. 20b). Enough water must be injected so that the rear of the gelant bank in the most-permeable zone outruns the front of the gelant bank in an adjacent less-permeable zone. In the third step of the process (Fig. 20c), the well is shut in to allow gelation to occur. Finally, if the gel treatment is applied in a waterflood injection well, water injection is resumed. Hopefully, a pathway will be available for water to crossflow from the high-permeability zone into the less-permeable zone(s) so that sweep efficiency can be improved (Fig. 20d).

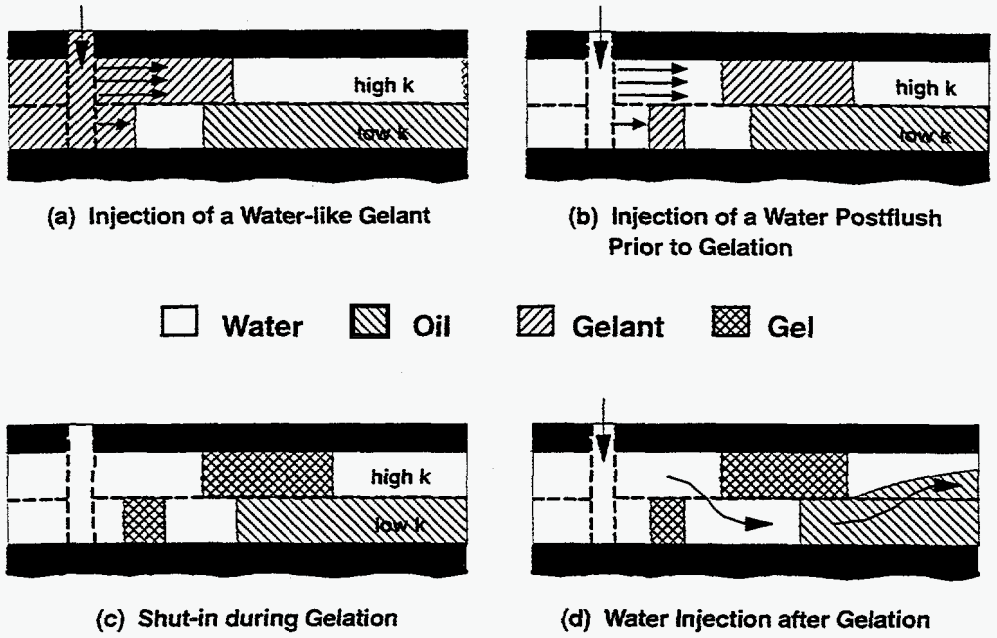

Fig. 20. Placement of a water-like gelant in a reservoir with crossflow.

If this scheme is feasible, then it could provide favorable injectivity characteristics. During water injection after gelation, much of the water leaving the wellbore should enter the most-permeable zone. If the cross-sectional area is relatively large in the region where water crossflows from the high-permeability zone into the low-permeability zone (Fig. 20d), then injectivity losses from the gel treatment could be minimized (particularly for unfractured injection wells, where flow is radial). In contrast, conventional gel treatments (i.e., those with no postflush prior to gelation) in unfractured injection wells should cause significant injectivity losses.[1]

The "incremental" oil from this scheme could be recovered relatively quickly. As shown in Fig. 20d, oil displaced from the less-permeable zones can crossflow into the most-permeable zone, where it can flow more rapidly to the production well.[47] Of course, this idea could be applied to production wells, to injection wells in CO_2 floods, steam floods, and other enhanced oil recovery processes, as well as to waterflood injection wells. Kvanvik *et al.*[48] proposed that the idea could also work if viscous, mobility-matched banks are used instead of fluids with water-like mobilities.

Limitations. A number of limitations should be recognized for this scheme. First, the gel treatment will not improve sweep efficiency beyond the greatest depth of gelant penetration in the reservoir.[2,44] Once beyond the gel bank in the most-permeable zone, fluids can crossflow back into the high-permeability channel. This provides an incentive to maximize the depth of gelant penetration in the high-permeability channels.

Gelation time is an important factor that limits the depth of gelant penetration in a reservoir. In concept, many variables (e.g., temperature, pH, salinity, and gelant composition) could be manipulated to achieve virtually any desired gelation time. If the gel treatment is confined to the region near the wellbore, then these variables may be useful in controlling gelation. However, if

the gelant is to penetrate a significant distance into the reservoir, control of gelation time is usually quite limited. For the most part, the temperature, pH, and salinity are set by the reservoir and are resistant to change. Until relatively recently, gelation times for common oilfield gelants were relatively short (0 to 10 days, typically) under reservoir conditions. If the offending channel is a very conductive fracture, then a typical gelant could penetrate a large distance into the reservoir before gelation. However, if the offending channel consists of a very permeable rock matrix, then very long gelation times (months to years) may be needed in order to achieve large depths of gelant penetration. (The different requirements for fractures vs. matrixes arise primarily because of their substantial differences in both permeability and pore volume.) Thus, there may be a need for new low-viscosity gelants with very long gelation times. In recent years, substantial progress has been made toward developing gelants with long gelation times, especially for use at elevated temperatures.[34,49-56]

One very important limitation is that the viscosity and resistance factor of the gelant should not exceed that of water. Viscous gelants will penetrate to a greater degree into the less-permeable zones.[1,44] Furthermore, before gelation, viscous gelants will crossflow continuously from the high-permeability channel into the adjacent less-permeable zones.[44] This creates a barrier of viscous gelant in the less-permeable zones all along the interface with the high-permeability channel. When a water postflush is injected, the barrier hinders crossflow of water from the high-permeability channel into the less-permeability zones. Thus, viscous fingers from a water postflush will break through the viscous gelant bank in the high-permeability channel before breakthrough in less-permeable zones. This will render the process ineffective. (Incidentally, Kvanvik *et al.*[48] have suggested a scheme where viscous gelants could be used, so long as mobility-matched banks were used throughout the process.)

In addition, the viscosity and resistance factor of the gelant should not increase during injection of either the gelant or the water postflush. Any increase in gelant resistance factor during this time will drive additional gelant into the less-permeable zones,[1,44] and thereby, jeopardize the process. If gel placement is not fast relative to the gelation time, gel aggregates may form during the placement process. Formation and flow of gel aggregates has been discussed with respect to gel treatments.[30,31,57] However, at present, their behavior has not been characterized sufficiently to quantify how they will impact gel placement.

The applicability of the scheme in Fig. 20 depends on the sweep efficiency in the reservoir prior to the gel treatment. In injection wells, the scheme is expected to work best if sweep efficiency is very poor prior to the gel treatment. Then, the water that is diverted into the less-permeable strata should primarily displace oil. In contrast, if sweep efficiency is high prior to the gel treatment or if gelant penetration is insufficient in the high-permeability channel, there may be little or no oil to displace in the less-permeable zones.

Can Pressure-Transient Effects Be Exploited to Minimize Gelant Penetration into Low-Permeability Zones? (Yes, under limited circumstances, and only if intra-wellbore crossflow is confirmed to occur for a sufficiently long period of time.)

Breston[58] speculated that selective placement can be achieved by a sudden reduction in injection pressure when the plugging agents reached the target zones (calculated from pipe dimensions and the injection rate). Conceptually, a sudden decrease in injection pressure would create a transient period during which fluids in the reservoir could flow back into the well (Fig. 21). The length of the transient period is inversely proportional to the formation permeability.[59] Breston's idea relies on the difference in transient times between the high- and low-permeability zones to achieve selective placement. The author asserted that due to the shorter transient time, enough plugging agents can be placed into high-permeability zones while the less-permeable zones are still backflowing. However, supporting evidence was not provided.

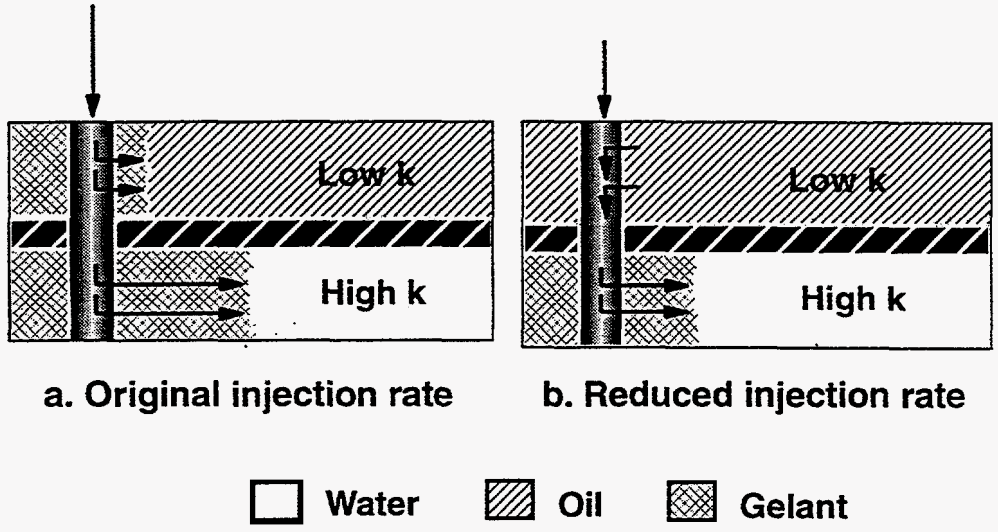

Fig. 21. "Transient" placement.

The feasibility of this idea depends on whether the difference in transient times is long enough to allow a realistic amount of the plugging agent to be placed into the high-permeability zone. Consider a reservoir with a 1,500-md high-permeability zone and a 10-md low-permeability zone. In this example, the injection pressure at the wellbore is suddenly reduced from p_{wo} to p_{w2} where $(p_{wo}-p_e)=2(p_{w2}-p_e)$. We assume a steady-state flow condition in the reservoir before the injection pressure reduction. The parameters in this example are listed in Table 3. Before the injection-pressure reduction, the radial distance into the reservoir, r_2, where the pressure is equal to p_{w2} can be determined by[13]

$$r_2 = \sqrt{r_e \cdot r_w} \qquad (7)$$

In this example, r_2 is $(372\text{x}0.3)^{0.5}$ = 10.5 ft. This indicates that before the injection-pressure reduction, reservoir pressure within a 10.5 ft radius from the well is greater than p_{w2}. A sudden reduction in injection pressure from p_{wo} to p_{w2} creates a pressure pulse that travels outward into the reservoir. The pressure in the reservoir would remain greater than the wellbore pressure, p_{w2}, until the pressure pulse reaches r_2. In order for the reservoir fluid to backflow into the well, reservoir pressure must be greater than the wellbore pressure. The transient time is therefore the

time required for the pressure pulse to reach r_2. In pressure-drawdown analysis, the transient time is defined as

$$t_{tr} = \frac{\phi \mu c r_e^2}{0.00264k}, \quad (8)$$

where ϕ is porosity, μ is fluid viscosity in cp, c is compressibility in psi^{-1}, r_e is drainage radius in ft, and k is formation permeability in md.[59] This equation calculates the time required for the pressure pulse to reach the drainage radius. The time required for the pressure pulse to reach r_2 can be estimated by substituting r_2 for r_e in the equation. In our example, the transient time for the high-permeability zone (k_1=1,500 md) is about 0.05 seconds and the transient time for the low-permeability zone (k_i=10 md) is only about 7 seconds. Breston's concept relies on the difference in transient times between the high- and low-permeability zones to achieve selective placement. Our example demonstrates that the difference in transient times (7-0.05=6.95 sec.) is obviously too short for this concept to have any practical value.

Table 3. Example Rock and Fluid Properties for Transient Time Calculations

k_1=1,500 md	k_i=10 md
ϕ=0.21	μ=0.7 cp
c=3x10^{-6} psi^{-1}	r_w=0.3 ft
r_e=372 ft (20 acre, 5 spot pattern)	

One other possible way of achieving selective plugging is to exploit the difference in formation pressures between high- and low-permeability zones. This is possible only when the zones are separated by an impermeable barrier and when the formation pressure in the low-permeability zone is significantly higher than that in the high-permeability zone. Selective placement could be achieved by injecting the plugging agent at an injection pressure which is high enough to place a significant amount of plugging agent into the high-permeability zone in a short period of time and yet low enough not to exceed the formation pressure in the low-permeability zone.[13]

The most effective method to establish whether or not the transient-placement concept is of value in a particular well is to (1) place a profiling tool in the well, (2) make a step change in injection or production rate to the desired value, and (3) measure how long the transient period lasts. If this procedure is not performed to satisfactorily demonstrate that the transient period lasts long enough, the transient-placement concept should not be used.[13]

Can Anisotropic Permeability or Pressure Distributions Around an Unfractured Well Be Exploited to Eliminate the Need to Protect Hydrocarbon-Productive Zones During Gelant Placement? (No.)

In the analysis of gel placement to this point, only linear and purely radial flow geometries were considered. However, flow in reservoirs is often anisotropic—the effective permeability and/or the pressure gradient is greater in one horizontal direction than in another direction. Anisotropic flow can occur in both fractured and unfractured reservoirs.[60] In the naturally fractured Spraberry field, Elkins and Skov[61] reported that the effective reservoir permeability along the main fracture trend was 13 times greater than that at right angles to this trend. As expected,[60] permeability anisotropy is significantly less in unfractured reservoirs. For example, Ramey[62] reported only a 56% permeability anisotropy for a channel-sand reservoir (i.e., k_x/k_y=1.56).

In fractured reservoirs, gel placement can be treated effectively as a linear flow problem.[16] However, unfractured anisotropic reservoirs can be viewed as flow geometries that are intermediate cases between linear and radial flow. In fact, a linear flow geometry can represent the extreme case of an anisotropic reservoir. Since the requirements for an effective gel placement are radically different for linear versus purely radial flow, questions arise about gel placement during anisotropic flow in unfractured reservoirs: How anisotropic must an unfractured reservoir be to allow gelant placement to approximate that for the linear flow case? Asked another way, how anisotropic must an unfractured reservoir be to achieve an acceptable gel placement during unrestricted gelant injection? These questions were addressed in Refs. 13 and 63 by developing two models of simple anisotropic flow systems and by performing sensitivity studies with these models. Both analytical and numerical methods were applied to solve the problem. We studied how the effectiveness of gel treatments is influenced by permeability variation, distance of gelant penetration, anisotropic pressure distributions, resistance factor, and residual resistance factor.

Our analyses showed that the range of permeability variations (permeability in the most-permeable direction divided by permeability in the least-permeable direction) must be greater than 1,000 (and usually greater than 10,000) before anisotropy can be exploited to achieve a satisfactory gel placement in unfractured wells. We doubt that any unfractured wells or reservoirs exist with this degree of anisotropy. In contrast, in wells and reservoirs where anisotropic flow is due to fractures, the linear flow geometry and the extreme permeability contrast between the fracture and the porous rock can aid gel placement substantially.[63]

Can Gravity and Fluid Density Differences Be Exploited to Optimize Gelant Placement? (Yes, for some cases in fractured wells. Usually, no, for unfractured wells.)

For most commercial gel treatments, the process of gel placement consists of two stages. First, the gelant is injected in a fluid form. Second, the well is shut in to allow gelation to take place. During the first stage in fractured wells, viscous forces virtually always dominate over gravity forces—that is, the gravity number is much less than one. To demonstrate, first consider a fracture with an effective permeability of 100 darcys, fluids with a density difference of 0.2 g/cm^3, a viscosity of 1 cp, and sin θ = 1 (i.e., the fracture is vertical). The dimensionless gravity number, G, provides a means to compare the importance of gravity forces relative to viscous forces during a displacement of oil by water.[64]

$$G = -\frac{k\Delta\rho g \sin\theta}{1.0133x10^6 u\mu} \qquad (9)$$

Gel Placement in Fractured Wells. For gel treatments in fractured production wells, gelant injection rates are typically very high—e.g., 50 to 500 BPD/ft of pay.[10] Thus, for a fracture with a width of 0.01 ft, the velocity in fractures during gelant injection typically ranges from 28,000 to 280,000 ft/d (10 to 100 cm/s). With these velocities, the G values range from 0.000193 to 0.00193. Note that the gravity number is substantially less than one. Even if the fracture was 100 times more permeable, the G values would still be much less than one. Thus, viscous forces dominate over gravity forces during gelant or gel injection into fractures. Therefore, the position of the gelant or gel front will not be significantly affected by gravity during injection.

When the well is shut in after gelant injection, how rapidly will gravity equilibrate the level of the gelant-oil interface in the fracture? If gravity alone acts as the driving force, then the vertical superficial velocity, u_z, is given by Eq. 10.[64]

$$u_z = -\frac{k\Delta\rho g}{1.0133x10^6\mu} \tag{10}$$

Fig. 22 illustrates u_z as a function of k/μ and $\Delta\rho$. Assume that oil has ready access to the fracture, either from the porous rock or from portions of the fracture beyond the gelant front. (This assumption will generally be valid for applications in production wells but not in injection wells unless oil is also injected.) Also assume that fluid displacements are piston-like (i.e., that capillary-pressure and relative-permeability effects are negligible). Given a fracture permeability of 100 darcys, a density difference of 0.2 g/cm^3, and a 1-cp fluid viscosity, then u_z is -55 ft/d. Thus, the rate of interface equilibration in a fracture can be quite rapid. For example, a fracture 55 ft high could be drained of gelant in 1 day if the gelation time is long enough.

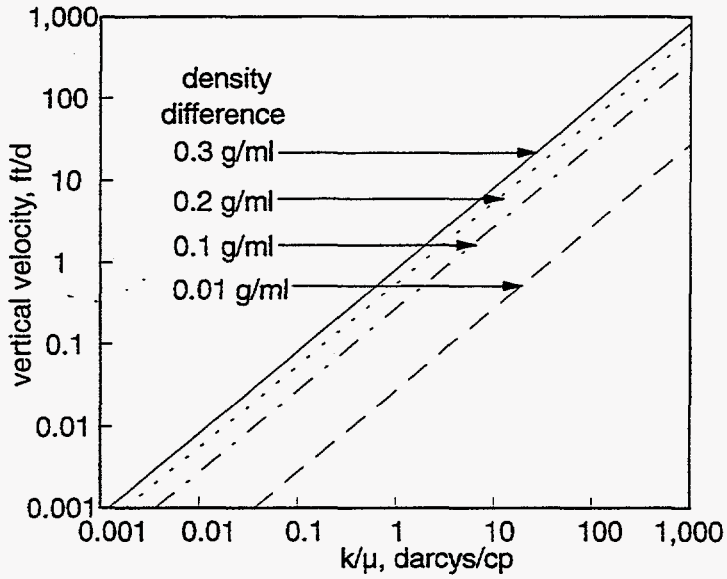

Fig. 22. Effect of gravity on gelant placement.

Gel Placement in Unfractured Wells. Next consider an unfractured production well with a matrix permeability of 1 darcy. For the same fluid properties used in the previous examples,

$$G = \frac{(1)(0.2)(980)(1)}{(1.0133x10^6(1)u} = \frac{0.000193}{u} \tag{11}$$

G will be less than 1 so long as u is greater than 0.000193 cm/s. If the gelant injection rate is 10 BPD/ft, then u > 0.000193 cm/s if the gelant is within a radius of 16.3 ft from the wellbore. Thus, during gelant injection in unfractured wells, viscous forces will dominate near the wellbore, but gravity becomes more important farther from the wellbore.

When the well is shut in after gelant injection, Eq. 10 can again be used to estimate the rate of settling for a gelant-oil interface. If k = 1 darcy, $\Delta\rho$= 0.2 g/cm^3, and μ = 1 cp, then u_z = -0.55 ft/d. Thus, even in a very permeable rock matrix, the rate of settling will be slow. The rate will

be less in less-permeable rock or if a more viscous gelant is used. In concept, gravity could be exploited during gelant placement if the offending channel or aquifer is located below oil-productive zones. However, in view of the slow settling rate in porous rock, relatively long gelation times (weeks, at least) will be needed.

In unfractured injection wells, slow settling rates and small density contrasts (between the gelant and the formation water) make gravity difficult to exploit during gelant placement.

Can Suspensions of Particles (Including Gel Particles) Show Better Placement Properties Than Gelants When Used as Blocking Agents? (No, except under rare circumstances.)

Placement. Several researchers proposed the use of particles as blocking agents (see Refs. 104-111 in Ref. 13). With particles, two different approaches can be taken to control placement. The first approach is commonly used in matrix acidizing.[65] If they are large enough relative to pore throats, particles can form a filter cake on the rock surfaces. Since the largest volume of the injected suspension enters the most-permeable zone, the largest filter cake forms on that zone, and that filter cake can restrict flow to the greatest extent in the most-permeable zone. However, at best this method will equalize injection rates in the different zones.[65] If too much of the suspension is injected, flow will be restricted in all zones. Also, any beneficial flow diversion occurs at the wellbore. If flow is reversed (e.g., return of an oil well to production), the filter cake can be removed, and the effect of the diverting agent will be reversed. Finally, if this diversion method is combined with another blocking agent, such as a gelant, an undesirable placement results—the gelant is diverted into rather than away from the less-permeable zones.

The second placement approach using particles (Fig. 23) relies on the relation between the particle size and the pore sizes of the zones of interest. In concept, a suspension of particles could penetrate readily into a high-permeability zone, while the particles are removed by filtration on the rock faces of less-permeable zones. If the fluid contains a gelant or other blocking agent, that blocking agent could be selectively placed in the high-permeability zone with minimum penetration into less-permeable zones.

For this second concept to work, several requirements must be fulfilled. First, the particles must be small enough to penetrate freely into the most-permeable zones. Second, the particles must be large enough to form an external filter cake on the rock surface of the less-permeable zones. Third, the particle size distribution must be sufficiently narrow. We developed a theoretical model to study the feasibility of using particles to prevent gelant penetration into low-permeability zones during the placement process.[13] Our analysis indicated that to achieve selective placement using particles with a normal size distribution, there is a maximum standard deviation of particle sizes that should not be exceeded for a given permeability contrast. For example, consider two zones with permeabilities of 10,000 md and 100 md, respectively. Assume a best-case scenario where all particles less than 33.3 μm in diameter will flow freely through the 10,000-md rock and where all particles greater than 3.33 μm in diameter will form an external filter cake on the 100-md rock. Therefore, if monodisperse particles were available, a selective placement of a blocking agent could be achieved using any particles that were smaller than 33.3 μm and larger than 3.33 μm.

In reality, particles in a given suspension have a distribution of sizes. We have shown[13] that for a given standard deviation of a normal particle-size distribution, the maximum selectivity for placement of a blocking agent is achieved by choosing the average of the critical particle sizes of the high- and low-permeability zones as the mean particle size [in this example, (33.3+3.33)/2 = 18.3 μm]. If particles with a mean size of 18 μm are used in our example, the standard deviation of the size distribution must be smaller than 9 μm to achieve better selectivity than a water-like gelant without particles.[13] To achieve the same selectivity as particles with a monodisperse size of 18 μm, the standard deviation must be smaller than 4 μm. The maximum allowable standard deviation for selective placement decreases with decreasing permeability contrast.[13]

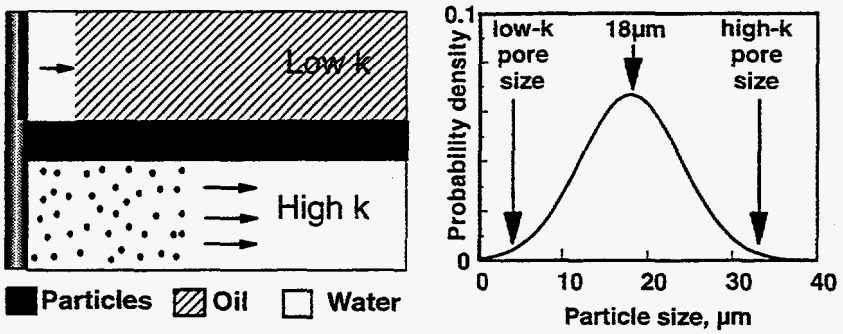

To achieve placement superior to gels, particles must:

- be small enough to flow freely into high-k zones,
- be large enough not to enter low-k zones,
- not aggregate or adsorb during placement,
- have a sufficiently narrow size distribution.

Fig. 23. Placement of particles.

The above analysis is actually optimistic since it assumes that the rock has a single pore size. Because porous media contain a range of pore sizes, the particles used must have a narrower size distribution than was indicated above to achieve selectivity during placement.[13] The utility of particles in controlling placement of blocking agents may also be limited by other factors that were not considered in our simple model. In particular, the ability of particles to penetrate into a given porous medium also depends on the influence of fluid velocity, particle concentration, and the surface chemistries of the particles and porous media.[66-68]

For intermediate-sized particles (those small enough to flow readily into the high-permeability zone but large enough not to enter the low-permeability zone), the relative distance of penetration, in concept, could be zero. On the surface, this behavior suggests a tremendous placement advantage over gelants. However, if the particles flow freely through the high-permeability rock, they may not provide a significant permeability reduction. Therefore, the particles by themselves are not expected to be an effective blocking agent in the high-permeability zones.

The above shortcoming could be remedied by incorporating a gelant or similar blocking agent with the suspended particles.[13] Intermediate-sized particles suspended in a gelant could readily enter the high-permeability zone. However, the particles would form a filter-cake on the surface of the low-permeability zone—thus, minimizing gelant penetration. Of course, some gelant will inevitably enter the low-permeability zone during placement. Even so, the potential exists to achieve a substantially better placement than that possible with a gelant alone.

Proper particle sizing is extremely important when combining particles with gelants. If particles are small enough to penetrate readily into all zones, gelant placement will be no better than that for a low-viscosity gelant without particles. If the particles are too large to penetrate into any zone, external filter cakes will form on all zones, and an excessive amount of gelant could enter the low-permeability zone (as expected from fluid diversion concepts in matrix acidizing[65]). In fact, the gelant could penetrate almost as far in the low-permeability zone as in the high-permeability zone.[13]

Permeability Reduction. The degree of permeability reduction caused by particles can be separated into two components: (1) that associated with an external filter cake formed at the surface of a given zone and (2) that associated with an "internal filter cake" formed from particles trapped inside the porous medium. Because the external filter cake can be removed or circumvented by mechanical means (e.g., jet washing, backflow, or perforation), we are concerned primarily with the permeability reduction associated with the internal filter cake. For particles trapped inside a porous medium, the degree of permeability reduction qualitatively follows the same trend as that for weak gels. In particular, formation damage factors or residual resistance factors tend to increase with increasing ratio of particle size to pore size.[69-71] (This behavior has been reported when the ratio of particle size to pore size ranges from 1/14 to 1/3.[71]) This parallel in behavior between particles and weak gels is not surprising since weak gels usually consist of a suspension of gel aggregates, which are a specific form of particulate. In concept, the potential improvements in placement that were discussed above with regard to particles could also be achieved using suspensions of gel aggregates. Of course, the limitations also apply. An extensive analysis by Midha *et al.*[57] indicates that suspensions of gel aggregates will be no more selective than gelants.

Hypothetically, particles could reduce the flow capacity of water zones to a greater extent than oil zones. Small particles could be injected that are soluble in oil but not soluble in water.[72,73] These particles must be sized so that they enter the porous rock and become trapped by deep-bed filtration. Upon returning the well to production, the particles could significantly reduce the permeability of watered-out zones. In contrast, in zones with high fractional oil flows, the particles may quickly dissolve—thus restoring a high oil permeability.

Can Precipitates and Other Products of Phase Transitions Show Better Placement Properties Than Gelants When Used as Blocking Agents? (No.)

Placement. Several investigators proposed the use of precipitates (or other products of phase transitions) as blocking agents for fluid diversion in oil recovery processes (see Refs. 92-107 in Ref. 10). Typically, these processes involve forming a blocking agent in situ by mixing two incompatible chemical solutions in the formation. Alternatively, chromatographic separation in a

formation can be exploited to form a blocking agent from a stable mixture. Llave and Dobson[74] described a recent example of the latter process. In their process, a low-viscosity surfactant-alcohol blend was injected. In the formation, the blend chromatographically separated, with the alcohol propagating more rapidly than the surfactant. After the alcohol was removed from the surfactant, the surfactant formulation became very viscous and restricted flow.

We surveyed the petroleum and patent literature to investigate whether blocking agents formed in situ from phase transitions have potential advantages over gels.[10] In most cases, the flow properties of the proposed materials (before the phase transition) are no different from those of gelants. Therefore, their placement characteristics are similar to those of gelants. Specifically, for a given distance of penetration into a high-permeability zone, the distance of penetration into a less-permeable zone will be no less for a precipitate or phase-transition product than for a gelant with a water-like mobility. Certainly, the mechanism of forming the blocking agent can be different for a gel versus a phase-transition product. This difference could allow one blocking agent to penetrate deeper overall into a formation than another blocking agent. However, it will not change the relative placement properties (i.e., the distance of penetration in one zone relative to that in a nearby zone during unrestricted injection).[1] Thus, placement of these materials is not better than that achieved using a low-viscosity gelant.

Permeability Reduction. Very little work has been reported on the permeability dependence of the permeability-reduction properties of precipitates. We suspect that they usually will be the same as those for particles. As mentioned earlier, residual resistance factors tend to increase with increasing ratio of particle size to pore size.[69-71] (Particles that enter porous rock reduce the flow capacity of low-permeability rock by a greater factor than in high-permeability rock.)

Thompson and Fogler[73] investigated the use of "reactive water-blocking agents" to plug water zones in preference to oil zones in production wells. These chemicals are dissolved in oil and then injected. They react upon contact with water to form a precipitate or solid barrier. Ideally, watered-out zones will be restricted by blocking agents formed at the front between the displaced water bank and the injected bank of reactive chemicals, while no blocking agent should form in zones with high oil saturations. To maximize formation of blocking agents in water zones, Thompson and Fogler proposed using a relatively viscous oil as a carrier fluid for the reactive chemicals. When the well is returned to production after injecting the reactive chemicals, water should finger through the bank of reactive chemicals—thereby promoting mixing and formation of the blocking agent. One of the main challenges in using these materials is that reaction with residual water in the oil-bearing zones could damage oil productivity. More work is needed to assess the potential of reactive water-blocking agents, especially their effects on oil productivity.

Can Microorganisms Show Better Placement Properties Than Gelants When Used as Blocking Agents? (No, except under rare circumstances.)

Many people have proposed the use of microorganisms as blocking agents (see Refs. 36-57 in Ref. 28). In most of these proposals, placement of the microorganisms is dictated by placement of the nutrients. Since the flow properties of the nutrients are no different from those of gelants, their placement characteristics are similar to those of gelants. Specifically, for a given distance of penetration into a high-permeability zone, the distance of penetration into a less-permeable

zone will be no less for the nutrient (and the microorganism) than for a gelant with a water-like mobility. If a viscous nutrient is used (e.g., molasses or corn syrup), microorganism penetration into less-permeable zones increases.[1,44]

From one perspective, microorganisms could be viewed as particles. Because of their narrow size distribution, certain microorganisms could, in concept, provide the advantageous placement characteristics associated with monodisperse particles (discussed earlier). A suspension of microorganisms could penetrate readily into a high-permeability zone, while size restrictions prevent them from entering less-permeable zones. Bae *et al.*[75] proposed the use of spores to act by this mechanism. They observed spores that propagate through Berea sandstone with permeabilities greater than 710 md but that do not propagate through cores with permeabilities less than 380 md. Once placed, nutrients could be provided so that the microorganisms could restrict flow (i.e., by growing or generating biomass or polymers). Thus, properly sized microorganisms conceptually could provide a placement similar to that for intermediate-sized particles suspended in a gelant.

Two important restrictions must be noted when using microorganisms in this mode. First, growth, aggregation of microorganisms, and adsorption onto pore walls must be limited during placement. Otherwise, these phenomena could greatly limit the distance of microorganism penetration into the high-permeability zones. Second, the microorganisms should be near-spherical in shape during placement. Elongated microorganisms act as particles with a significant size distribution.[28] As mentioned earlier, the placement advantage for particles will be lost unless the size distribution is very narrow.

Can Foams Show Better Placement Properties Than Gelants When Used as Blocking Agents? (Yes, under limited circumstances.)

Placement. Considerable theoretical, laboratory, and field work has been performed to evaluate the use of foams as mobility-control agents during steam and high-pressure gas floods (see Refs. 2-69 in Ref. 13). Much less work has been done to evaluate the use of foams as blocking agents. The distinction between a blocking agent and a mobility-control agent is an important concept to understand. A mobility-control agent should penetrate as much as possible into the less-permeable zones so that oil can be displaced from poorly swept zones. In contrast, we wish to minimize penetration of blocking agents into the less-permeable, oil-productive zones. Any blocking agent that enters the less-permeable zones can hinder subsequent injected fluids (e.g., water, CO_2, steam) from entering and displacing oil from those zones.

Many field results demonstrate that foams usually act more effectively as mobility-control agents than as blocking agents. For example, in cases where vertical injection profiles were measured before, during, and after foam injection, the profiles were consistently improved during foam injection—demonstrating the ability of the low-mobility foams to shift flow from high-permeability zones into less-permeable zones.[76-80] Also, when gas or water injection was resumed after foam injection, the profiles quickly reverted to profiles that were the same or worse than those observed before foam injection.[76-81] This behavior is consistent with expectations for injection of a high-mobility fluid following a bank of low-mobility fluid in a heterogeneous system.[44] This behavior is opposite to that desired for a blocking agent.

Nevertheless, in concept, several phenomena could allow foams to be superior to gels as blocking agents, in some circumstances. At present, these circumstances are hypothetical; very few conditions have been verified experimentally or in field applications. Details of our analyses of these circumstances are presented in Refs. 13, 28, and 82. In what follows, we summarize the findings of these analyses.

Two phenomena, the limiting capillary pressure[82-85] (see Fig. 24) and the minimum pressure gradient for foam generation,[76] could allow low-mobility foams to form in high-permeability zones but not in low-permeability zones. Exploiting these phenomena during foam placement requires that (1) under given reservoir conditions, a gas/liquid composition must be identified that will foam in high-permeability zones but not in low-permeability zones, (2) the foam must not easily collapse or wash out from the high-permeability zones, and (3) the aqueous phase must not contain a gelant or other reactive blocking agent.

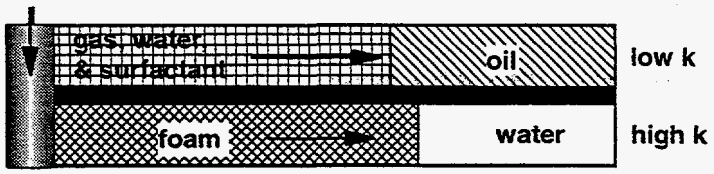

Limiting capillary pressure:

- Could allow a low-mobility foam to form in high-k zones but not in low-k zones.
- Much lab work needed to identify the foam.
- Aqueous phase must not contain a gelant.
- Foam must be persistent in the high-k zone.

Fig. 24. Exploiting limiting capillary pressure to optimize foam placement.

An ideal placement could be realized if foam forms in the high-permeability zone but not in the low-permeability zone. In contrast, an extremely unfavorable placement results if foam forms in both zones. The foam can penetrate almost as far in the low-permeability zone as in the high-permeability zone. This behavior is expected for viscous fluids when free crossflow can occur.[44,46] However, if crossflow cannot occur, the relative distance of penetration into the low-permeability zone is significantly greater than expected for simple viscous fluids.[13] If gelant is included with the foam, a very undesirable placement results regardless of whether foam forms in the less-permeable zone.[13]

In cyclic steam projects, foam placement could be aided by gravity effects combined with very large mobility contrasts between the foam and the displaced oil. For cyclic steam injection projects where the foam was intended to act as a blocking agent, a common observation for successful field applications was that steam and oil flow after the foam treatment was diverted away from upper zones in favor of the middle or lower zones.[86] These results suggest that gravity effects aided foam placement in the upper zones.

A circumstance where the presence of a preformed gel could aid placement of a foam can be inferred from the work of Craighead *et al.*[87] During hydraulic fracturing, foamed gels show significantly lower leakoff rates than foams or foamed polymers.[87] Logically, preformed foamed gels may propagate substantial distances along fractures with minimum leakoff. This argument parallels that given for injecting preformed gels into fractured systems.[16,17] However, a potential advantage over ordinary gels is that the foamed gels may be more likely to extrude through fractures without developing excessive pressure gradients. This concept needs to be tested experimentally.

Permeability Reduction. Problems with foam propagation and stability present challenges for foam applications both as mobility-control agents and as blocking agents.[13] In many cases, foam stability is significantly reduced by the presence of oil.[88,89] Hypothetically, this phenomenon could be exploited to optimize the use of a foam blocking agent in oil production wells. When oil wells are returned to production after foam injection, foams could collapse more rapidly in oil zones than in water zones. This behavior is most likely to be exploitable if the water zones contain no residual oil. Foam washout from the water zones could be reduced by incorporating a polymer or gel into the foam. If a gelant is used, the foam must be produced from the oil zones before gelation occurs; otherwise, the oil zones could be damaged.[13]

Another potential advantage of foamed gels is that they may allow more control in achieving low or intermediate residual resistance factors.[90] To explain, strong gels (without foam) can provide predictable and reproducible residual resistance factors because gelation in the porous medium is fairly complete.[8] Because these gels fill most of the aqueous pore space,[8] residual resistance factors are usually very high (10^3-10^6). However, we sometimes desire lower residual resistance factors (e.g., 1-100), that are associated with weak gels. Unfortunately, for the reasons mentioned earlier, weak gels provide low to intermediate residual resistance factors that are often unpredictable.[8] If a foamed gel is used that incorporates a strong gel in the aqueous phase, the thin gel films that separate the gas bubbles should be formed reproducibly, and they may allow intermediate residual resistance factors to be attained more reliably. This concept also needs to be tested experimentally.

For foams, gas residual resistance factors can increase with increasing permeability.[88] This behavior could be exploited when using foam as a gas blocking agent. A similar phenomenon has not been observed for water residual resistance factors in the presence of foam.[88] Gels and foams are known to show different permeability reductions for different phases.[27,88,89] Experimental work is needed to establish the permeability reduction properties of foamed polymers and foamed gels.[91]

Can Emulsions Show Better Placement Properties Than Gelants When Used as Blocking Agents? (No.)

Analysis of the literature (Refs. 70-103 in Ref. 13) suggests no reason to believe that emulsions have any placement or permeability-reduction advantages over gelants and gels.[13] For concentrated emulsions (either oil-in-water or water-in-oil), their behavior in porous media can be described using standard relative-permeability concepts.[92-93] Therefore, the placement

properties of concentrated emulsions are similar to those of viscous gelants.[18] Also, the literature indicates that concentrated emulsions provide very low permeability-reduction values (residual resistance factors less than 1.5).[13,92,93] Furthermore, residual resistance factors provided by concentrated emulsions do not increase with increasing initial rock permeability.[92,93]

Dilute emulsions show behavior that can be described by a modified deep-bed filtration theory.[94-96] Ref. 13 contains a detailed examination of the literature and models that describe the flow of dilute emulsions through porous media. We can summarize the results of this analysis as follows: although several features of emulsion flow through porous media remain unanswered, our analysis of the literature indicates that emulsions or emulsion/gel combinations will not perform significantly better than gels as blocking agents, particularly in the areas of placement characteristics and permeability-reduction properties. Our calculations indicate that at best, the placement properties of emulsions will approach those for a low-viscosity gelant.

Other Special Situations and Methods.

Certain other circumstances may be exploited to improve gel placement if zone isolation cannot be used. For example, before a gel treatment, the productive interval in a well might be plugged with debris, while a watered-out zone is open. If crossflow does not occur, the gel treatment could be applied with a reduced risk of gel entering productive zones. After the gel treatment, acid could be spotted on the productive intervals to remove near-wellbore damage and increase injectivity.[1]

In some cases, watered-out zones may contain natural, hydraulic, or thermally induced fractures while oil-productive zones do not.[97] In certain circumstances, selective plugging of the water zones could occur without the use of zone isolation. Alternatively, the various zones in a reservoir may contain fractures, but since the fractures do not contain proppants, they remain closed unless the injection pressure is sufficiently high. Also, the pressure at which a fracture opens varies from one zone to the next. If at a given pressure, the fractures are open in the watered-out zones but are closed in the hydrocarbon-productive zones, a blocking agent can be placed primarily in the most offensive fractures. Hopefully, after the gel has been placed, damage to the oil zones (either fractured or unfractured) will be minimal. For this concept to work, a given fracture must not cut through most or all zones. Fractures that cut through multiple zones will allow vertical fluid movement throughout their heights.

In another case, a watered-out channel may be located some distance above a less-permeable, productive interval. If the tubing between the two zones contains enough buffer fluid (e.g., water) and the permeability contrast is high enough, gelants can be placed in the watered-out channel without contacting the productive interval. In contrast, if a watered-out channel is located below a productive zone, the need for zone isolation during gel placement is accentuated. Considering typical casing or tubing volumes, this approach generally will require very small gelant volumes or very large distances between zones. Perhaps, a more practical idea involves the use of coiled tubing.[98] By locating the end of the coiled tubing at the interval to be plugged, one may minimize gelant injection into hydrocarbon zones (if the injection volume is sufficiently small).

In other cases,[99] hydrocarbon-productive zones have been protected during gelant injection by simultaneously injecting gelant down the tubing and oil down the tubing annulus (or vice versa). If the pressures, injection rates, and tubing location are balanced properly, gelant enters the water zones while oil enters the oil zones.

Conclusions

Basic calculations using the Darcy equation reveal three important facts.[1] First, gelants and similar fluid blocking agents can penetrate a significant distance into all open zones. Second, an acceptable gelant placement is much easier to achieve in linear flow than in radial flow. Third, if flow is radial, then hydrocarbon-productive zones must be protected during gelant placement. These facts mean that excess channeling and water production problems can be treated much more readily if they are caused by linear-flow phenomena, such as vertical fractures, fractured systems, or flow behind pipe. Even so, placement of blocking agents is very important in linear flow as well as in radial flow. When flow is radial (e.g., unfractured wells), field engineers would be well-advised not to apply blocking-agent treatments unless hydrocarbon productive zones are protected during placement of the blocking agent.

A strong need exists for the development of new ideas to optimize placement of gels and other blocking agents, both in linear and radial systems.

3. GEL PROPERTIES IN FRACTURES AND TUBES

Gels have often been used to reduce fluid channeling in reservoirs.[12] The objective of these gel treatments is to substantially reduce flow through high-permeability channels without damaging hydrocarbon-productive zones. The most successful applications for this purpose have occurred when treating linear flow problems—either fractures[100-102] or flow behind pipe.[98,103] In fractured reservoirs, some of the most successful treatments used relatively large volumes (e.g., 10,000 to 37,000 bbl/well) of Cr(III)-acetate-HPAM gel.[100,102] In these applications, the gel injection times were substantially longer than the gelation time (e.g., by factors ranging from 10 to 100). Since these gels (after gelation) do not flow through porous rock,[17] they must extrude through fractures during the placement process.

Ideally, a blocking agent should penetrate as far down the length of a fracture as possible while penetrating ("leaking off") to the minimum extent into the porous rock. By minimizing gelant leakoff, near-wellbore damage may be minimized.[16,17,105] Of course, various materials have been used to control leakoff during hydraulic fracturing.[106] However, a very logical choice of leakoff material is what we will call "preformed gel." In contrast to gelants, gels cannot flow intact through porous rock.[17,29-31] Therefore, in concept, leakoff could be virtually eliminated by forming the gel before injection into the fracture. Since the densities of water-based gels are very similar to that of water, these gels should have fewer problems with gravity segregation than other fluid-loss additives.[106]

This chapter examines the placement properties of preformed gels when used as blocking agents for conformance control in fractures. Results of new experiments are reported that characterize how gel extrusion through fractures and tubes is affected by fracture or tube conductivity, fracture or tube length, gel age, and gel velocity. In Chapter 4, the results from our experiments are used during a modeling study to compare the placement of preformed gels with those of gelants with a water-like viscosity.

Review of Gel Behavior in Fractures

In concept, leakoff could be minimized by injecting preformed gels instead of gelants. In our previous work,[16,17] we investigated the properties in fractures for several one-day-old gels, including Cr(III)-acetate-HPAM, Cr(III)-xanthan, resorcinol-formaldehyde, Al-citrate-HPAM, hydroquinone-hexamethylenetetramine-HPAM, Cr(VI)-HPAM-AMPS, and Cr(III)-acetate-HPAM-AMPS. We focused on the Cr(III)-acetate-HPAM gel. Tracer studies performed before and after gel placement revealed that this gel can effectively heal fractures with minimum damage to the porous rock. During brine injection after gel placement, preformed gels were more resistant to washout than gels formed in situ from gelants. However, high resistance factors (apparent viscosities) and pressure gradients were often observed during injection of preformed gels. For fractures with conductivities ranging from 0.33 to 6.4 darcy-ft, pressure gradients ranged from 40 to 300 psi/ft during gel injection.[17] (Incidentally, fracture conductivity is the product of fracture permeability and fracture width, $k_f w_f$.) These high pressure gradients raised concern about our ability to place preformed gels deep into fractured systems. However, the

fractures used in our experiments had relatively low conductivities, so perhaps, pressure gradients may not be prohibitively high during gel extrusion through more conductive fractures.

Preformed gels showed an apparent shear-thinning behavior during extrusion through fractures—gel resistance factors decreased with increased flow rate.[17] At high flow rates, the pressure gradient was almost independent of gel injection rate.[17] For example, in a fracture with a conductivity of 6.2 darcy-ft, the pressure gradient increased from 60 to 75 psi/ft as the average superficial velocity in the fracture increased from 310 to 3,100 ft/d. This behavior suggests that the gel experienced "slip" when extruding through fractures at high rates.

In contrast to the shear-thinning behavior observed during gel extrusion through fractures, flow-rate-independent behavior was usually seen during brine or oil injection after placement of preformed gels in fractures.[17,28] This behavior was expected. If the gel effectively plugs the fracture without damaging the porous rock, then normal, Newtonian flow of oil and water occurs in the porous rock.

Most of our previous experiments used one-day-old gels in 6-inch fractured cores that had low fracture conductivities. Therefore, a number of important questions remain to be answered for flow of preformed gels in fractures. First, how do gel resistance factors and pressure gradients vary with fracture conductivity or width? Second, how do gel properties vary with fracture length? Third, how does the age of the gel (i.e., gel "curing" time) affect the flow of preformed gels in fractures? Finally, how do the flow properties of different preformed gels compare in fractures? These questions are addressed in this chapter.

Core Characterization

Core Preparation. To answer the above questions, we performed experiments using fractured Berea sandstone cores. Before fracturing, the cores had a nominal permeability to brine of 650 md. Cores of two lengths were used. One set of cores were 14-15 cm (6 inches) in length and 3.6 cm (1.4 inches) in diameter. These cores were fractured lengthwise, and the two halves of the core were repositioned and cast in epoxy or a metal alloy. Two internal pressure taps were drilled 2 cm from the inlet sandface. One tap was located 90° from the fracture to measure pressure in the porous rock, while the other tap was drilled to measure pressure in the fracture. Fig. 25 shows a schematic of the first type of fractured core.

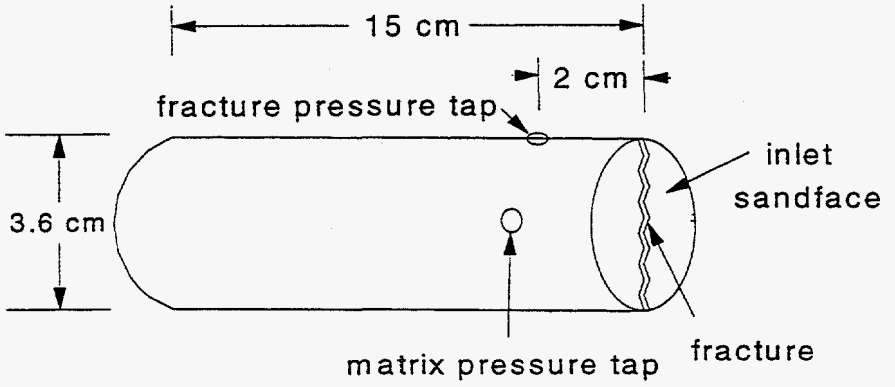

Fig. 25. Short fractured core.

The second set of cores (Fig. 26) were 114-122 cm (3.7-4.0 ft) in length (L) and 3.81 cm (1.5 inches) in height (h_f) and width. (So, the cross-sectional area of the cores was 14.5 cm^2 or 2.25 in^2.) Again, these cores were fractured lengthwise, and the two halves of the core were repositioned and cast in epoxy. Four internal pressure taps were spaced equally along the length of the fracture (i.e., to measure pressure in the fracture). During our corefloods, the fractures were always oriented vertically. All experiments were performed at 105°F (41°C).

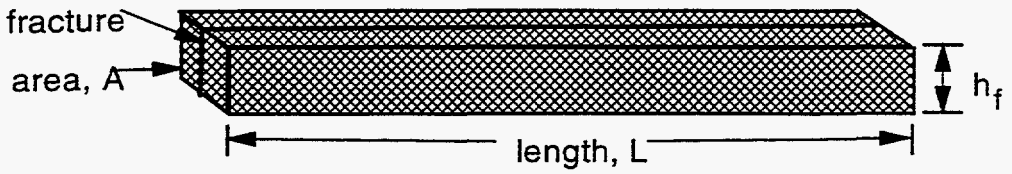

Fig. 26. Long fractured cores.

Tracer Studies. We routinely performed water-tracer studies before and after gel placement during our experiments. These tracer studies were used to characterize pore volumes and dispersivities of the cores. These studies involved injecting a brine bank that contained potassium iodide as a tracer. The tracer concentration in the effluent was monitored at a wavelength of 230 nm. In Fig. 27, the curve with the open circles illustrates the results from a tracer study for a short (14.5-cm or 5.7-inch) unfractured Berea core that was saturated with brine. Dispersivities of unfractured Berea sandstone cores were typically 0.1 cm (0.04 inches), and the effluent tracer concentration reached 50% of the injected concentration after injecting 1 PV of tracer solution.

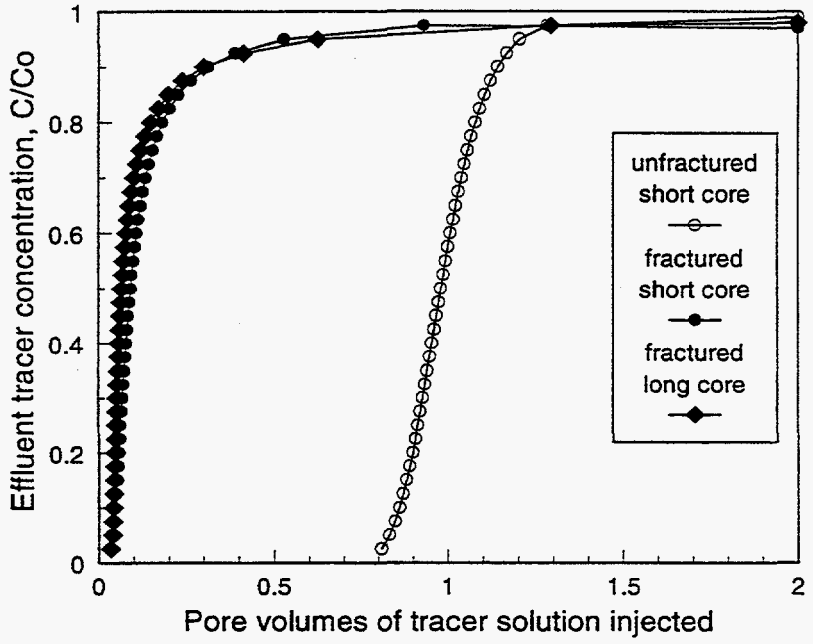

Fig. 27. Tracer results for unfractured and fractured short (14.5-cm or 5.7-inch) and long (115-cm or 3.8-ft) Berea sandstone cores (no gel present).

The solid circles in Fig. 27 show the tracer results from a short (14.5-cm or 5.7-inch) fractured Berea core. For this fractured core, the first tracer was detected in the effluent after injecting 0.032 PV of tracer solution. In contrast, for the unfractured core, the first tracer was detected after injecting 0.8 PV.

The solid diamonds in Fig. 27 show the tracer results from a long (115-cm or 3.8 ft) fractured Berea core. For this fractured core, the first tracer was detected in the effluent after injecting 0.035 PV of tracer solution. Fig. 27 shows that the tracer results were similar for the short and long fractured cores. The average conductivities were about the same for the short and long fractured cores (3.9 and 4.5 darcy-ft, respectively).

Fracture Width, Permeability, and Conductivity. In our work, we routinely use conductivity to characterize fractures. Fracture conductivity ($k_f w_f$) is the product of fracture permeability (k_f) and fracture width (w_f). We report fracture conductivities because they can be determined conveniently and accurately from pressure drops, flow rates, and the Darcy equation.[10] For our experiments to date, fracture conductivities have ranged from 0.75 to 1,860 darcy-ft.

For many people, the flow properties of fractures are understood more readily if a given fracture conductivity is separated into its components of permeability and width. To achieve this separation, one of the components must be measured by an independent method. In concept, fracture width could be measured directly if the fracture faces were smooth and parallel; unfortunately, they usually are neither.

We used results from tracer studies to make an independent estimate of the average width of the fractures in our core experiments. The cores were initially saturated with brine with no tracer. Brine with a potassium iodide tracer was then injected, and the tracer concentration in the effluent was measured spectrophotometrically. Since the flow capacities of our fractures were at least 12 times greater than the flow capacities of the adjacent rock,[13] the first tracer detected in the core effluent gives a good estimate of the fracture volume (V_f). Since the lengths (L_f) and heights (h_f) of our fractures are known accurately, fracture widths can be calculated using Eq. 12.

$$w_f = \frac{V_f}{L_f h_f} \tag{12}$$

By dividing fracture conductivity by fracture width, fracture permeability can be estimated. These calculations were used to generate Fig. 28, which plots fracture width versus fracture permeability for many of our fractured cores. Fracture widths ranged from 0.02 to 0.18 cm (0.008 to 0.071 inches), and the estimated fracture permeabilities ranged from 1,650 to 360,000 darcys.

The solid line in Fig. 28 shows the relation predicted between fracture width and fracture permeability for laminar flow through a slit (parallel plates).[104] The theoretical relation is given by Eq. 13, where w_f is in cm and k_f is in darcys. The predictions match our data reasonably well.

$$k_f = \frac{w_f^2 x 1.013 x 10^8}{12} \tag{13}$$

Eq. 14 provides an alternative form of Eq. 13, where w_f is in inches and $k_f w_f$ is in darcy-ft.

$$w_f = 0.00604(k_f w_f)^{1/3} \quad (14)$$

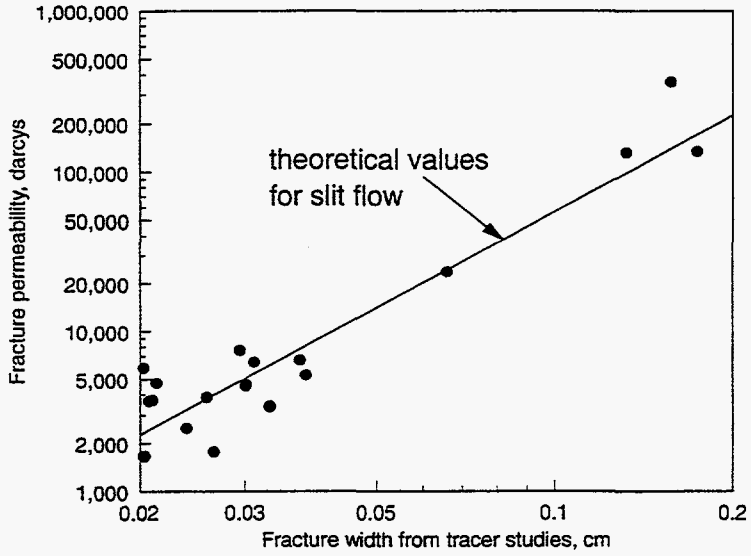

Fig. 28. Fracture permeability versus fracture width.

Fig. 28 or Table 4 can be used to estimate fracture widths and permeabilities from fracture conductivities. The values in Table 4 were calculated using Eq. 14.

Table 4. Fracture Widths and Permeabilities from Eq. 14

$k_f w_f$, darcy-ft	w_f, inches	k_f, darcys
1	0.006	2,000
10	0.013	9,230
100	0.028	42,900
1,000	0.060	200,000
10,000	0.130	923,000

Gel Used. Most experiments described in this chapter used a Cr(III)-acetate-HPAM gel. This gel contained 0.5% HPAM (Allied Colloids Alcoflood 935®, Mw=5×10^6 daltons, degree of hydrolysis: 5-10%), 0.0417% Cr(III)-acetate, and 1% NaCl at pH 6. The gelation time for this formulation was about 5 hours at 105°F.

Resistance Factors Versus Fracture Conductivity

How does the ability of a given gel to extrude through a fracture vary with fracture conductivity? For a Cr(III)-acetate-HPAM gel (composition given above) that was aged 24 hours before injection, Fig. 29 plots pressure gradient or resistance factor in the fracture versus fracture conductivity for 23 experiments where preformed gels were forced through fractures that were typically 15 cm (6 inches) in length. In these experiments, the injection rate was constant at 200 cm^3/hr (12.2 in^3/hr), and at least 50 fracture volumes of gel were injected during the measurement of resistance factors. Fracture conductivities ranged from 1.5 to 700 darcy-ft.

Estimated fracture "permeabilities" ranged from 2,600 to 152,000 darcys.[28] Gel resistance factors averaged about 3,000 for fracture conductivities below 15 darcy-ft (although there was a fair amount of data scatter). Resistance factors increased as fracture conductivities increased above 15 darcy-ft. Pressure gradients were generally inversely proportional to fracture conductivity. At an injection rate of 200 cm^3/hr, pressure gradients varied from 10 to 250 psi/ft for the range of fracture conductivities shown in Fig. 29.

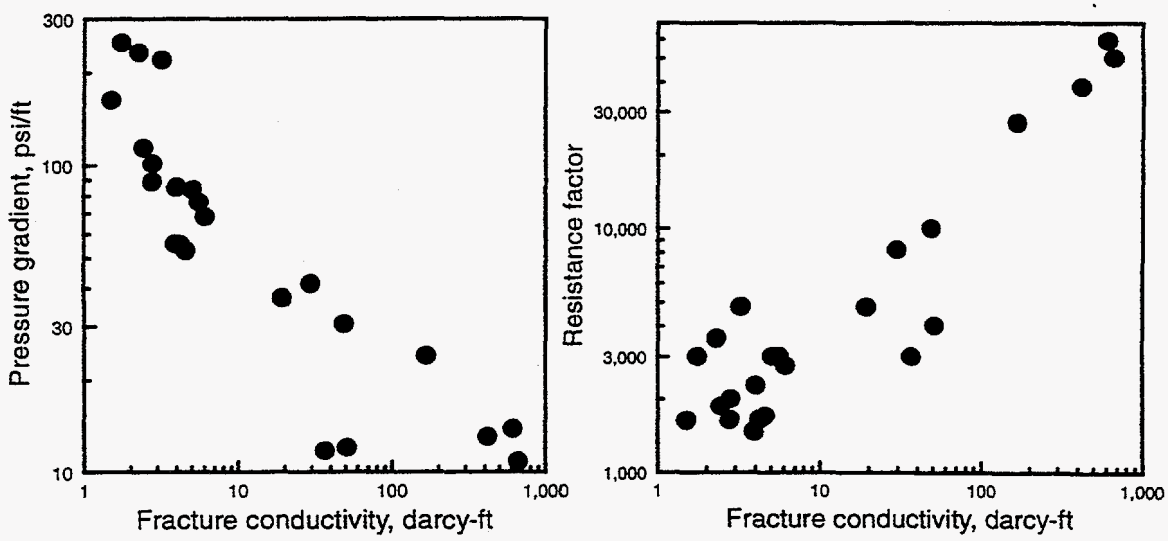

Fig. 29. Gel: 0.5% HPAM, 0.0417% Cr(III)-acetate, 1% NaCl, 105°F, Gel time = 5 hours, 24-hr injection delay, 200 cm^3/hr (12.2 in^3/hr) rate.

Gel Behavior Versus Tube Diameter

The behavior shown in Fig. 29 was counter-intuitive. The gel resistance factors unexpectedly increased with increased fracture conductivity (and therefore, fracture width). To investigate this behavior further, we forced preformed gels (same composition and age as that mentioned above) through tubes of various diameters. The inside diameters of these tubes were 0.009, 0.03, 0.04, 0.079, 0.245, and 0.325 inches (0.023, 0.076, 0.102, 0.201, 0.622, and 0.826 cm, respectively). For comparison, the estimated average fracture widths ranged from 0.0067 to 0.055 inches (0.017 to 0.14 cm) for the core experiments shown in Fig. 29. Except for the 0.03- and 0.325-inch tubes (which were 15 ft in length), our tubes were 3 ft long. The results from these experiments were plotted three different ways (see Figs. 30, 31, and 32). The data scatter associated with the 0.009-, 0.04-, and 0.079-inch tubes resulted during replicate experiments.

Fig. 30 plots pressure gradients versus superficial velocities (fluxes). For most of the tubes, the pressure gradient increased noticeably with increased superficial velocity until about 5,000 ft/d. Above 5,000 ft/d, increased velocity had a much less significant effect on the pressure gradient. This behavior suggests that gel "slip" became important above 5,000 ft/d (i.e., instead of laminar flow, the gel extruded through the tube as a plug, while an apparent discontinuity occurred in the velocity profile at or near the gel-tube interface.) Our observations at high flow rates were consistent with our previous results for gel extrusion through fractures. As mentioned earlier, at high flow rates in fractures, the pressure gradient was almost independent of gel injection rate.[17]

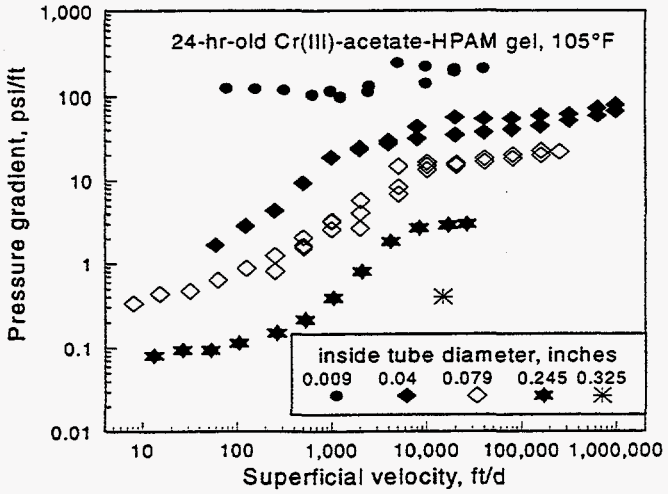

Fig. 30. Pressure gradient versus velocity for gel in tubes.

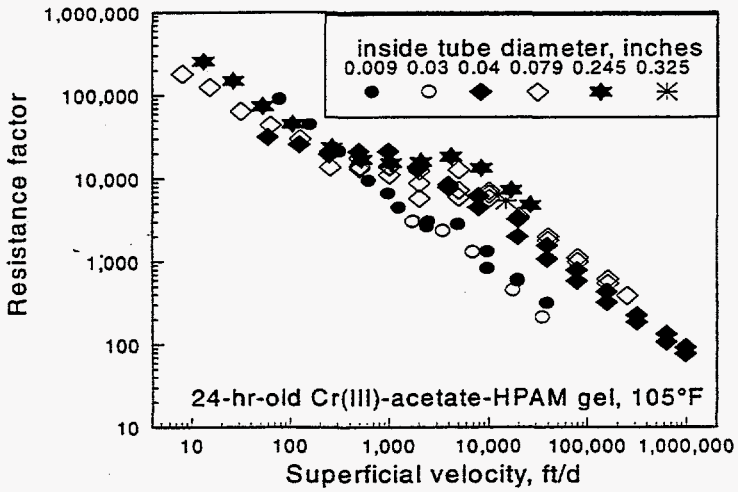

Fig. 31. Resistance factor versus velocity for gel in tubes.

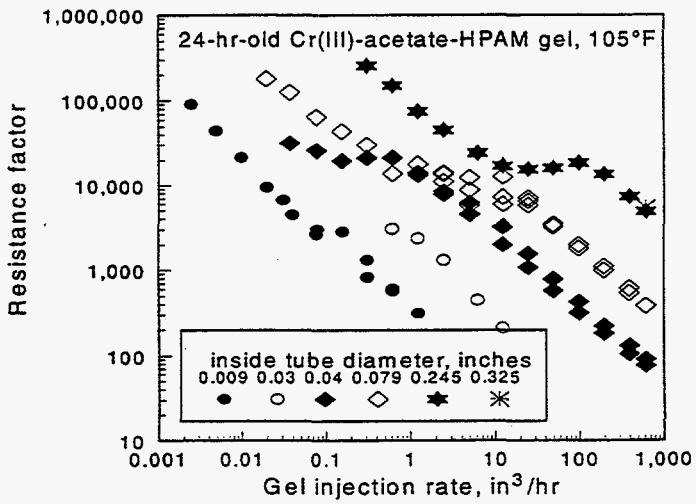

Fig. 32. Resistance factor versus volumetric injection rate for gel in tubes.

At a given velocity in the tubes, the pressure gradient decreased significantly with increased tube diameter. For example, around 20,000 ft/d, the pressure gradients were 208, 57, 16, 3, and 0.4 psi/ft for tube diameters of 0.009, 0.04, 0.079, 0.245, and 0.325 inches, respectively.

Fig. 31 plots resistance factors versus superficial velocities for our tube experiments. At a given velocity, the resistance factor was calculated by dividing the pressure drop during gel injection by the pressure drop during water injection (before gel placement). The pressure drop, Δp, during water injection was calculated using $\Delta p=8q\mu L/(\pi r^4)$, where q was injection rate, μ was water viscosity, L was the tube length, and r was the tube radius.[104]

For tubes with inside diameters of 0.04-, 0.079-, and 0.245-inches, the resistance-factor curves were very similar (Fig. 31). However, these curves separated significantly when the volumetric injection rate was plotted on the x-axis instead of superficial velocity. For our experiments in the tubes, Fig. 32 plots resistance factors versus volumetric injection rates (in in^3/hr). Especially at high volumetric injection rates, the resistance factors increased significantly with increased tube diameter. For example, at a gel injection rate of 98 in^3/hr (1,600 cm^3/hr), the resistance factors were 317, 1,800, and 18,400 for tube diameters of 0.04-, 0.079-, and 0.245-inches, respectively.

The above behavior explains the unexpected result shown in Fig. 29, where gel injection into the fractures occurred at 12.2 in^3/hr (200 cm^3/hr). For a fixed volumetric injection rate, the average gel velocity varies inversely with fracture width. For a shear-thinning material, the resistance factor increased with decreased superficial velocity. Consequently, for a given volumetric injection rate and for moderate to high fracture conductivities, the resistance factor increased with increased fracture width (and conductivity).

Comparison of Tube and Fracture Data

In Fig. 33, we compare resistance factors in tubes with those in fractures. The solid circles in Fig. 33 show the data for the 0.009- and 0.03-inch tubes, which were provided in Fig. 31. The small squares in Fig. 33 represent the remainder of the tube data taken from Fig. 31, for tube diameters ranging from 0.04 to 0.325 inches. The open circles and diamonds in Fig. 33 show data from our floods in fractured cores. Inclusion of the fracture data in Fig. 33 required an ability to estimate average fracture widths. Fracture widths were estimated using Eq. 14.

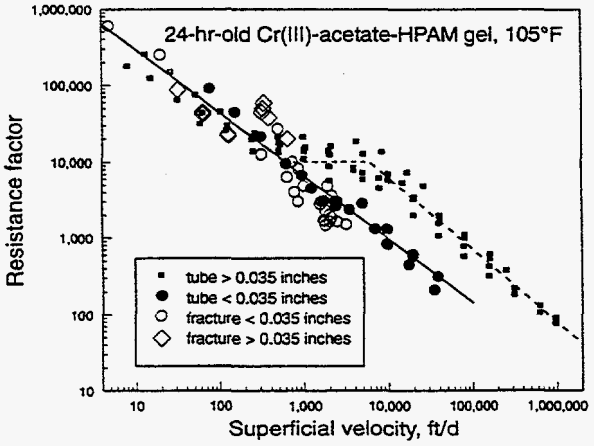

Fig. 33. Comparison of resistance factors in tubes and fractures.

Fig. 33 shows that the fracture data were in reasonable agreement with the tube data. For tubes with diameters less than 0.035 inches or fractures with estimated widths less than 0.035 inches, the resistance factors, F_r, were described fairly well using Eq. 15,

$$F_r = 2x10^6 u^{-0.83} \quad \text{if } w_f < 0.035 \text{ inches,} \tag{15}$$

where u was the superficial velocity in ft/d. The solid line in Fig. 33 illustrates Eq. 15.

For tubes with diameters greater than 0.035 inches (and presumably, for fractures with widths greater than 0.035 inches), the resistance factors were described using Eq. 16.

$$F_r = 2x10^6 u^{-0.83}, \text{ if } u \le 600 \text{ ft/d}$$
$$F_r = 10{,}000, \text{ if } 600 < u < 6{,}200 \text{ ft/d} \tag{16}$$
$$F_r = 4x10^7 u^{-0.95}, \text{ if } u \ge 6{,}200 \text{ ft/d}$$

The dashed curve in Fig. 33 illustrates Eq. 16 for velocities above 600 ft/d. Below 600 ft/d, Eq. 16 predicts the same values as Eq. 15.

The results in Fig. 33 suggest that gel behavior in tubes can parallel that in fractures. In both tubes and fractures, resistance factors correlate with velocity and opening size (fracture width or tube diameter), and at high velocities, the pressure gradient is insensitive to gel velocity. Since experiments are much easier to perform in tubes than in fractures, tube experiments may provide a good way to screen gels and estimate gel behavior in fractures.

Gel Resistance Factors in Longer Fractures

Most of our previous experiments used fractured cores that were fairly short (6 inches or 15 cm). Of course, we are interested in assessing gel propagation through longer fractures. We performed an experiment using a fractured Berea sandstone core that was 3.8 ft (116 cm) in length and 2.25 in^2 (14.5 cm^2) in cross-section (square). Four internal pressure taps were spaced equally along the length of the fracture. The conductivities of the five 9-inch fracture sections of the core were 4.2, 5.1, 5.6, 2.8, and 4.6 darcy-ft. A tracer study performed before gel injection indicated that the volume associated with the fracture was about 0.8 in^3 (13 cm^3). For comparison, the total core pore volume was 22.9 in^3 (375 cm^3).

Using a 24-hr-old Cr(III)-acetate-HPAM gel with the same composition as that mentioned earlier, we forced 67 fracture volumes of gel through the fractured core at a rate of about 1,600 ft/d (12.2 in^3/hr or 200 cm^3/hr). Fig. 34 shows resistance factors in the five core sections as a function of the volume of gel injected. Resistance factors in all core sections were more or less stable after injecting 35 fracture volumes of gel. The magnitude of the stabilized values varied from section to section. In the first and last sections ($k_f w_f$ = 4.2 and 4.6 darcy-ft), the stabilized resistance factors averaged 1,700. In the second and third sections ($k_f w_f$ = 5.1 and 5.6 darcy-ft), values averaged 3,100. In the fourth section ($k_f w_f$ = 2.8 darcy-ft), the stabilized value averaged 2,000. End effects may have been at least partly responsible for the relatively low values observed in the first and last sections.

Interestingly, about 35 fracture volumes of gel were injected before gel was produced from the core. The relatively slow propagation of the gel through the fracture can be seen from the resistance factor data in Fig. 34. This slow rate of gel propagation suggests that the gel was

dehydrated as it extruded through the core—i.e., water from the gel leaked off into the porous rock while the polymer and chromium were left behind in the fracture. This suggestion is consistent with an observation made during a previous experiment[13]—the gel found in a fracture (upon disassembly of the core after the experiment) was significantly more rigid (Sydansk gel code[105]=I) than the gel was before injection (Sydansk gel code=D). In a separate study,[28] we showed that compared to mechanical degradation, gel dehydration had a much greater influence on gel properties during extrusion through relatively short fractures.

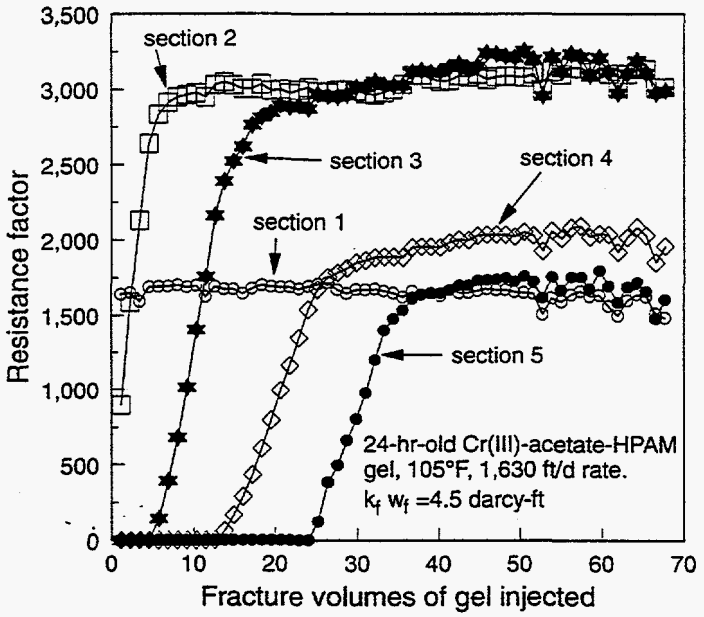

Fig. 34. Resistance factor versus volume of gel injected in a 3.8-ft-long fractured core.

The slow rate of gel propagation through the fracture is consistent with field observations that were reported earlier.[13] In some injection-well treatments, tracer studies were first performed to determine interwell transit times for water. Very rapid transit times were observed, confirming fractures as the cause of the channeling. When a Cr(III)-acetate-HPAM gel was injected, no gel was detected at the offset producers, even though the gel volume was ten times greater than the volume associated with transit of the water tracer between the wells. We note that other factors could also account for the delayed propagation of gels through fractures in field applications.[13] These factors include leakoff of the viscous gelant before gelation, and extrusion of gel into alternate fracture pathways (in naturally fractured systems).

We performed two similar experiments using long fractured cores. These cores were also 3.8 to 4.0 ft in length and 2.25 in^2 in cross-section. Four internal pressure taps were spaced equally along the length of the fracture. The average conductivities of these fractures were 568 darcy-ft and 1,860 darcy-ft. Estimated fracture widths were 0.051 inches and 0.063 inches, respectively, and the estimated fracture permeabilities were 133,000 darcys and 360,000 darcys, respectively. Fracture volumes, determined from tracer studies, were 3.5 in^3 (57 cm^3) and 4.5 in^3 (74 cm^3), respectively. Again, we forced preformed Cr(III)-acetate-HPAM gels through these fractures. The gels were aged at 105°F for either 10 or 24 hours before injection. By observing the effluent

from a given core and the pressures along the core, we monitored the gel front in the fracture during gel injection. Fig. 35 shows the results for experiments in the long fractured cores. The positions of the gel fronts were plotted versus the fracture volumes of gel injected.

The curve without data points in Fig. 35 shows the ideal case expected if gel propagation was not retarded by gel dehydration or other factors. In other words, the fracture would be completely filled with gel after injecting one fracture volume of gel. For the three corefloods, gel transport was retarded to varying degrees, depending on the fracture conductivity and the age of the gel.

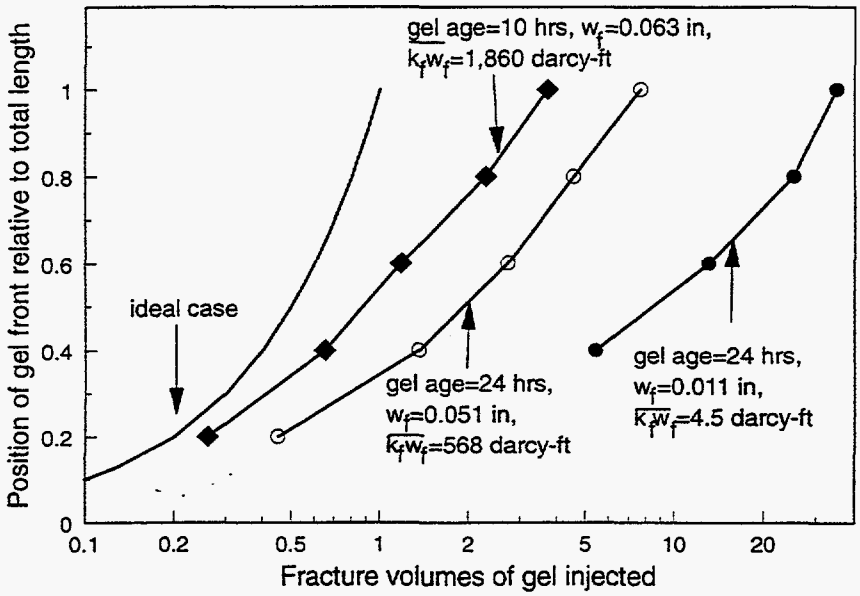

Fig. 35. Gel propagation through fractures (3.8-4.0 ft long).

The greatest retardation occurred for the 24-hr-old gel in the least conductive fracture (average $k_f w_f$=4.5 darcy-ft). In that case, 35 fracture volumes were required for the gel to reach the end of the core (solid circles in Fig. 35). An average pressure gradient of 65.4 psi/ft was required to extrude the gel through this fracture. For comparison, a 24-hr-old gel in a fracture with $k_f w_f$=568 darcy-ft reached the end of the fracture after injecting 7.7 fracture volumes of gel (open circles in Fig. 35). In this case, the average pressure gradient was 10.8 psi/ft during gel injection. For the third coreflood (solid diamonds in Fig. 35), a 10-hr-old gel was extruded through a fracture with $k_f w_f$=1,860 darcy-ft. In this experiment, the gel reached the core outlet after injecting 3.7 fracture volumes of gel, and the average pressure gradient was 9.9 psi/ft.

The results in Fig. 35 indicate that the rate of gel propagation decreased and the degree of gel dehydration increased as fracture conductivity decreased. Of course, for a given injection rate, the pressure gradient increased with decreased fracture conductivity. It seems likely that the level of gel dehydration is closely tied to the pressure gradient experienced by the gel.

Gel Propagation in Tubes

Can gel dehydration and a delay in gel propagation be observed during gel extrusion through tubes, as well as in fractures? Two experiments were performed to answer this question. Both

experiments used tubes that were 15 ft in length with four equally spaced internal pressure taps (making five 3-ft sections). The inside diameters of the two tubes were 0.03 inches and 0.325 inches. In both experiments, we used a Cr(III)-acetate-HPAM gel that was aged 24 hours before injection. In the 0.03-inch tube, gel was injected at a superficial velocity of 34,500 ft/d. The rate of gel propagation was determined by monitoring the effluent and the pressure drops in the five sections of the tube. The gel front reached 20%, 40%, 60%, 80%, and 100% of the tube length after injecting 1.3, 2.9, 3.9, 5.3, and 6.3 tube volumes of gel, respectively. After 11 tube volumes, resistance factors were 210, 176, 155, 130, and 122 for the five tube sections.

Since 6.3 tube volumes of gel injection were required before gel was produced, the gel experienced significant dehydration and delay. For comparison, Fig. 35 shows that 7.7 fracture volumes of gel were injected before gel was produced from the fracture that averaged 0.051 inches in width. Thus, the gel propagation delay factors were comparable in tubes and fractures—at least, when the opening size was from 0.03 to 0.051 inches.

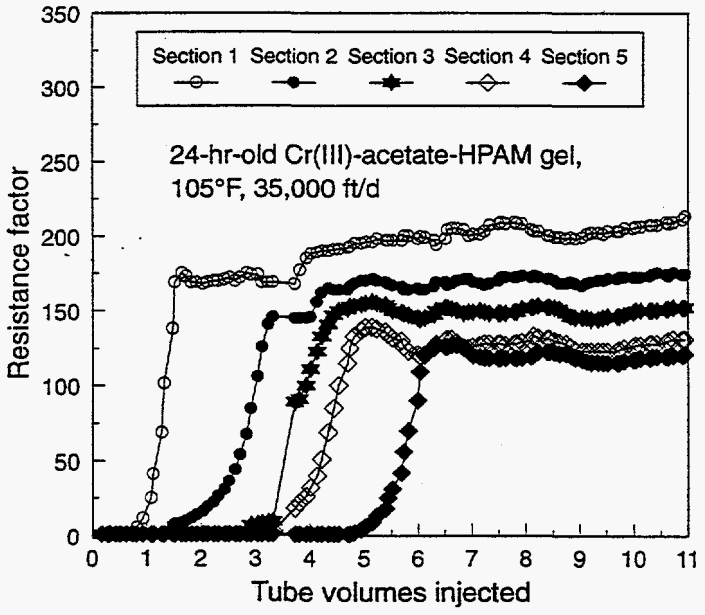

Fig. 36. Extrusion of a 24-hr-old Cr(III)-acetate-HPAM gel through a 0.03-inch-ID, 15-ft-long tube at 35,000 ft/d. 105°F

At least two possible explanations can be offered for the decrease in resistance factor with increased tube length. First, the gel may experience continuous mechanical degradation as it extrudes farther down the tube. This explanation is not consistent with the behavior that we observed in fractures. In 4-ft-long fractures, the resistance factors did not decrease with increased length of penetration along the fracture.[16] One might expect the rough surfaces of fracture faces to cause more mechanical degradation than the smooth surfaces of our tubes.

The second explanation is tied to the gel-dehydration phenomenon. When gel dehydration occurs in fractures, the free water from the dehydration process leaks off into the porous rock, while the crosslinked polymer (or more concentrated gel) remains behind in the fracture. However, when water is expelled from the gel in a tube, it cannot leak off through the tube

walls—it must flow along with the gel. Because water is more mobile than gel, the water may flow more rapidly than the concentrated gel. Thus, in relatively short tubes (perhaps, 20 ft or less), the gel front can propagate much more slowly than the front associated with the water that left the gel. Presumably for the experiment shown in Fig. 36, the first water that left the gel arrived at the tube outlet after injecting about 1 tube volume of gel, while the gel front required 6.3 tube volumes to reach the tube outlet. However, once the tube was filled with gel, the water that left the gel in the first tube section must flow along with the gel in the subsequent sections. If the gel dehydrates to a greater degree in each subsequent tube section, more free water becomes available, so the resistance factors decrease with increased length along the tube. This effect will be discussed further when we discuss gel propagation through 100-ft-long tubes.

A similar experiment was performed using the 15-ft tube with an inside diameter of 0.325 inches. In this experiment, the gel arrived at the tube outlet after injecting 1 tube volume of gel. In other words, the gel experienced no dehydration or delay in the tube. This result suggests that gels may not experience dehydration or delay when extruding through tubes or fractures with opening sizes of at least 0.325 inches.

Effect of Velocity on Gel Propagation Through Tubes

Because gel-extrusion experiments are much easier to perform in tubes than in fractures, we hope that results from tube experiments can quickly provide valuable insights into gel behavior in fractures. Therefore, we conducted a number of experiments to examine the impact of extrusion velocity, tube diameter, gel age, and tube length on the behavior of a Cr(III)-acetate-HPAM gel in 6-ft-long tubes. Each tube had one internal pressure tap that divided the tube into two 3-ft-long sections. The following figures and tables show gel breakthrough values, pressure gradients, and resistance factors during various experiments. The breakthrough values indicate the apparent number of tube volumes required to fill a given tube section with gel. The pressure gradients indicate the average psi/ft in a given section once that section was filled with gel.

In Fig. 36, the extrusion rate was fixed at 35,000 ft/d. What range of velocities are expected during flow through fractures in field applications? This question is addressed in Fig. 37. In wells with fractures, injection rates are typically in the range from 1 to 100 BPD/ft of net pay. If a vertical fracture has two wings of fixed height and the effective average fracture width is known, straight-forward calculations can provide the average superficial velocity in the fracture. Fig. 37 suggests that superficial velocities in fractures typically range from 100 to 100,000 ft/d.

Fig. 38 illustrates the effect of velocity on propagation delays for a 24-hr-old Cr(III)-acetate-HPAM gel as it extrudes through a 0.03-inch-ID, 6-ft-long tube. Experiments were performed using superficial velocities of 350, 3,500, and 35,000 ft/d. By monitoring the pressure gradients and tube effluent, gel breakthrough values can be determined in the two tube sections. Note that significant pressure fluctuations can occur even after the tubes are filled with gel. Apparently, temporary gel plugs or "screen-outs" occur in the tube, thus causing the pressure gradient to increase temporarily. When the pressure gradient becomes too high, the gel plug breaks and the pressure gradient drops until a new gel plug forms.

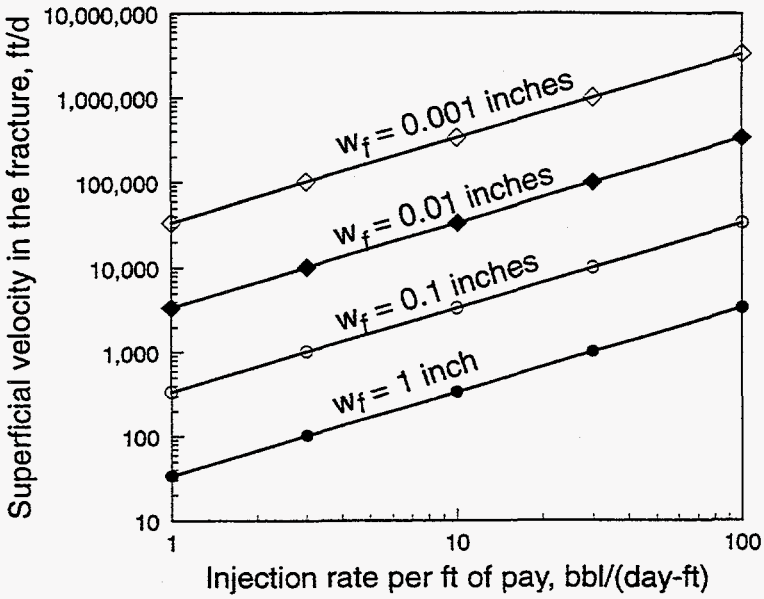

Fig. 37. Velocities in a two-wing fracture.

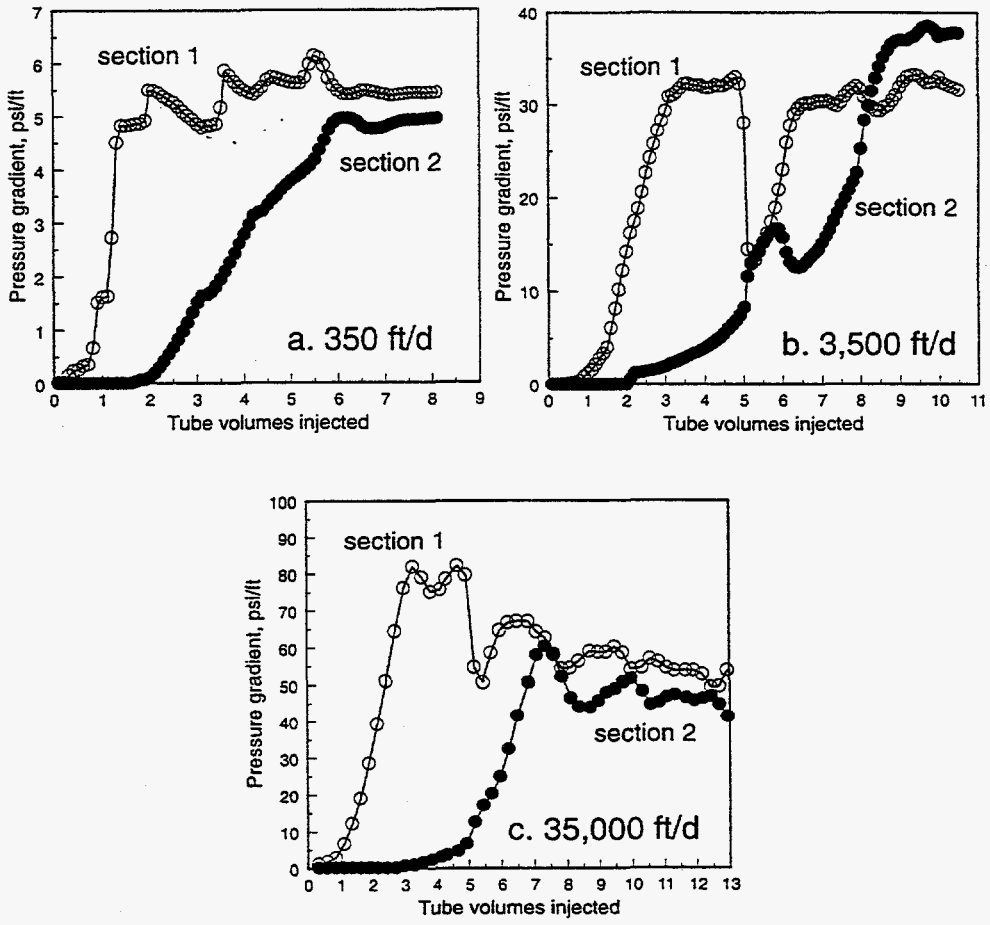

Fig. 38. Effect of velocity on extrusion of a 24-hr-old Cr(III)-acetate-HPAM gel through a 0.03-inch-ID, 6-ft-long tube.

Table 5 summarizes the results illustrated in Fig. 38. For the three superficial velocities, this table indicates that 2.2 to 3.0 tube volumes of gel were required to achieve gel breakthrough in Section 1, while 5.9 to 6.8 tube volumes were required to achieve gel breakthrough in Section 2. Thus, propagation of gel through this tube was delayed by a factor of about 6, independent of extrusion velocity. This result was somewhat surprising since we expected greater dehydration of the gel to occur when higher pressure gradients were applied. Note that the pressure gradients (average values when both tube sections were filled with gel) were 4.7-5.4 psi/ft at 350 ft/d, 28.3-29.3 psi/ft at 3,500 ft/d, and 48.4-61.5 psi/ft at 35,000 ft/d.

Table 5. Effect of Velocity on Gel Extrusion of a 24-hr-old Cr(III)-Acetate-HPAM Gel Through a 0.03-inch-ID, 6-ft-long Tube. 105°F

Superficial velocity, ft/d:	350	3,500	35,000
Breakthrough in Section 1, tube volumes	2.2	3.0	2.4
Breakthrough in Section 2, tube volumes	5.9	6.2	6.8
Resistance factor in Section 1	2,680	1,445	303
Resistance factor in Section 2	2,320	1,396	239
Pressure gradient in Section 1, psi/ft	5.4	29.3	61.5
Pressure gradient in Section 2, psi/ft	4.7	28.3	48.4

Some uncertainty exists about the breakthrough values for these short, small-diameter tubes. The total volume in a 0.03-inch-ID, 6-ft-long tube is only 0.051 in^3 or 0.83 cm^3. When injecting a 0.5% HPAM solution (20 cp, no crosslinker), the breakthrough in Section 2 was about 3 tube volumes. We expected breakthrough in 1 tube volume. We suspect that the compressibility of the system (i.e., from the transducers and fluid in the transducer lines) was at least partly responsible for the delayed breakthrough. Certainly, additional work is needed to remove this artifact. An obvious method to remove the artifact involves using longer, larger-volume tubes. However, as will be noted later, this approach introduces other complications. Until this artifact is minimized or eliminated, we must admit that the uncertainty for the breakthrough values associated with this tube may be plus-or-minus 2-3 tube volumes. For the same tube length, this uncertainty will be greater for smaller-diameter tubes and less for greater-diameter tubes.

Effect of Tube Inside Diameter (ID) on Gel Propagation Through Tubes

We performed several experiments where 24-hr-old Cr(III)-acetate-HPAM gels were extruded through tubes of various diameters, ranging from 0.009 to 0.325 inches. All of these tubes were 6 ft long, the superficial velocity was fixed at 35,000 ft/d, and the temperature was 105°F. The results from these experiments are summarized in Table 6, while Fig. 39 plots pressure gradients versus tube volumes injected for 4 of the 6 experiments. As expected, the delay in gel propagation (breakthrough) increased with decreased tube diameter. This trend is qualitatively consistent with the behavior that we observed in fractured cores (Fig. 35). For tube diameters of at least 0.245 inches, no delay in breakthrough was observed. This result suggests that this gel would not experience dehydration or delay in fractures with widths of at least 0.245 inches. When the tubes were completely filled with gel, for a velocity of 35,000 ft/d, the average pressure gradients increased with decreased tube diameter. This behavior was expected. We also noted that the pressure fluctuations became much smaller in tubes with the largest diameters.

Table 6. Effect of Tube Inside Diameter on Gel Extrusion of a 24-hr-old Cr(III)-Acetate-HPAM Gel Through a 6-ft-long tube at 35,000 ft/d. 105°F

	Breakthrough, tube volumes		Pressure gradient, psi/ft	
Tube ID, inches	Section 1	Section 2	Section 1	Section 2
0.009	33	64	123	71.4
0.03	2.4	6.8	61.5	48.4
0.04	1.3	3.4	28.0	26.5
0.079	0.8	1.8	16.4	16.1
0.245	0.5	1.0	1.9	2.0
0.325	0.5	1.0	0.4	0.4

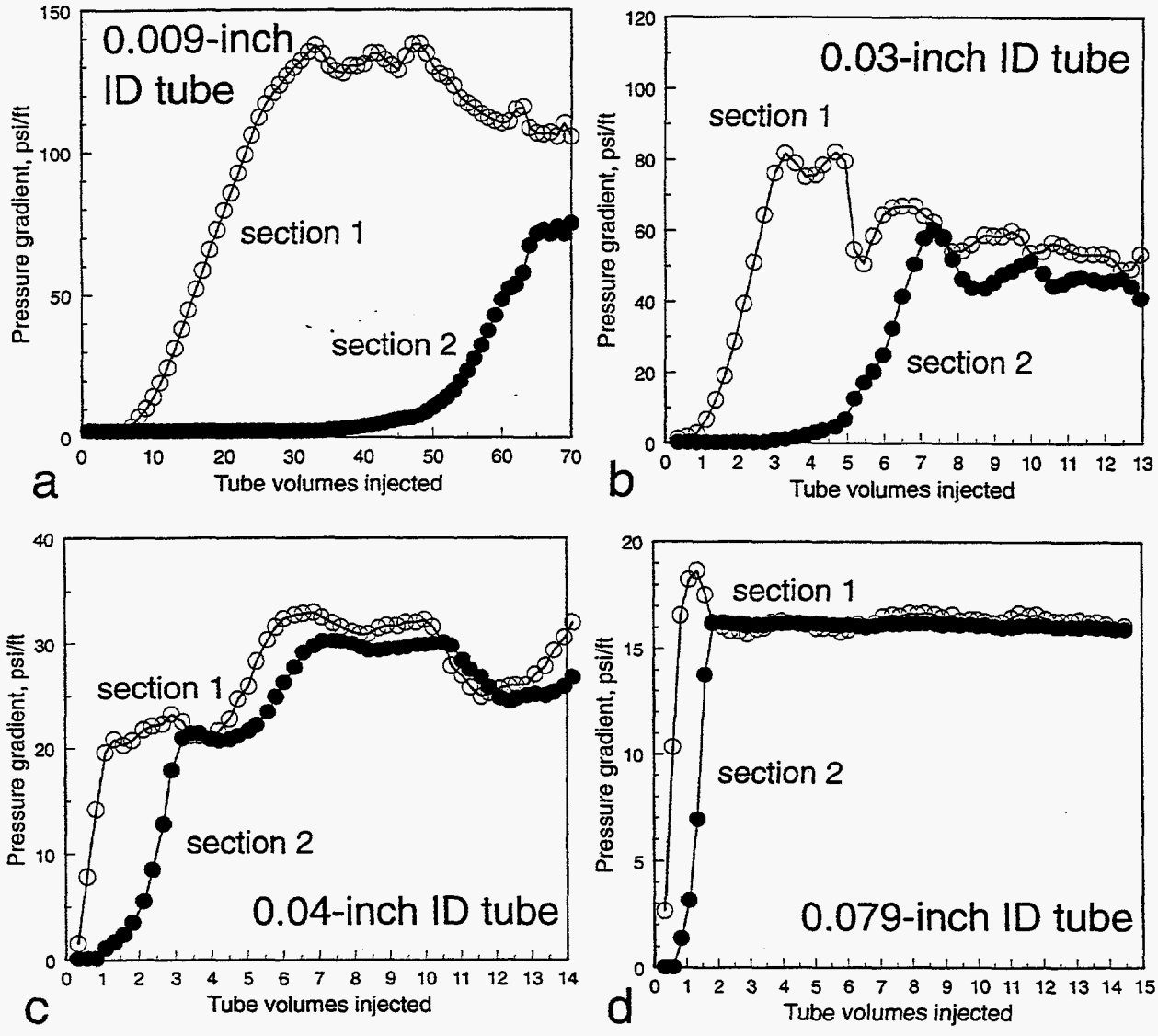

Fig. 39. Effect of tube inside diameter (ID) on extrusion of a 24-hr-old Cr(III)-acetate-HPAM gel through 6-ft-long tubes at 35,000 ft/d. 105°F.

Effect of Gel Age on Gel Propagation Through Fractures and Tubes

Most of our previous experiments used gels that were aged for 24 hours before injection. Therefore, we were interested in how gel performance varies with the age of the gel (or the gel "curing" time). We performed an experiment where a fractured core (6 inches or 15 cm long) and a single batch of gel were used. The conductivity of the fracture in this core (Core 32) was 2.8 darcy-ft. (The effective average fracture width was 0.0085 inches or 0.022 cm.) A large volume of Cr(III)-acetate-HPAM gel (same composition as that used previously) was prepared and placed in a transfer vessel between an ISCO pump and the fractured core. At predetermined times, 60 fracture volumes (60 cm^3 or 3.7 in^3) of this gel were injected into the fractured core using a constant rate of 12.2 in^3/hr or 200 cm^3/hr. (The average superficial velocity in the fracture was 2,050 ft/d.) The injection delays (time since the gelant was prepared) ranged from 5 to 240 hours. Fig. 40 shows the resistance factors and pressure gradients that were observed during the experiment. Recall that the gelation time for this formulation was about 5 hours at 105°F. Resistance factors increased rapidly between 5 and 24 hours after gelant preparation. Thereafter, the resistance factors increased more gradually until a value of 16,240 was reached 240 hours (10 days) after gelant preparation.

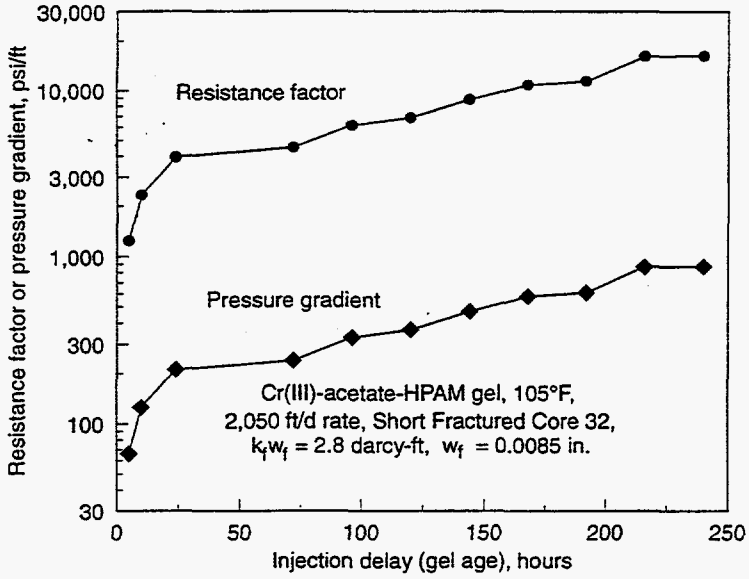

Fig. 40. Effect of gel age on extrusion of gel through a fracture.

We performed an analogous experiment where Cr(III)-acetate-HPAM gels with various ages were extruded through 0.03-inch-ID, 6-ft-long tubes. Fig. 41 provides the detail for the plots of pressure gradient versus tube volumes injected, while Table 7 summarizes the results from these experiments. Surprisingly, the delay in gel propagation was about the same (~6 tube volumes for breakthrough) for gel ages between 5 and 240 hours. We expected breakthrough to increase with increased gel age and rigidity. Table 7 also lists average pressure gradients and standard deviations when Sections 1 and 2 of the tubes were filled with gel. In qualitative agreement with Fig. 40, the most pronounced increase in pressure gradient occurred for gel ages between 5

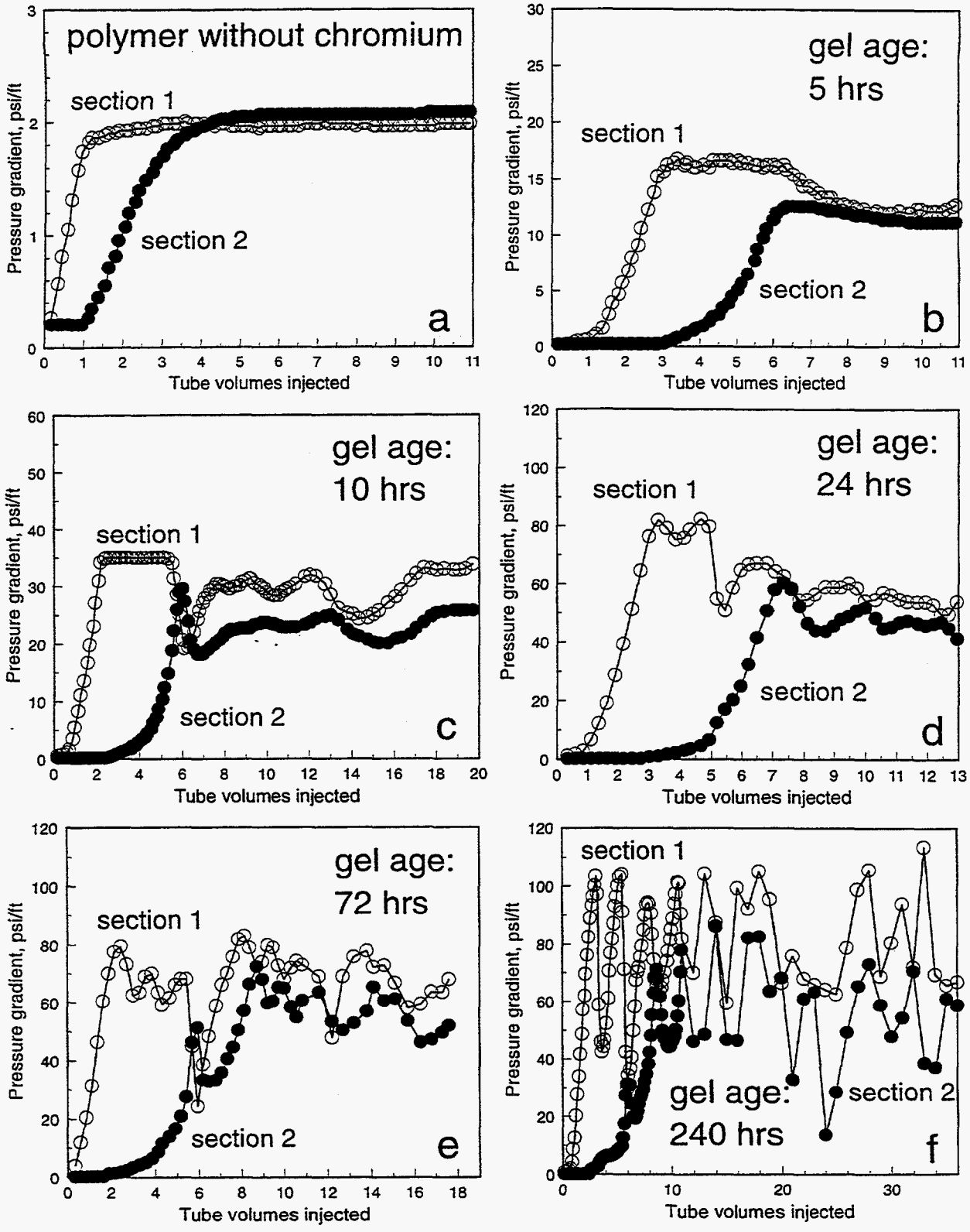

Fig. 41. Effect of gel age on gel extrusion of Cr(III)-acetate-HPAM gels through a 0.03-inch-ID, 6-ft-long tube at 35,000 ft/d. 105°F.

and 24 hours. After 24 hours, the increase in pressure gradient was more moderate with increased gel age. Between 24 and 240 hours, the pressure gradient in the tube experienced a 24% increase in Section 1 and no significant increase in Section 2. In the fracture (Fig. 40), the pressure gradient experienced a 3-fold increase between gel ages of 24 and 240 hours. However, two differences between the tube and fracture experiments could cause the quantitative differences in the behavior. First, the average superficial velocities were 2,050 ft/d for the fracture experiment and 35,000 for the tube experiments. Second, the average width was 0.0085 inches for the fracture, while the inside diameter was 0.03 inches for the tube experiments.

Table 7. Effect of Gel Age on Gel Extrusion of a Cr(III)-Acetate-HPAM Gel Through a 0.03-inch-ID, 6-ft-long tube at 35,000 ft/d. 105°F

	Breakthrough, tube volumes		Pressure gradient, psi/ft	
Gel age, days	Section 1	Section 2	Section 1	Section 2
5	2.4	5.8	14.3±1.9	11.7±0.6
10	1.9	5.5	30.5±4.0	22.7±2.4
24	2.4	6.8	61.5±9.8	48.4±4.8
72	2.0	6.3	67.1±11.4	52.9±11.2
240	3.0	5.8	76.3±19.3	47.7±18.0

Comparison of Different Gels

In addition to the Cr(III)-acetate-HPAM gel, we also examined several other gels in tubes and fractures. These gels included (1) resorcinol-formaldehyde (3% resorcinol, 3% formaldehyde, 1% KCl, 0.1% $CaCl_2$, pH 9), (2) Cr(III)-xanthan (0.4% Pfizer Flocon 4800 xanthan, 0.047% $CrCl_3$, 0.5% KCl, pH 4), (3) Cr(VI)-redox-PAM/AMPS (0.3% Drilling Specialties HE-100 PAM/AMPS, 0.15% $Na_2S_2O_3$, 0.05% $Na_2Cr_2O_7$, 2% KCl, pH 5), and (4) HQ-HMT-HPAM (0.1% hydroquinone, 0.25% hexamethylenetetramine, 0.5445% Allied Colloids 935 HPAM, 1% $NaHCO_3$, pH 8.2, aged for 24 hours at 230°F, then quenched).

Fig. 42 shows the detailed plots of pressure gradient versus tube volumes injected for these gels. Table 8 lists these gels in decreasing order of rigidity. The second column in Table 8 lists the Sydansk gel code[105]—Code J indicates a ringing rigid gel, while Code D indicates a moderately flowing gel. The third and fourth columns in Table 8 lists propagation delay factors in 0.03-inch-ID, 6-ft-long tubes. For example, for the resorcinol-formaldehyde gel, 4.8 tube volumes of gel were injected before gel was produced from the tube. The fifth and sixth columns list the pressure gradients and the stability of the pressure measurements during gel injection. The most rigid gel, resorcinol-formaldehyde, experienced the highest average pressure gradients (108 psi/ft in the first tube section), and the pressure measurements were erratic, indicating the sporadic formation and breakage of gel plugs in the tube. The Cr(III)-xanthan gel also showed erratic pressure behavior (especially in Section 1). The other three gels showed stable pressure behavior as the gels were extruded through the tubes. Except for the resorcinol-formaldehyde gel, we were surprised that the pressure gradients did not correlate with gel rigidity or propagation delay factor. We expected that pressure gradients and propagation delay factors would increase with increased gel rigidity. More work will be needed to understand the differences that we see.

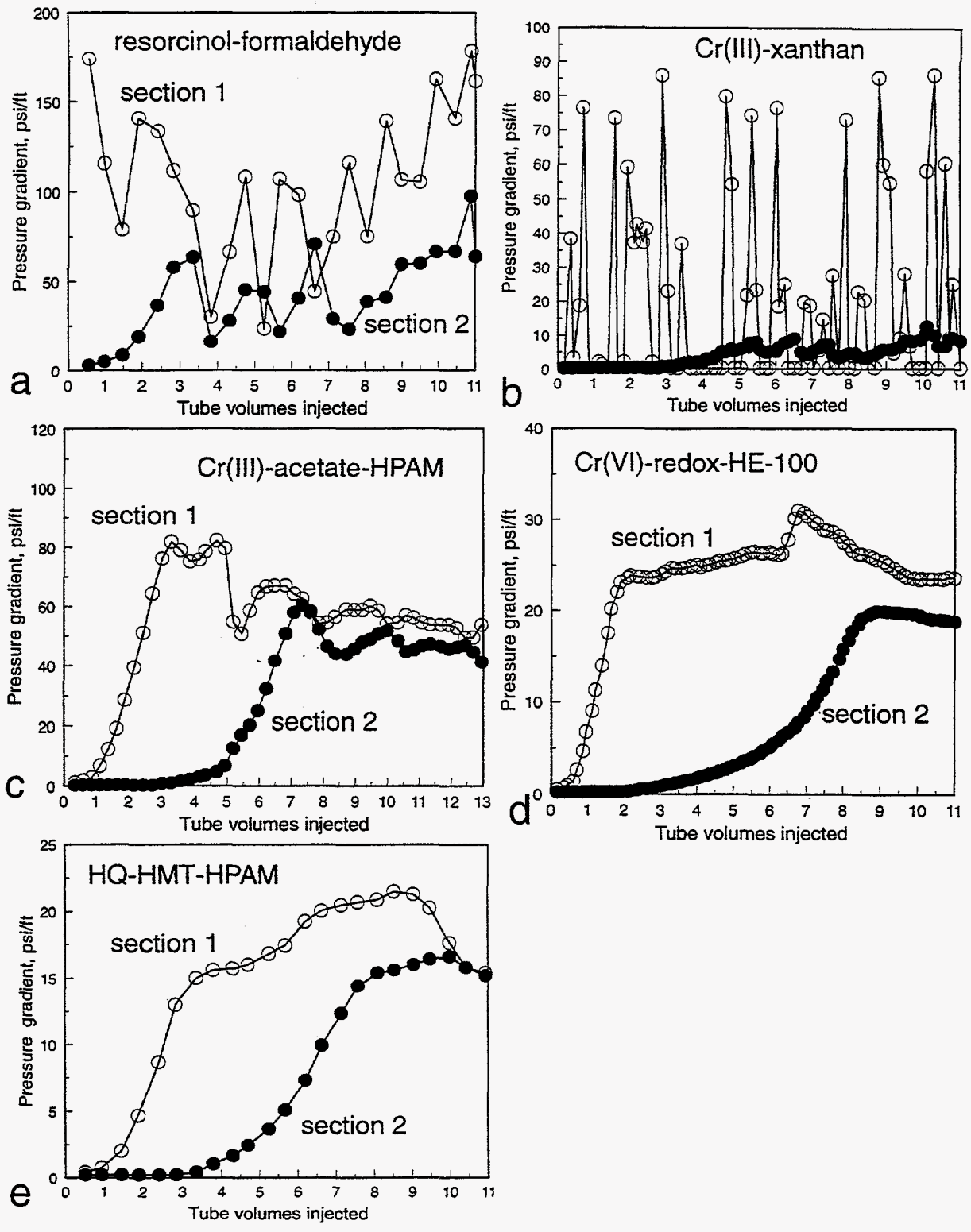

Fig. 42. Extrusion of 24-hr-old gels through 0.03-inch-ID, 6-ft-long tubes at 35,000 ft/d. 105°F.

Table 8. Extrusion of 24-hr-old Gels Through 0.03-inch-ID, 6-ft-long tubes at 35,000 ft/d. 105°F

Gel	Sydansk gel code	Breakthrough, tube volumes		Pressure gradient, psi/ft	
		Section 1	Section 2	Section 1	Section 2
resorcinol-formaldehyde	J	1.0	4.8	108±42.5	49.1±20.9
Cr(III)-xanthan	H-I	4.5	9.6	20.5±27.2	6.4±2.1
Cr(VI)-redox-HE-100	G	1.8	4 to 9	25.6±2.1	19.4±0.5
Cr(III)-acetate-HPAM	E	2.4	6.8	61.5±9.8	48.4±4.8
HQ-HMT-HPAM	D	3.3	7.6	18.4±2.3	15.9±0.5

For comparison, Table 9 lists results from analogous experiments where preformed gels were extruded through 6-inch-long fractured cores instead of tubes.[13]

Table 9. Extrusion of 24-hr-old Gels Through 6-inch-long Fractures at ~2,000 ft/d. 105°F

Gel	Estimated fracture width, inches	Pressure gradient, psi/ft	Pressure behavior
resorcinol-formaldehyde	0.0112	>830	plugged
Cr(III)-xanthan	0.0064	250	erratic
Cr(VI)-redox-HE-100	0.0078	290	stable
Cr(III)-acetate-HPAM	0.0073	250	stable
HQ-HMT-HPAM	0.0115	48	stable

Column 2 in Table 9 lists the average fracture width for each case (calculated using Eq. 14 and fracture conductivity data). The average fracture width was 0.0088 inches (0.022 cm). Thus, the average fracture width was less than one-third the inside tube diameters for the previous experiment. Not surprisingly, the pressure gradients during gel extrusion through the fractures were substantially greater than those in the tubes (Column 3 of Table 9). The last column of Table 9 indicates that the resorcinol-formaldehyde gel plugged the fracture (pressure gradients increased rapidly and continuously). For the other four gels, the pressure behavior was similar to that observed in tubes—erratic pressure drops were noted for the Cr(III)-xanthan gel, but stable pressures were seen for the other three gels. We are not suggesting that one gel is necessarily better than another. Presumably, the performance of all of these gels could be altered by adjusting chemical concentrations.

Fig. 43 plots pressure gradient versus superficial velocity for four of the 24-hr-old gels in 0.03-inch-ID, 6-ft-long tubes. Three of the gels showed qualitatively similar behavior—with pressure gradients, perhaps, approaching constant values at low and/or high superficial velocities. For the resorcinol-formaldehyde gel, severe plugging occurred at velocities below 10,000 ft/d, so limited data were collected.

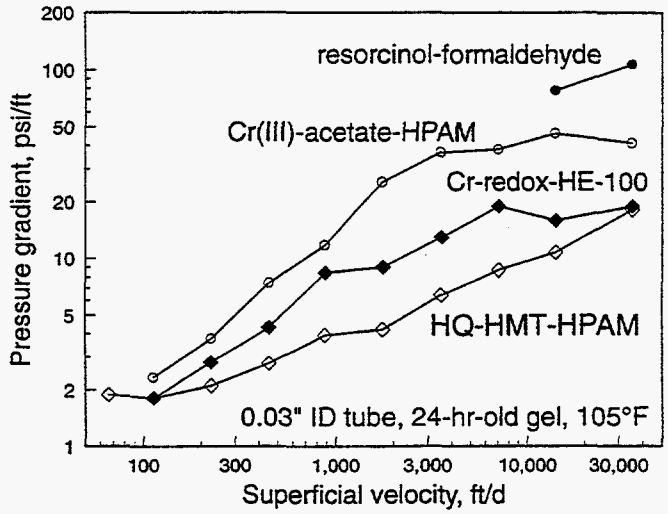

Fig. 43. Pressure gradient versus velocity for four 24-hr-old gels in 0.03-inch-ID, 6-ft-long tubes.

Effect of Length on Gel Propagation Through Tubes

Our experiments to date used relatively short tubes (3 to 15 ft) and fractured cores (0.5 to 4 ft). Since fractures in field applications are typically more than 100 ft in length, we wish to determine gel properties as a function of fracture length. Unfortunately, creating very long fractures is difficult in the laboratory. However, long tubes are readily available. If we find a satisfactory relation between the behavior of gels in fractures versus tubes, we hope that gel-extrusion experiments in long tubes will indicate the performance of gels in long fractures.

We performed several experiments in a 0.03-inch-ID, 100-ft-long tube. The tube had four equally spaced internal pressure taps that divided the tube into five 20-ft sections. The total tube volume was 0.85 in^3 or 13.9 cm^3. Fig. 44 plots resistance factors and pressure gradients observed in each of the five 20-ft sections as a function of tube volumes of gel injected at 35,000 ft/d.

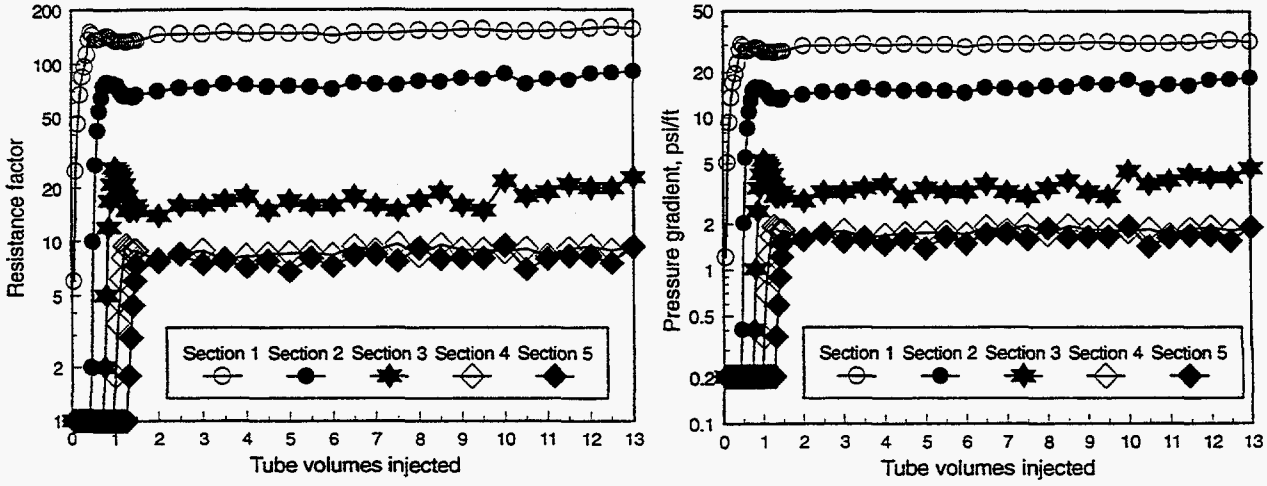

Fig. 44. Extrusion of a 24-hr-old Cr(III)-acetate-HPAM gel through a 100-ft-long, 0.03-inch-ID tube at 35,000 ft/d. 105°F.

We noted that the gel arrived at the tube outlet after injecting only 1.3 tube volumes, instead of 6 tube volumes, as observed in the 6-ft and 15-ft tubes (Figs. 36 and 38). As mentioned during the discussion of Fig. 36, we suspect that in the 6-ft and 15-ft tubes, the water expelled from the gel flowed ahead of the less-mobile gel—allowing the water front to flow about 6 times faster than the gel front. However, in the 100-ft tube, the water that was expelled from the gel had insufficient opportunity to flow ahead of the gel. Instead, it was forced to mix and form a dispersion with the gel.

After injecting two tube volumes of gel, the pressure gradients in the five tube sections averaged 29.2, 15.3, 3.7, 1.8, and 1.6 psi/ft, respectively, while the resistance factors averaged 144, 75.6, 18.2, 8.9, and 8.0, respectively. Thus, the gel apparently experienced severe degradation during extrusion through the 100-ft-long tube. As mentioned during the discussion of Fig. 36, two explanations could account for this behavior. First, the gel could experience continuous mechanical degradation as it extrudes farther down the tube. Second, water expelled from the gel during the gel-dehydration process could lubricate the flow of gel in the down-stream sections of the tube. Since the ratio of free water to gel increases with increased tube length, the resistance factor decreases with increasing tube length.

If the second mechanism mentioned above is correct, gel extrusion experiments in long tubes are not representative of gel extrusion through long fractures. In fractures, water that leaves the gel can leak off into the porous rock, leaving the concentrated gel behind to extrude through the fracture. However, in tubes, water that is expelled from the gel must flow along with the more concentrated gel. If the dehydration effect occurs soon after the gel enters a tube and if the free water could be removed early in the extrusion process, perhaps, the gel behavior in the tube may satisfactorily imitate that in a fracture. To test this idea, we repeated the extrusion experiment with the 0.03-inch-ID, 100-ft-long tube, except that a 0.5 μm steel filter was placed at the end of each of the first three internal pressure taps. These filters did not interfere with gel flow through the tube, but they allowed free water to leave the tube at these points. During extrusion of 10 tube volumes (139 cm^3) of 24-hr-old Cr(III)-acetate-HPAM gel through the tube at 35,000 ft/d, the volumes of filtrate collected at the first (20-ft), second (40-ft), and third (60-ft) taps were only 3.2 cm^3, 2.6 cm^3, and 2.7 cm^3, respectively. Thus, only about 2% of the total throughput left the tube at each of the three filters. If the gel was dehydrated by a factor of 6 (as suggested by Figs. 36 and 38), our filters were very ineffective at removing the free water from the tube.

Analysis of the three filtrates revealed HPAM concentrations of 68 ppm (C/C_o=1.4%), 190 ppm (C/C_o=3.8%), and 380 ppm (C/C_o=7.6%), respectively. These results suggest that very little polymer passed through the filters. However, since the polymer concentrations in the filtrates increased with increased length along the tube, perhaps, mechanical degradation of the polymer and gel was important as they flowed through the tube.

Analysis of the filtrates also revealed chromium concentrations of 13.3 ppm (C/C_o=14.1%), 14.4 ppm (C/C_o=15.2%), and 10.5 ppm (C/C_o=11.1%), respectively. Thus, the free water contained about the same level of chromium, regardless of the distance along the tube.

Table 10 compares the resistance factors in the five tube sections for this experiment with those from the previous experiment. For a given tube section, the resistance factors were about the same for both experiments. This result also indicates that our filters were ineffective at removing free water from the tube.

Table 10. Extrusion of 24-hr-old Cr(III)-Acetate-HPAM Gels Through 0.03-inch-ID, 100-ft-long Tubes. 105°F

	Resistance factor				
Experiment	Section 1	Section 2	Section 3	Section 4	Section 5
No filters	144	75.6	18.2	8.9	8.0
0.5 μm filters at 20, 40, and 60 ft	135	62.1	11.1	7.2	6.3
2.5-inch Berea sandstone core with 0.04-inch hole at tube inlet	134	62.2	12.3	8.9	7.9

We performed another experiment where a 650-md Berea core with a 0.04-inch-ID hole was mounted at the inlet of a 0.03-inch-ID, 100-ft-long tube (see Fig. 45). The core was 1.4 inches (3.6 cm) in diameter and 2.5 inches (6.37 cm) in length, with a pore volume of 0.836 in^3 (13.7 cm^3). A 0.04-inch-ID hole was drilled axially through the center of the core. The outlet from the 0.04-inch-ID hole led directly into a 0.03-inch-ID, 100-ft-long tube. The core was cast in epoxy so that gel could be forced through the 0.04-inch-ID hole and the 100-ft-long tube in series. A tap was drilled to penetrate a short distance into the porous rock, so that leakoff fluid could drain from the core. Thus, the core acted as a tangential filter to remove water that emanated from the gel during the first part of the flow path. As with all of our experiments, the tube and core were saturated with water at the beginning of the gel experiment.

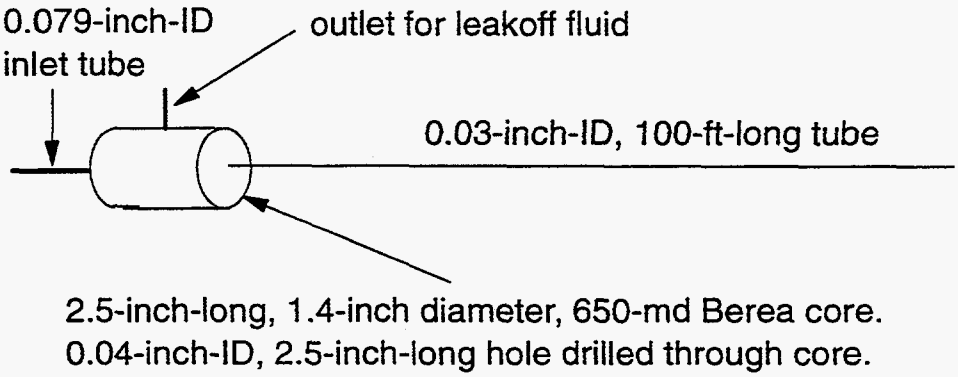

Fig. 45. Schematic of the core-tube experiment.

Fifteen tube volumes of a 24-hr-old Cr(III)-acetate-HPAM gel were forced through this core and tube using the same rate used in the previous experiments (35,000 ft/d in the 0.03-inch-ID tube). The third data row of Table 10 lists the average resistance factors observed in the five sections of the 0.03-inch-ID, 100-ft-long tube. Table 10 shows that the behavior observed during this experiment was not significantly different from that seen during the two previous experiments.

Fig. 46 plots the volume of leakoff fluid produced from the core versus the total volume of gel injected. The slopes of the first and second parts of the plot in Fig. 46 were 0.43 and 0.039, respectively. Fig. 47 replots the data from Fig. 46 using the common method used to evaluate fluid-loss additives for hydraulic fracturing. Fig. 47 plots the leakoff (in gallons per ft^2 of rock surface area) versus the square root of the injection time (in $min^{1/2}$). The intercept from this plot gives a "spurt loss" of 1.68 gal/ft^2, while the slope from the plot gives a "leakoff coefficient" of 0.0258 $ft/(min)^{1/2}$. A total of 26.5 cm^3 of leakoff fluid was collected during injection of 206 cm^3 (15 tube volumes) of gel. Analysis of the leakoff fluid revealed that the first 12 cm^3 contained 100-ppm HPAM and 12-ppm chromium, while the next 12 cm^3 contained 100-ppm HPAM and 26-ppm chromium.

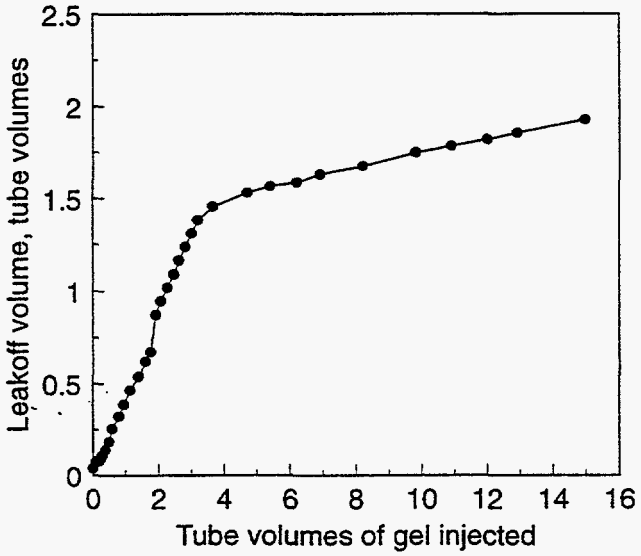

Fig. 46. Fluid leakoff volume versus volume of Cr(III)-acetate-HPAM gel injected for experiment shown in Fig. 45.

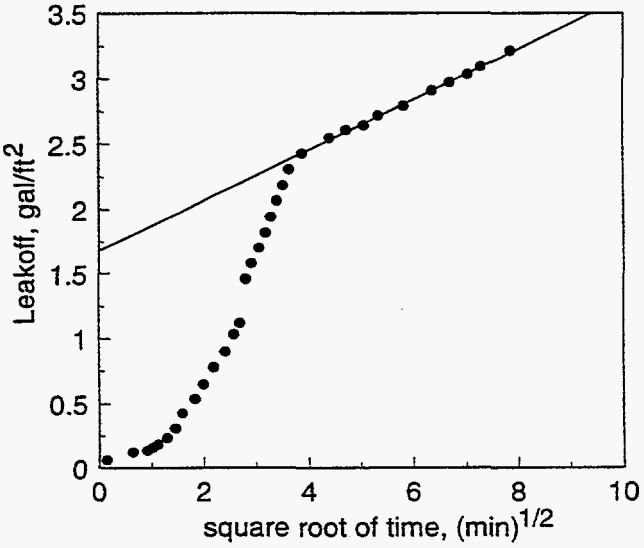

Fig. 47. Replot of Fig. 46 using a common fluid-loss plot.

Recycling Experiments

We performed several experiments where a 24-hr-old Cr(III)-acetate-HPAM gel was recycled through a 0.03-inch-ID, 15-ft-long tube at 35,000 ft/d. (No cores or filters were placed in line during these experiments.) Table 11 summarizes the results. In the first cycle, 200 tube volumes (450 cm^3) of gel were injected. Resistance factors ranged from 198 in the first tube section to 116 in the fifth tube section. (Table 11 also lists standard deviations associated with the resistance factors to give an idea of the fluctuations that occurred.) The effluent from the first cycle was reinjected into the same tube at the same rate. The second data row in Table 11 shows that during the second cycle of gel injection, resistance factors ranged from 92.2 in Section 1 to 73.9 in Section 5. Thus, the resistance factors decreased monotonically with increased distance through the tube. Fluctuations in the resistance factors were greater during the second cycle than during the first cycle (i.e., the standard deviations were typically ± 5% during the first cycle but ± 20% during the second cycle). This result probably occurred because the gelant injected during the first cycle was homogeneous, but during the second cycle, the injectant consisted of gel and free water that separated during the first injection cycle. Thus, during the second cycle, uneven amounts of free water and gel flowed through the tube at any given time. Low resistance factors occurred during high ratios of free water to gel, while high resistance factors were observed during low ratios of free water to gel.

Table 11. Recycling of a 24-hr-old Cr(III)-Acetate-HPAM Gel Through a 0.03-inch-ID, 15-ft-long Tube. 105°F

	Resistance factor				
Cycle	Section 1	Section 2	Section 3	Section 4	Section 5
1-fresh gel	198±10.6	148±7.3	132±5.9	120±5.5	116±6.0
2-recycle effluent from cycle 1	92.2±17.4	80.7±17.2	81.5±15.7	74.1±16.1	73.9±18.5
3-recycle effluent from cycle 2 after decanting free water	114±59.8	92.3±56.0	82.0±49.7	62.6±44.6	59.1±46.7
4-recycle effluent from cycle 3	22.7±18.4	15.6±22.1	25.4±22.1	20.9±23.1	20.4±27.3

The effluent from Cycle 2 consisted of gel and free water. We decanted 128 grams of free water from this effluent—leaving 325 grams of gel. This gel was then forced through the tube during the third cycle. Our expectation during this process was that the concentrated gel might experience less mechanical degradation during the third cycle. However, Table 11 shows that although the average resistance factor in Section 1 was higher during Cycle 3 than Cycle 2 (114 versus 92.2), the average resistance factors during Cycle 3 decreased more dramatically as the gel extruded through the tube (i.e., from 114 in Section 1 to 59.1 in Section 5). Also, very large fluctuations were noted during the third cycle (± 52% to ± 79%). Thus, decanting the water after Cycle 2 did not reduce the apparent level of mechanical degradation, and it did not reduce the resistance-factor fluctuations during gel extrusion.

All of the effluent from Cycle 3 was reinjected during Cycle 4. Table 11 shows that the resistance factors were low (averaging about 20) in all five tube sections. Also, large resistance-factor fluctuations were noted in all five sections. The standard deviations were typically about ± 100%.

A recycling experiment was also performed with a 24-hr-old Cr(III)-acetate-HPAM in a 0.03-inch-ID, 100-ft-long tube. During the first cycle of injection, resistance factors in the five tube sections averaged 163 ± 5, 91 ± 4, 27.5 ± 2.7, 9.9 ± 0.9, and 8.6 ± 1.9. All of the effluent was reinjected into the tube, resulting in resistance factors averaging 40.9 ± 39.8, 13.5 ± 12.1, 10.1 ± 6.7, 9.5 ± 6.4, and 8.4 ± 6.0, respectively. Consistent with our results in the 15-ft-long tube, the gel appeared to experience significant mechanical degradation with increased tube length, and the resistance factors became much more erratic during the second cycle of gel injection.

Certainly, more work is needed to establish the properties of gels as they extrude through long fractures. At present, our results suggest that two possibilities exist. First, gel extrusion experiments in tubes may provide a reasonable imitation of gel extrusion through fractures even though water cannot leakoff during our tube experiments. If this possibility is correct, our gels experience severe mechanical degradation as they extrude through long tubes or fractures. Of course, this possibility poses important limitations on field applications of existing gel technology. The second possibility is that experiments in long tubes cannot properly imitate gel behavior in long fractures, because the water that separates from the gel cannot be removed during the extrusion experiment. Our challenge, now, is to determine which of these possibilities is correct.

Conclusions

This chapter examined the placement properties of preformed gels when used as blocking agents for conformance control in fractures. Results of new experiments were reported that characterized how gel extrusion through fractures and tubes was affected by fracture or tube conductivity, fracture or tube length, gel age, and gel velocity. Our work focused on a gel that contained 0.5% HPAM (Allied Colloids Alcoflood 935), 0.0417% Cr(III)-acetate, and 1% NaCl at 105°F. We found the following:

1. During gel extrusion through short (0.5 to 15 ft) fractures and tubes at high velocities, pressure gradients were insensitive to flow rate.
2. Gels exhibited shear-thinning behavior in short fractures and tubes that correlated with the gel superficial velocity and the fracture width or tube diameter.
3. In short fractures or tubes with sufficiently small opening sizes, gels dehydrated during extrusion, thus reducing the rate of gel propagation. This effect was more pronounced as the opening size decreased.
4. The delay in gel propagation in short tubes was insensitive to velocity and gel age.
5. Gel resistance factors in fractures increased rapidly with increased gel age during the first 24 hours but increased more gradually during the next 200 hours.
6. Pressure gradients became more erratic with increasing gel age.
7. The behavior of Cr(III)-acetate-HPAM, resorcinol-formaldehyde, Cr(III)-xanthan, Cr(VI)-redox-HE-100, and hydroquinone-hexamethylenetetramine-HPAM gels in short tubes was qualitatively consistent with that in short fractures.
8. For different types of gels, the delay in gel propagation in short tubes did not correlate with gel rigidity or pressure gradient.
9. In 0.03-inch-ID, 100-ft-long tubes, resistance factors decreased substantially with increased length along the tube. This behavior was quite different from that in short fractures or tubes.

Therefore, we are presently uncertain whether gel extrusion through long tubes can adequately imitate gel extrusion through long fractures.

4. PLACEMENT OF PREFORMED GELS VERSUS WATER-LIKE GELANTS

Fracture Model

We now wish to use our experimental results from Chapter 3 to assess whether preformed gels have placement advantages over gels formed in situ from gelants. We focused on a simple model of a fractured reservoir, illustrated in Fig. 48. Consider an injector-producer pair where Fracture 1 allows injected water to channel directly from the injection well to the production well. For Fracture 1, L_{f1} is the effective length, and k_1 is the effective permeability. (Conversions between fracture conductivities, widths, and permeabilities can be made using Eq. 14.) This reservoir also contains a second fracture, Fracture 2, that has a beneficial role in oil recovery. Specifically, Fracture 2 meanders from the injection well to the production well in a much less direct path than Fracture 1. Because of its length and orientation, Fracture 2 allows the injected water to be distributed evenly in the reservoir and allows a high water injectivity (relative to the case where no fractures exist). (Of course, Fracture 1 also allows a high water injectivity, but most of that water channels directly to the production well.) Fracture 2 also acts as a conduit for oil flowing to the production well so that a relatively high oil productivity can be maintained. Fracture 2 has an effective length, L_{f2}, and an effective permeability, k_2. Generally, Fracture 2 will be longer and have a lower conductivity (and lower effective fracture permeability) than Fracture 1.

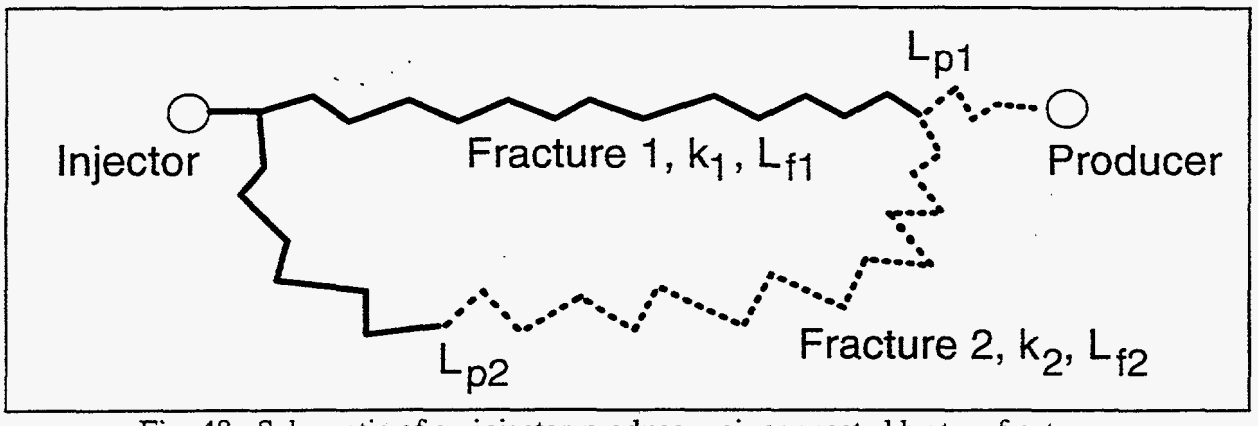

Fig. 48. Schematic of an injector-producer pair connected by two fractures.

Ideally, a gel treatment will substantially reduce the flow capacity of Fracture 1 while having little or no effect on the flow capacity of Fracture 2. Thus, we wish to maximize penetration of gel into Fracture 1 and minimize gel penetration into Fracture 2. The question is then raised, for a given distance (L_{p1}) of gel penetration into Fracture 1, how far (L_{p2}) will the gel penetrate into Fracture 2? We used the analytical and numerical methods described in Refs. 4 and 28 to answer this question. In these analyses, we assumed that (1) fluids were incompressible, (2) fractures were initially filled with fluids with water-like viscosities, (3) displacement was miscible and piston-like, (4) dispersion, capillary effects, and gravity effects were negligible, (5) flow of gel in a given fracture was effectively linear, and (6) all factors that can retard gel propagation (such as dehydration, leakoff, adsorption, and mechanical entrapment) were included in a propagation delay factor, a_r. In the base case for our numerical studies, Fracture 1 had an effective length of 500 ft, and a pressure drop of 1,000 psi was applied between the injector and the producer.

During sensitivity studies, the following results were insensitive to the length of Fracture 1 (between 50 and 5,000 ft) and to the pressure drop (between 100 and 10,000 psi).

Effects of Fracture Permeability Differences

In most circumstances, Fracture 1 will be more permeable than Fracture 2. So, how does the degree of gel penetration, L_{p2}/L_{p1}, vary with the fracture permeability ratio, k_1/k_2? Fig. 49 answers this question for several cases of gel resistance factor. (In this figure, both fractures were assumed to have the same length.) The curve with the open circles illustrates the case where the gel resistance factor was fixed at a value of 3,000. In this case, when Fracture 1 was 10 times more permeable than Fracture 2, the gel penetrated 31.6% as far in Fracture 2 as it did in Fracture 1 (L_{p2}/L_{p1}=0.316).

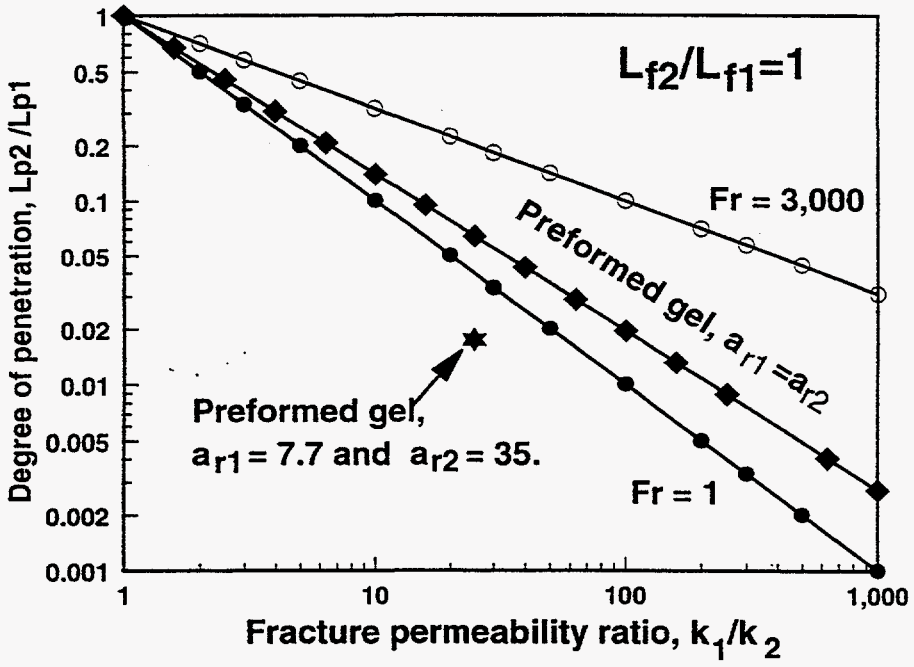

Fig. 49. Comparison of degree of penetration calculations for water-like gelants and preformed gels.

The curve with the solid diamonds illustrates a second case, where the gel resistance factors followed the behavior shown in Fig. 33 (described by Eqs. 15 and 16). For these gel resistance factors, Fig. 49 shows significantly lower degrees of penetration than when F_r=3,000. When Fracture 1 was 10 times more permeable than Fracture 2, the degree of penetration was 0.14.

The third and best case (solid circles) involved the use of a gelant with a water-like viscosity, where F_r=1. In that case, when Fracture 1 was 10 times more permeable than Fracture 2, the gel penetrated 10% as far in Fracture 2 as it did in Fracture 1 (L_{p2}/L_{p1}=0.10).

In the three cases considered above, the gel propagation delay factor (a_r) was assumed to be the same in Fractures 1 and 2. However, for a given preformed gel, Fig. 35 indicates that the a_r value

should decrease with increasing fracture conductivity. In particular, Fig. 35 suggests that the a_r values are 35 and 7.7 when $k_f w_f$ values are 4.5 darcy-ft and 568 darcy-ft, respectively. (In other words, 35 fracture volumes of gel must be injected to fill the 4.5-darcy-ft fracture, while 7.7 fracture volumes of gel must be injected to fill the 568-darcy-ft fracture.) Using Eq. 14, we can determine that a conductivity ratio of 568 to 4.5 translates to a fracture permeability ratio of 25.

We calculated the degree of penetration assuming that (1) gel resistance factors were given by Eqs. 15 and 16, (2) a_{r1}=7.7 in Fracture 1, (3) a_{r2}=35 in Fracture 2, and (4) the fracture permeability ratio was 25. As indicated by the star in Fig. 49, the calculated degree of penetration was 0.0175. For comparison, if the gel propagation delay factor was the same in both fractures, the degree of penetration was 0.064 for a permeability ratio of 25. For a water-like gelant with the same permeability ratio, the degree of penetration was 0.040. Therefore, in this particular case, the "real" preformed gel (i.e., showing resistance factors given by Eqs. 15 and 16 and gel propagation delay factors of 7.7 and 35 in Fractures 1 and 2, respectively) provided a degree of gel penetration that was less than half that for a water-like gelant.

Effect of Fracture Length Differences

In the above discussion, we assumed that Fractures 1 and 2 had the same length. In reality, Fracture 1 (the most direct channel between the wells) will probably be shorter than Fracture 2. How will the degree of gel penetration, L_{p2}/L_{p1}, be affected by the fracture length ratio, L_{f2}/L_{f1}? This question is addressed in Fig. 50 for a fixed fracture permeability ratio, k_1/k_2=25. The curve with the solid diamonds applies for the case where gel resistance factors were described by Eqs. 15 and 16, but the gel propagation delay factors were equal in both fractures ($a_{r1}=a_{r2}$). For this case, the degree of penetration was 0.064, independent of the fracture length ratio. This interesting result can be understood by realizing that for most practical situations, the gel resistance factors are large (see Fig. 33). Consequently, the resistance to flow in the gel-filled portions of the fracture is much larger than that in the portions of the fracture that do not contain gel. Then, an analysis[4] reveals that the frontal gel velocity in Fracture 2 relative to that in Fracture 1 is approximately k_1/k_2 raised to the power associated with the shear-thinning behavior for the gel. For example, the velocity exponent in Eq. 15 is -0.83. For a fracture permeability ratio of 25, $(k_1/k_2)^{-0.83}$ = 0.069, which is close to the degree of penetration (0.064) calculated from our more rigorous numerical analysis.

The curve with the stars applies for the case where gel resistance factors were described by Eqs. 15 and 16, but the gel propagation delay factors were 7.7 and 35 in Fractures 1 and 2, respectively. For this case, the degree of penetration was 0.0175, independent of the fracture length ratio. Of course, because the dehydration effect was significantly greater in Fracture 2 than in Fracture 1 (i.e., 35>7.7), the gel front moved even more slowly in Fracture 2. Consequently, the degree of penetration for this case (0.0175) was significantly less than that for the previous case, where the gel propagation delay factor was assumed to be the same in both fractures. Using rationale similar to that from the previous paragraph, the degree of penetration can be estimated using a simple analysis. First, calculate the product, $(k_1/k_2)(a_{r2}/a_{r1})$. Second, raise this product to the velocity exponent associated with the shear-thinning gel. In this case, we calculate $(25\text{x}35\div7.7)^{-0.83}$, which equals 0.0197. Again, this value is close to the value calculated from our more rigorous numerical analysis (0.0175).

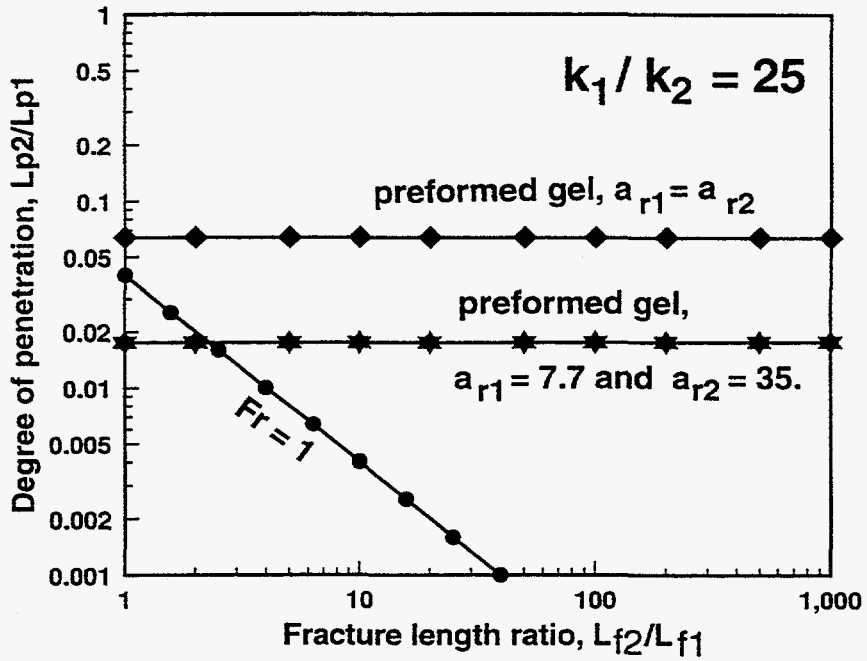

Fig. 50. Degree of penetration versus fracture length ratio.

The curve with the solid circles plots the degree of penetration versus the fracture length ratio for a water-like gelant (F_r=1). In contrast to the two cases above where preformed gels were considered, the degree of penetration for the water-like gelant decreased significantly with increased fracture length ratio. When Fracture 2 was more than twice the length of Fracture 1, the water-like gelant provided degrees of penetration that were less than those for the preformed gels.

Fracture Length Ratios in Field Applications

The results presented in Figs. 49 and 50 suggest that the placement characteristics of preformed gels may be as good or better than those of water-like gelants if the fracture length ratio has a value of 2 or less. In fractured systems with high fracture length ratios, gelants with water-like viscosities may have a significant placement advantage.

What fracture-length ratios are expected in field applications? This question is addressed in Fig. 51. Consider a naturally fractured reservoir with a pattern of north-south and east-west fractures. Assume that a waterflood has been applied with a five-spot pattern of injection and production wells. The shortest fracture, Fracture 1, channels directly between the two wells and has a length, L_{f1}. One can choose a number of longer fracture pathways between the two wells. For practical purposes, the longest fracture pathway (Fracture 2 in Fig. 51) begins at the injection well, extends perpendicular to Fracture 1 until almost reaching a nearby offset production well, turns 90° to parallel Fracture 1 until almost reaching the next injection well in the pattern, turns 90° and continues directly to the production well to meet Fracture 1. Assuming that Fractures 1 and 2 have the same degree of tortuosity per unit of length, and assuming that the five-spot pattern is square, the ratio, L_{f2}/L_{f1}, has a value around 3.

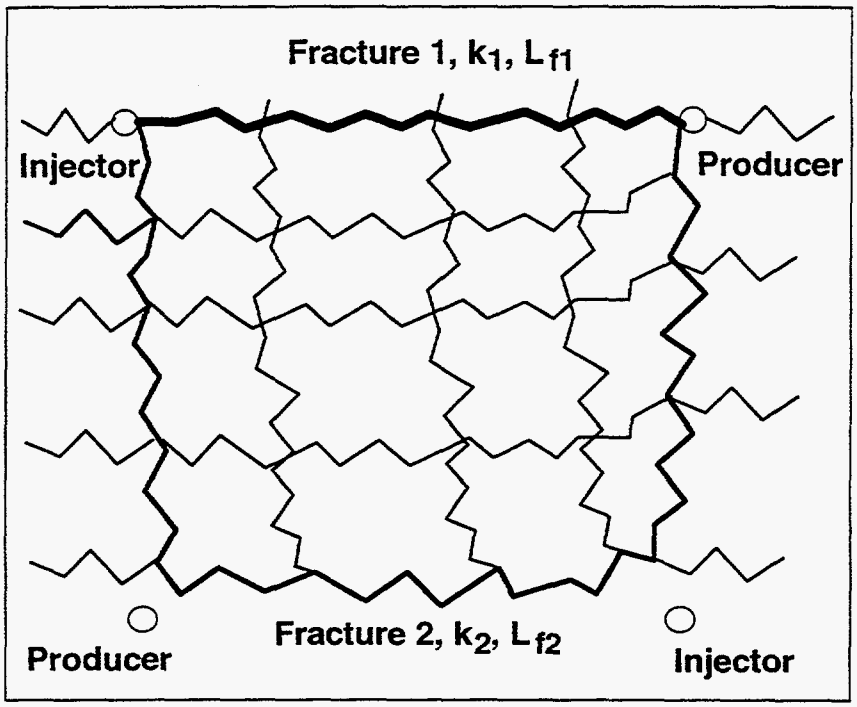

Fig. 51. In naturally fractured reservoirs, usually, $L_{f2}/L_{f1} < 3$.

Certainly, one can envision longer, more circuitous fracture pathways than that illustrated by Fracture 2 in Fig. 51. Upon first consideration, one might pick a pathway that jigs and jags in random directions, doubles back, and/or crosses itself on its way from the injector to the producer. However, one must honor the flow constraints imposed by the streamlines and equipotential lines of the flow system. These constraints preclude pathways that double back and/or cross each other. The constraints also reduce the number of overly circuitous pathways. Thus, the longest practical length for Fracture 2 will be approximately that illustrated in Fig. 51.

Arguments can be made that L_{f2}/L_{f1} should be less than 3. For example, a fracture flow path from one injection well probably will not closely approach another injection well in the way suggested in the lower right part of Fig. 51.

Since L_{f2}/L_{f1} is generally less than 3, Fig. 50 suggests that in most applications, a preformed gel may show placement properties that are at least as desirable as those for a gelant with a water-like viscosity. Of course, this suggestion assumes that preformed gels exhibit the behavior shown in Figs. 33 and 35. As mentioned in Chapter 3, more work is needed to determine if the behavior shown in Figs. 33 and 35 (which was found in relatively short fractures of 4 feet or less) is also observed during gel extrusion in longer fractures (e.g., >100 ft). Also, more work is needed to determine whether the behavior shown in Figs. 33 and 35 is basically the same for other gel compositions.

In the modeling described to this point, the various fracture pathways did not have pressure communication except at the endpoints of the fracture pathways (Fig. 48). Currently, we are actively modeling naturally fractured systems with multiple points of pressure communication (Fig. 51). Results from these studies will be reported in the near future.

Other Considerations in Field Applications

Of course, several other factors can influence the relative merits of using preformed gels versus gelants. First, water-like gelants are usually more expensive than polymer-based gels. Water-like gelants typically require from 5% to 30% concentrations of active chemicals, whereas polymer-based gels typically require 0.3% to 2% concentrations. Second, gelation chemistry for gelants is often quite sensitive to contact with reservoir rocks and fluids. In contrast, the effect of gelation chemistry is minimized with preformed gels because the gelation reactions are largely finished before reservoir contact occurs. Third, gravity effects are much more important for gelants than for preformed gels. During gelant injection, viscous forces in fractures usually dominate over gravity forces, so the shape of the gelant front is not greatly distorted by gravity.[17] However, after gelant injection stops, gravity segregation (of gelant and reservoir fluids) can occur very rapidly in a fracture.[17] If minimum gravity segregation is desired, the gelation time must be carefully controlled to coincide with the gelant injection time. In contrast, gravity segregation usually is not important for preformed gels because they have high resistance factors.

On the other hand, water-like gelants have at least two advantages over preformed gels. First, because of their low viscosities, water-like gelants exhibit relatively high injectivities, regardless of the conductivities of the fractures in the reservoir. In contrast, preformed gels may experience significant injectivity problems if the fractures are not sufficiently conductive. Since engineers often do not know the conductivities of the fractures near a well, preformed gels have a greater risk of plugging the well before the desired volume of gel is injected.

A second advantage of water-like gelants is that they can be easily displaced away from the wellbore before gelation using a water or oil postflush. This allows placement of the gel deep into the fracture while leaving the near-wellbore part of the fracture open (upper left of Fig. 4). As mentioned earlier, this placement process allows sweep efficiency to be improved while maintaining a high injectivity or productivity for the well. (As illustrated in the lower right part of Fig. 4, viscous gelants *do not* share this advantage with water-like gelants.[28]) In contrast, preformed gels are more difficult to displace from the near-wellbore part of the fracture. To achieve a placement like that in the upper left of Fig. 4 using preformed gels, perhaps, one could incorporate a gel-degrading chemical (e.g., an oxidizer, enzyme, hydrolysis agent, or delayed complexing agent) into the last volume of gel injected. Gel without the degrading chemical is injected first to penetrate into and plug the far-wellbore portions of the fracture. This gel is then followed by gel that contains the degrading agent that destroys the gel (after an appropriate delay) in the near-wellbore portion of the fracture. Of course, this idea remains to be tested experimentally.

Conclusions

During a numerical study comparing the placement properties of preformed gels and water-like gelants in a simple two-fracture reservoir, the following conclusions were reached:

1. The gel-dehydration effect can aid gel placement by minimizing the degree of gel penetration (i.e., the distance of gel penetration into a given fracture pathway divided by that for the most-conductive fracture pathway between an injector-producer pair).

2. For preformed gels, the degree of penetration was insensitive to the fracture length ratio (i.e., the length of a less-conductive fracture divided by the length of the most-conductive fracture in the system).
3. In contrast, for gelants with a water-like viscosity, the degree of penetration decreased dramatically with increased fracture length ratio.
4. For fracture length ratios below 2, preformed gels may have a placement advantage over water-like gelants.
5. In most field applications, fracture length ratios will be less than 3.

5. SCHEMES TO OPTIMIZE GEL PLACEMENT IN FRACTURES

Part of our project focuses on schemes to optimize placement of blocking agents in fractures and narrow channels behind pipe. Ideally, we desire schemes that will provide the placement illustrated by the upper left part of Fig. 4. To achieve this objective, the blocking agent must possess three properties. First, during the placement process, it must flow readily through the fracture without screening out or developing excessive pressure gradients. Second, it must become immobile at a predictable and controllable time. Third, some mechanism must be available to remove the blocking agent from the near-wellbore portion of the fracture without damaging the blocking agent in the far-wellbore part of the fracture. This chapter summarizes our preliminary investigations of several schemes.

Injection of Mechanically Degraded Cr(III)-Acetate-HPAM Gels

A concern during injection of preformed gels is that the gel may "screen out" or develop excessive pressure gradients. In relatively low-conductivity fractures, we noted pressure gradients over 300 psi/ft during gel extrusion.[17] In one approach to reduce this concern, we allowed the gelation reaction for a conventional gel to proceed to completion and then mechanically degraded the gel to a desired fluidity. We examined the performance of a 5-day-old Cr(III)-acetate-HPAM gel that was sheared in a blender.[28] Our objective was to determine whether this mechanical degradation can reduce gel resistance factors while still providing effective fluid diversion in a fractured core. In this work, we used the same composition of Cr(III)-acetate-HPAM gel that was described in Chapter 3 (0.5% Allied Colloids Alcoflood 935® HPAM, 0.0417% Cr(III)-acetate, 1% NaCl, pH 6). After preparation, the gel was allowed to set for 5 days at 105°F. Then, it was sheared for 1 minute in a Waring blender at 75% of full power. After shearing, the product had a smooth consistency (no chunks).

Short Core. We injected 300 fracture volumes (315 cm^3) of sheared Cr(III)-acetate-HPAM gel through a fractured Berea sandstone core (Core 21). The core was 14.7 cm (5.7 inches) in length and 3.6 cm (1.4 inches) in diameter. The fracture conductivity was 0.75 darcy-ft. The estimated average fracture width (from Eq. 14) was 0.014 cm (0.0055 inches)

Fig. 52 shows resistance factors and pressure gradients during gel injection at a rate of 200 cm^3/hr (superficial velocity ≈ 3,100 ft/d). During injection of 300 fracture volumes of gel, the resistance factor steadily increased from 45 to 200, while the pressure gradient increased from 9 to 38 psi/ft. These values are lower (and therefore more desirable) than values that we observed during most previous experiments.[28] However, the steady increase in these values still raises a concern that unacceptably high pressure gradients could develop unless the fractures are very conductive.

Fig. 53 shows tracer results associated with this experiment. The solid circles show tracer results for the fractured core during brine injection before gel was injected. The first tracer was detected in the core effluent after injecting 0.03 PV of tracer solution. The tracer concentration in the effluent reached 50% of the injected concentration after injecting 0.09 PV of tracer solution. In contrast, the open circles show the tracer results during brine injection for a Berea core before

fracturing and before gel injection. This data shows the results expected for a tracer study during brine injection after a gel treatment that effectively healed a fracture without damaging the porous rock.[17] In this case, tracer was first detected in the core effluent after 0.81 PV of tracer solution, while the 50% tracer concentration was reached at 1.0 PV.

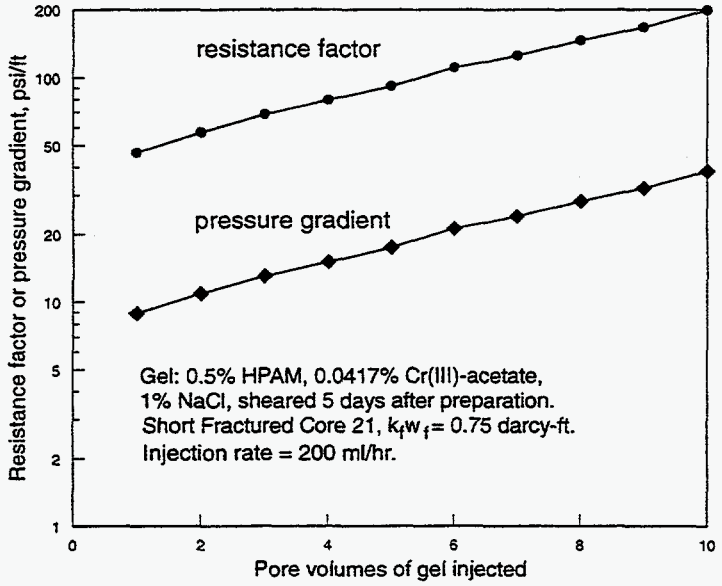

Fig. 52. Resistance factors and pressure gradients during placement of a sheared Cr(III)-acetate-HPAM gel in Short Fractured Core 21.

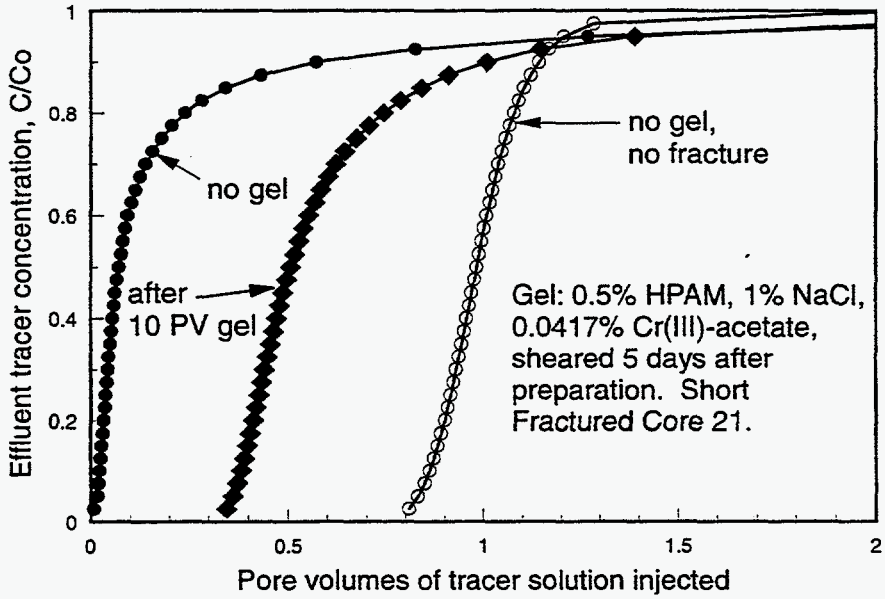

Fig. 53. Tracer results before versus after placement of a sheared Cr(III)-acetate-HPAM gel in Short Fractured Core 21.

The solid diamonds in Fig. 53 show tracer results that were obtained during brine injection after placement of the mechanically degraded gel. In this study, tracer breakthrough occurred at 0.345

PV and C/C_o=50% at 0.505 PV. Thus, the treatment improved sweep efficiency somewhat in the core, but the fracture was not healed.

Long Core. We repeated the above experiment using a fractured core (Long Fractured Core 3) that was 114.5 cm (3.8 ft) in length. The average conductivity of the fracture was 1.5 darcy-ft, and the effective average fracture width was 0.018 cm (0.0069 inches). We used a Cr(III)-acetate-HPAM gel with the same composition and aging time (5 days at 105°F) as that used in Short Fractured Core 21. The gel was also sheared in a Waring blender in the same way (1 minute at 75% of full power). We injected 750 cm^3 (2.1 core PV or 60 fracture volumes) of sheared gel at a rate of 400 cm^3/hr (4,600 ft/d). Consistent with the results observed in the short core, progressive plugging occurred in all five sections of the fractured core. The resistance factors reached the highest values in the first two sections, exceeding 1,000.

Effect of Shearing Time Using gel that had been sheared for 1 minute in a Waring blender, the above results suggest that gel propagation through fractures is still a potential problem. How does the gel resistance factor vary with shearing time? To answer this question, we performed a series of experients using Short Fractured Core 33. This core was 14.4 cm (5.7 inches) in length. The fracture conductivity was 3.9 darcy-ft. The effective average fracture width was 0.024 cm (0.0095 inches). A Cr(III)-acetate-HPAM gel was prepared with the same composition as that mentioned earlier, and this gel was aged for five days at 105°F. This gel was separated into five batches of equal size. Then, each batch was sheared in a Waring blender at 75% of full power for time periods ranging from 15 to 90 seconds (specifically, 15, 30, 45, 60, and 90 seconds).

After preparation, we injected 10 PV (326 cm^3 or about 300 fracture volumes) of each batch of sheared gel into Short Fractured Core 33 using a rate of 200 cm^3/hr (1,800 ft/d). The most sheared gel was injected first and the least-sheared gel was injected last. Fig. 54 shows the resistance factors that were observed during gel injection. While injecting 10 PV (300 fracture volumes) of gel, the resistance factors steadily increased from 11 to 200 for the 90-second-sheared gel, from 230 to 330 for the 60-second-sheared gel, and from 450 to 1,600 for the 45-second-sheared gel. For the 30-second-sheared gel and the 15-second-sheared gel, the resistance factors were fairly stable—averaging 2,200 and 3,100, respectively. Thus, as expected, the average resistance factor decreases with increasing shearing time.

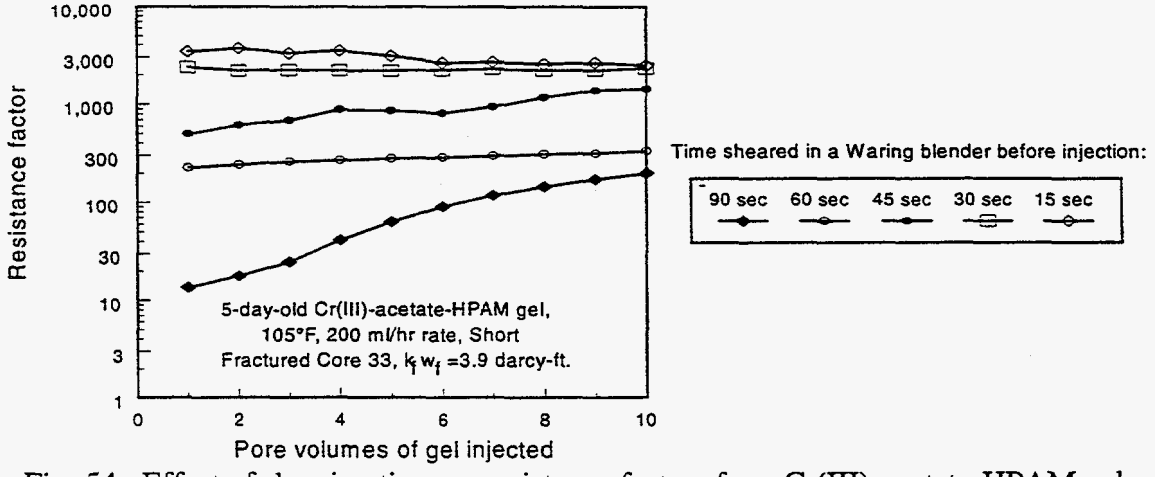

Fig. 54. Effect of shearing time on resistance factors for a Cr(III)-acetate-HPAM gel.

Tracer results indicated that the gel treatment significantly improved sweep efficiency in the core, but it did not completely heal the fracture.[28]

In summary, our investigation has not shown sheared preformed gels to be superior to preformed gels that were not sheared. However, our studies have not been extensive enough to abandon hope that sheared gels may prove useful.

Two-Stage Reactions

We are also investigating blocking agents that are formed from two-stage reactions. For these blocking agents, the product from the first reaction must be very fluid, but it must have enough particulate or gel content to prevent leakoff into porous rock. If this reaction is effectively complete before the fluid leaves the wellbore, the fluid can penetrate to the maximum extent into the fracture or channel. A number of methods could be used to ensure that this reaction is completed before injection, including control of temperature, reactant concentrations, and pH.

The second reaction stage must occur after the blocking agent has been placed in the desired location. This reaction should produce an immobile material at a predictable time. The second reaction must be effective under reservoir conditions, immobilizing the product of the first reaction at a predetermined time. Many examples of two-stage reactions can be envisioned, including (1) polymers that can be crosslinked using two different chemicals (with two different gelation times), (2) preformed gels that can be further crosslinked after injection, and (3) mixtures of two different gelant systems having substantially different gelation rates.

Injection of Cr(III) After Placement of a Mechanically Degraded Cr(III)-Acetate-HPAM Gel. The first two-stage reaction that we investigated involved injecting a sheared gel, followed by a crosslinker solution. In concept, the sheared gel could exhibit a low resistance factor and pressure gradient during gel injection. Then, when a crosslinker solution was injected after gel placement, hopefully, a more effective gel could be formed that might plug the fracture. We investigated this idea using Short Fractured Core 34. This core was 14.4 cm (5.7 inches) in length. After fracturing, the fracture conductivity was 2.5 darcy-ft, and the effective average fracture width was 0.021 cm (0.0082 inches). We used a Cr(III)-acetate-HPAM gel with the same composition and aging time (5 days at 105°F) as that used in previous experiments. The gel was also sheared in a Waring blender in the same way (1 minute at 75% of full power). After shearing, the viscosity of this gel was 6.6 cp. We injected 10 PV (317 cm^3 or 300 fracture volumes) of sheared gel at a rate of 200 cm^3/hr (2,100 ft/d). The left side of Fig. 55 shows how the resistance factor and pressure gradient increased while injecting 10 PV of gel.

After gel placement, we immediately injected 10 PV (317 cm^3 or 300 fracture volumes) of a crosslinker solution that contained 0.0288% $CrCl_3$ and 1% NaCl. The right side of Fig. 55 shows that the resistance factor and pressure gradient continued to increase, but not as rapidly as during gel injection.

After injecting the crosslinker solution, the core was shut in for three days. Then, we injected 25 PV of brine, followed by a tracer study. The tracer results indicated that this treatment had no beneficial effect on sweep efficiency.[28]

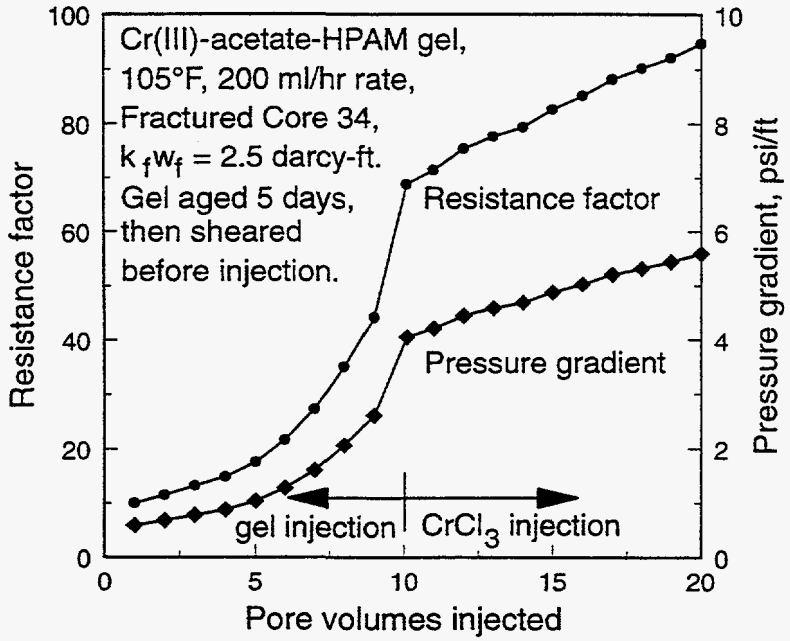

Fig. 55. Effect of $CrCl_3$ injection after placement of a Cr(III)-acetate-HPAM gel.

Injection of Cr(III) After Placement of a Hydroquinone-Hexamethylenetetramine-HPAM Gel. Following similar logic to that described above, we performed another experiment where a hydroquinone-hexamethylenetetramine-HPAM gel was injected instead of a sheared Cr(III)-acetate-HPAM gel. The gelant contained 0.5445% Allied Colloids Alcoflood® 935 HPAM, 0.25% hydroquinone, 0.1% hexamethylenetetramine, and 1% $NaHCO_3$. This gelant requires high temperatures for the gelation reaction to proceed at a significant rate. Based on our previous experience,[13] we aged the gelant for 18 hours at 230°F, followed by quenching to 105°F, to make a gel that exhibits fairly low resistance factors and pressure gradients during injection. Then, we injected 10 PV (325 cm^3 or 300 fracture volumes) of this gel into Short Fractured Core 35 using a rate of 200 cm^3/hr (1,900 ft/d). This core was 14.5 cm (5.7 inches) in length. The fracture conductivity was 3.3 darcy-ft, and the effective average fracture width was 0.023 cm (0.0090 inches).

During gel injection, the resistance factor was stable at 340, and the pressure gradient was stable at 15 psi/ft (left side of Fig. 56). After gel injection, we injected 10 PV of crosslinker solution that contained 0.0288% $CrCl_3$ and 1% NaCl. (Throughout this experiment, the rate was maintained constant at 200 cm^3/hr.) During injection of the crosslinker solution, the resistance factor and pressure gradient averaged 21 and 1 psi/ft, respectively. Next, 20 PV of 1%-NaCl brine (without crosslinker) were injected. During this brine injection, the resistance factor and pressure gradient were about the same as those observed during crosslinker injection (Fig. 56). After brine injection, an additional 10 PV of crosslinker solution (same composition as before) were injected, with no effect on the resistance factor or pressure gradient. Then, the core was shut in for 3 days, followed by injection of an additional 20 PV of 1%-NaCl brine. Again, the resistance factor and pressure gradient were unaffected. Finally, a tracer study was performed. As in the previous experiment, the tracer study indicated that the gel treatment did not improve sweep efficiency in the core.[28]

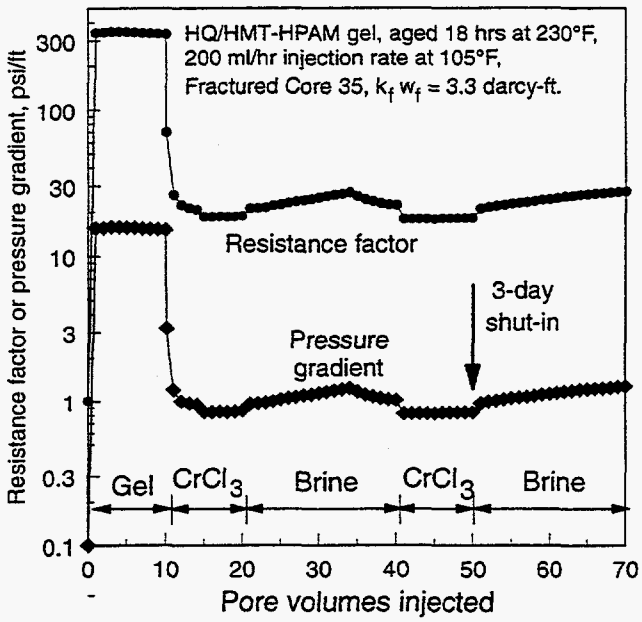

Fig. 56. Effect of $CrCl_3$ injection after placement of a HQ/HMT-HPAM gel.

Injection of Cr(III) After Placement of an HPAM Water-in-Oil Emulsion. We also investigated whether fractures can be treated by injecting a concentrated HPAM water-in-oil emulsion, followed by injection of a crosslinker solution. We used the emulsion-form polymer, Allied Colloids Alcomer® 123L. This product consists of 25% HPAM that is dispersed in water, that is, in turn, dispersed in oil. This water-in-oil emulsion was used directly as supplied from the manufacturer. This emulsion is shear-thinning and exhibits a viscosity of 76 cp at 11 s^{-1} and 105°F.

We performed experiments with this emulsion in five short fractured cores (14.5 cm or 5.7 inches in length). Properties of the five fractured cores are listed in Table 12. Table 13 lists the injection sequence for each of these experiments. All experiments were performed at 105°F. Table 14 summarizes the experimental results.

Table 12. Properties of Cores Used in HPAM Emulsion Experiments

Core no.	36	37	38	39	40
$k_f w_f$, darcy-ft	2.5	1.1	1.5	1.3	1.9
$k_f w_f h_f / A k_m$	41.5	18.5	25.2	21.0	32.7
V_f, cm^3	1.0	1.0	0.8	0.8	1.2
w_f, cm	0.020	0.020	0.016	0.016	0.024
k_f, darcys	3,900	1,700	2,900	2,400	2,500

Table 13. Sequences Followed During Experiments with HPAM Emulsions (105°F)

Step	Core 36	Core 37	Core 38	Core 39	Core 40
1	brine saturated	brine saturated	oil saturated	oil saturated	brine saturated, 10 PV $CrCl_3$
2	1 PV emulsion	1 PV emulsion	2 PV emulsion	1 PV emulsion	0.25 PV emulsion
3	34 PV brine	1-day shut-in	10 PV $CrCl_3$	0.7 PV $CrCl_3$*	1-day shut-in
4	10 PV $CrCl_3$, 1-day shut-in	10 PV $CrCl_3$, 1-day shut-in	26 PV oil	20 PV oil	27 PV brine
5	11 PV brine	22 PV brine	oil tracer	oil tracer	brine tracer

* $CrCl_3$ placement occurred at 0.32 cm^3/hr injection rate during this experiment only. In the other experiments, $CrCl_3$ placement occurred at 200 cm^3/hr injection rate.

Table 14. Summary of Results of Experiments with HPAM Emulsions (105°F)

	Core 36	Core 37	Core 38	Core 39	Core 40
Maximum F_r during emulsion injection	85	77	30	52	80
Maximum F_{rr} during $CrCl_3$ injection	4,000	370	28	85,000	--
Maximum F_{rr} during water or oil injection	3,700	105	5	4,000	91
Tracer indicates sweep improvement?	not available	not available	no	no	no

Short Fractured Core 36 was first saturated with brine (1% NaCl). Then, 31 cm^3 (1 core PV or 31 fracture volumes) of Alcomer 123L HPAM emulsion were injected. (Unless stated otherwise, the injection rate was 200 cm^3/hr.) The resistance factor in the second section of the fracture reached a value of 85 during emulsion injection (Table 14). For comparison, the emulsion viscosity approaches 50 cp at high shear rates. After emulsion injection, 34 PV of 1%-NaCl brine were injected. During this step, the maximum residual resistance factor (F_{rrw}) was 130. Next, 10 PV of crosslinker solution (0.0288% $CrCl_3$, 1% NaCl) were injected. During this step, F_{rrw} reached a maximum of 4,000. After injecting the crosslinker solution, the core was shut in for 1 day, followed by injection of 11 PV of brine. During this final step, F_{rrw} was 3,700. Unfortunately, we could not perform a tracer study at the end of this experiment because emulsified polymer was continually produced—interfering with our tracer detector.

The above experiment was repeated in Short Fractured Core 37, with certain modifications (see Table 13). Again, the core was first saturated with brine (1% NaCl), and 1 PV of HPAM emulsion was injected (resulting in a maximum F_r of 77), followed by a 1-day shut-in. Then, 10 PV of crosslinker solution were injected, resulting in a maximum F_{rrw} value of 370. After a 1-

day shut-in period, 22 PV of brine were injected, resulting in a maximum F_{rrw} value of 105. At the end of this experiment, produced emulsion, again, precluded a successful tracer study.

In an attempt to minimize the production of emulsion from the core (so that a post-treatment tracer study could be performed), two floods were conducted using oil-saturated cores (Short Fractured Cores 38 and 39). These cores were first completely saturated with Soltrol 130 oil. In Core 38, the F_r value reached a maximum value of 30 during injection of 2 PV (60 fracture volumes) of emulsion (Tables 13 and 14). Then, 10 PV of $CrCl_3$ crosslinker solution (again, containing 0.0288% $CrCl_3$ and 1% NaCl) were injected, resulting in a maximum F_{rrw} value of 28. During the subsequent injection of 26 PV of Soltrol 130 oil, the residual resistance factor fell to a value of 5. Finally, we were able to complete oil-tracer studies both before and after placement of the crosslinked emulsion. The tracer studies showed that this emulsion treatment was completely ineffective at improving sweep efficiency in Core 38.[28]

The above experiment was repeated in Short Fractured Core 39, with certain modifications. The core was first saturated with Soltrol 130 oil. Then, 1 PV (30 fracture volumes) of HPAM emulsion was injected at a rate of 200 cm^3/hr. The maximum F_r was 52 during this step. Next, 0.7 PV of $CrCl_3$ crosslinker solution was injected at a rate of 0.32 cm^3/hr. This slow rate was chosen to maximize diffusion into and reaction with the HPAM. The residual resistance factor reached a very high value (85,000) during this step. After injecting the crosslinker, 20 PV of Soltrol 130 oil were injected at 200 cm^3/hr, resulting in an F_{rrw} value of 4,000. Finally, an oil-tracer study was conducted. Unfortunately, the tracer results indicated that the crosslinked-emulsion treatment was ineffective.

The final experiment was performed in Short Fractured Core 40. This core was first saturated with brine (1% NaCl), and then, 10 PV of $CrCl_3$ crosslinker solution were injected. Our intent was to saturate the core with crosslinker before the emulsion was placed. (All steps in this experiment used a rate of 200 cm^3/hr.) Next, 0.25 PV (6 fracture volumes) of emulsion were injected, resulting in a maximum F_r value of 80. This F_r value is comparable to those observed during emulsion placement in Cores 36 and 37 (see Table 14). This result suggests that the HPAM did not react extensively with the resident $CrCl_3$ crosslinker during the placement process. After emulsion placement, Core 40 was shut in for 1 day, followed by injection of 27 PV of brine. The F_{rrw} during brine injection was 91. Finally, we were able to complete a brine-tracer study at the end of this experiment. Unfortunately, tracer studies showed that this crosslinked-emulsion treatment was also ineffective at improving sweep efficiency in the fractured core.[28]

Mobility-Matched Postflushes

We are also investigating the use of mobility-matched postflushes during placement of blocking agents. In fractured systems, ideally, the blocking agent should plug the fracture far from the wellbore, while leaving the fracture open to flow near the well. This situation could reduce fluid channeling through the reservoir while maintaining a high injectivity or productivity for the well. In contrast, if the blocking agent simply heals the entire fracture or fracture system, the ultimate injectivity or productivity of the well may be unacceptably low.[16]

Theoretical work and flow visualization studies suggest that a postflush could aid placement if the effective viscosity of the blocking agent was not greater than that for the postflush fluid (or more generally, if a favorable mobility ratio exists during the displacement).[17,44,48] To be effective, the postflush must be injected before the mobility of the blocking agent becomes too low. At least two approaches are available for the design of the postflush. In one approach, a nonreactive postflush is injected that has the same effective viscosity in the fracture as that of the blocking agent that is being displaced. In a second approach, the postflush could have the same composition as the blocking agent, except that it must also contain a chemical (e.g., enzyme or oxidizing agent) that degrades the blocking agent or prevents the blocking agent from forming.

Water Postflush Displacing a Water-Like Gelant. We used a 4-ft-long (122-cm) fractured core to test the effectiveness of a water postflush in displacing a gelant with a water-like viscosity. Four internal pressure taps were spaced equally along the fracture. Table 15 lists the properties of the fractured core. The average fracture conductivity was 0.85 darcy-ft, the effective average fracture width (from Eq. 14) was 0.015 cm (0.0057 inches), and the fracture volume (measured from tracer studies) was 11.2 cm^3. We injected 7 cm^3 (0.6 fracture volumes) of a freshly prepared resorcinol-formaldehyde gelant at a rate of 200 cm^3/hr. The gel contained 3% resorcinol, 3% formaldehyde, 0.5% KCl, and 0.1% $CaCl_2$.

Table 15. Properties of Long Fractured Core 11

Section	1	2	3	4	5
Length, inches	9.6	9.6	9.6	9.6	9.6
$k_f w_f$, darcy-ft	0.62	1.62	0.85	0.60	0.58
V_f, cm^3	2.1	2.6	2.1	2.4	2.0
F_{rr}	30	4.0	4.0	1.8	1.1

After gelant injection, the core was shut in for 40 minutes. Then, 5 cm^3 (0.5 fracture volumes) of brine were injected at 200 cm^3/hr. (The 40-minute shut-in was actually a mistake. We intended to inject brine immediately after the gelant. We suspect that gravity segregation during this shut-in may have caused the failure of the treatment. Therefore, this experiment will be repeated.) Next, the core was shut in for several days, followed by brine injection and tracer studies. During brine injection, the residual resistance factors in Sections 1 through 5 of the core were 30, 4, 4, 1.8, and 1.1, respectively. Thus, the primary plugging effect occurred in the first (inlet) core section. Tracer studies indicated that the gel treatment caused a minor improvement in sweep efficiency in the first core section. However, no improvement was observed in the other four core sections. Of course, we had hoped that this treatment would have plugged the fracture in the last half of the core—thus, improving sweep efficiency in those sections while leaving the fracture open in the first half of the core. This experiment will be repeated, with some modifications, to try to achieve a more positive result.

Injecting a Degrading Agent After Placement of a Preformed Gel

We also examined the idea of injecting a degrading agent after placement of a preformed gel. In this experiment, we used a 4-ft-long core with an average fracture conductivity of 26.2 darcy-ft and an average fracture width of 0.018 inches (0.046 cm). We forced 800 cm^3 (37 fracture volumes) of a 24-hr-old Cr(III)-acetate-HPAM gel (same composition as that mentioned earlier)

at a rate of 200 cm^3/hr (900 ft/d). The average resistance factors in Sections 1 through 5 of the core were 2,000, 3,290, 7,430, 4,960, and 4,430, respectively. After gel placement, a tracer study indicated that the gel had effectively healed the fracture. Next, 127 cm^3 (0.32 core PV) of 2% sodium pyrophosphate were injected at 200 cm^3/hr. Then, the core was shut in for three days. Since sodium pyrophosphate is very effective at degrading or "degelling" Cr(III)-acetate-HPAM gels,[49,50] we hoped that this bank of degrading agent would destroy the gel in the first third of the fracture. However, subsequent tracer studies and residual-resistance-factor measurements indicated that the sodium pyrophosphate treatment had virtually no effect. Therefore, we displaced the old pyrophosphate solution from the core and injected 151 cm^3 (0.38 core PV) of 7.5%-sodium-pyrophosphate solution. Again, subsequent tracer studies and residual-resistance-factor measurements did not indicate significant destruction of the gel in any part of the fracture. Thus, it appears that a stronger degrading agent or a longer shut-in time may be needed.

Conclusions

In summary, we were not able to improve the placement of gels in fractured cores using (1) injection of mechanically degraded Cr(III)-acetate-HPAM gels, (2) injection of mechanically degraded Cr(III)-acetate-HPAM gels, followed by injection of a $CrCl_3$ solution, (3) injection of a partially crosslinked hydroquinone-hexamethylenetetramine-HPAM gel, followed by a $CrCl_3$ solution, (4) injection of an HPAM water-in-oil emulsion, preceded or followed by a $CrCl_3$ solution, (5) injection of a water-like gelant, followed by a water postflush before gelation, and (6) injection of a preformed Cr(III)-acetate-HPAM gel, followed by a pyrophosphate solution. However, our efforts to date must be regarded as preliminary.

In the future, these and other placement schemes will be investigated if they show promise. We will aggressively combine our experimental results with analytical and numerical analyses to establish the optimum blocking-agent type, blocking-agent volumes, and placement technique to achieve the best results in hydraulically fractured and naturally fractured reservoirs.

6. DISPROPORTIONATE PERMEABILITY REDUCTION

The ability of blocking agents to reduce the permeability to water much more than to oil is critical to the success of water-shutoff treatments in production wells if zones cannot be isolated.[18,25] Results from the literature and our own experimental work[19-23,107-110] have shown that many polymers and gels exhibit this disproportionate permeability reduction. In our previous studies, we extensively examined the possible mechanisms for this disproportionate permeability reduction.[27,28] Although we still do not have a plausible explanation for this phenomenon, many interesting leads have been generated during the course of the study. Our previous studies ruled out gravity and lubrication effects as possible mechanisms. Also, gel shrinking and swelling are unlikely to be responsible for this phenomenon. Our experimental results indicate that wettability may play a role; however, its effects are unclear. Based on a micromodel study by Dawe and Zhang,[111] we have proposed that the competition between capillary forces and gel elasticity might contribute to disproportionate permeability reduction. In this study, we report results from experiments designed to verify this theory. We also discuss the use of small glass tubes to visualize disproportionate permeability reduction. Based on results from core experiments using an oil-based gel, we proposed that disproportionate permeability reduction might be caused by oil and water following segregated pathways on a microscopic scale. We speculate that if this theory is valid, a simultaneous injection of oil and an aqueous gelant during placement should enhance disproportionate permeability reduction. We continue our study of this theory by using different gelant/oil volume ratios during placement. Also, we examine the effects of polymer washout during multiple cycles of water/oil injection after a gel treatment.

Effects of Capillary Forces and Gel Elasticity on Disproportionate Permeability Reduction

Based on visual micromodel experiments by Dawe and Zhang,[111] we proposed that capillary forces and gel elasticity might contribute to the disproportionate permeability reduction.[28] In reviewing the video of the micromodel experiments, we observed that during oil injection, oil drops forced their way through an aqueous gel and the gel acted as an elastic material, creating just enough room for the oil drops to squeeze through. During water injection, most of the water flowed through the pathways created by oil, except the pathways were more constricted. Dawe and Zhang [111] reported that the gel reduced the permeability to water significantly more than to oil. We suspect that the disproportionate permeability reduction was caused by the competition between capillary forces and gel elasticity. As illustrated in Fig. 57, when an oil droplet is extruding through an aqueous gel, there are two competing forces that act against each other. On the one hand, a capillary force is trying to open the channel. On the other hand, the elastic confining force exerted by the gel on the oil droplet is trying to close the channel. The final radius of the oil droplet depends on the balance between the two forces. The effective permeability to oil increases with increasing radius of the flow path around the oil droplet. In contrast, when water flows through the same channel, there is no capillary force to open the channel. Therefore, the effective permeability to water should be less than that to oil. Two possible ways exist to test this theory: (1) vary the capillary forces and (2) change the gel elasticity.

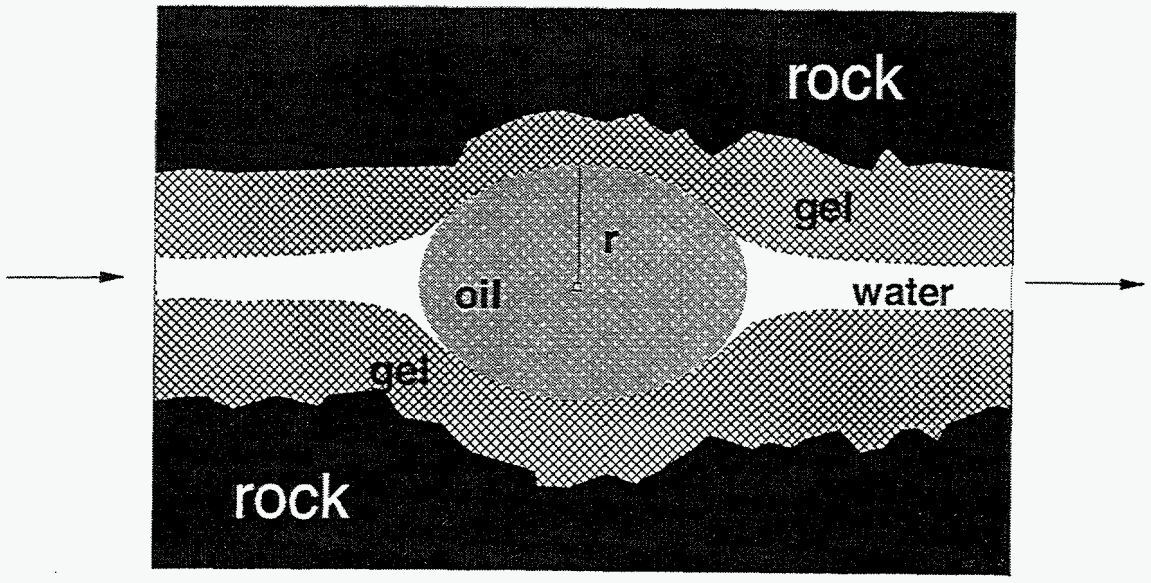

Fig. 57. Effect of capillary forces and gel elasticity on disproportionate permeability reduction.

Effects of Interfacial Tension on Disproportionate Permeability Reduction. For an oil droplet in water, the capillary pressure across the interface, P_c, is proportional to the interfacial tension, σ, divided by the oil-drop radius, r. Reducing the interfacial tension decreases the capillary pressure. With a weaker capillary force to counter a given elastic force from the gel, the radius of the flow channel around the oil droplets is reduced. Therefore, if this theory is valid, lowering the interfacial tension should reduce the permeability to oil while the water permeability should not be affected. In other words, the disproportionate permeability reduction should become less pronounced if the oil-water interfacial tension is reduced. To test this theory, we used an oil-soluble surfactant, Shell Neodol(R) 1-3 (a C_{11} alcohol ethoxylate), to lower the oil-water interfacial tension. The addition of 0.1% surfactant into the oil phase lowered the oil-water interfacial tension from 42.5 dyne/cm to 8 dyne/cm. Incidentally, the critical micelle concentration was 0.1% for this surfactant in 1% NaCl brine at 41°C.

A high-permeability Berea sandstone core was used as the porous medium. In the core experiment, we used an aqueous gel containing 0.5% HPAM (Alcoflood 935), 0.1667% Cr(III)-acetate, and 1% NaCl. Soltrol 130 was the oil used. The core was first saturated with brine (1% NaCl), and permeability and porosity were determined. The core was then oil-flooded, followed by waterflooding. (Tables A-1a through A-1i list endpoint mobilities and residual saturations for all cores used in this study.)

Six PV of gelant were injected into the core at residual water saturation. To delay the gelation during placement, the gelant was injected at room temperature (26°C). After gelant injection, the temperature was raised to 41°C, and the core was shut in for three days to allow the gelation to complete. After the shut-in period, we first injected brine to determine the residual resistance factor for water, F_{rrw}. Because of its high value, F_{rrw} was measured at a single rate of 0.013 ft/d.

Table 16 shows that F_{rrw} was 6,350. Then, oil without surfactant was injected at different flow rates to determine the residual resistance factor for oil, F_{rro}. As shown in Table 16, F_{rro} was Newtonian (flow-rate independent), with a value of 77 (second data row). (Detailed residual-resistance-factor data are listed in Tables A-2a through A-2i.)

Table 16. Summary of F_{rrw} and F_{rro} After Treatment
Core: 420-md Berea Sandstone (SSH-118)
Gel: 0.5% HPAM (Alcoflood 935), 0.1667% Cr(III)-Acetate, and 1% NaCl
Surfactant: 0.1% Shell Neodol(R) 1-3 (a C_{11} Alcohol Ethoxylate)

Injectant	PV injected	Residual resistance factor
brine	0.14	6,350
oil (without surfactant)	12.2	77
oil (with surfactant)	11.7	50
brine	6.5	$143\ u^{-0.54}$

Next, we injected oil with 0.1% surfactant. According to our theory, lowering the interfacial tension should reduce the effective permeability to oil. During oil injection, F_{rro} was Newtonian, with a value of 50 (third data row of Table 16). A comparison of the F_{rro} values with versus without surfactant indicated that lowering the interfacial tension from 42.5 dyne/cm (0% surfactant) to 8 dyne/cm (0.1% surfactant) did not reduce the permeability to oil (i.e., increase F_{rro}). After oil injection, brine was injected again using different flow velocities. During brine injection, F_{rrw} exhibited a strong shear-thinning behavior, which can be described by a power-law equation (fourth data row of Table 16). Table 16 shows that the gel reduced the permeability to water much more than to oil throughout the oil/water injection cycles. These findings do not appear to support the theory that interfacial-tension variations affect the disproportionate permeability reduction. We suspect that the addition of the oil-soluble surfactant in the oil phase may have changed the surface properties of both the water and oil phases. To eliminate this complication, we are searching for a third phase with significantly different surface properties than those of Soltrol 130. Also, the third phase should be insoluble in both Soltrol 130 oil and the brine.

Effects of Gel Elasticity on Disproportionate Permeability Reduction. In concept, increasing gel elasticity should allow the capillary force to open a larger path around the oil droplet, resulting in a higher effective permeability to oil. One way to increase the elasticity of a gel is to incorporate gas into the system. Therefore, if this theory is valid, we expect a gelled foam to show a more pronounced disproportionate permeability reduction. In a previous study,[28] we examined the ability of a gelled foam to reduce permeability to water and oil. Results from core experiments showed that the disproportionate permeability reduction was not more pronounced for a gelled foam than for a gel without foam or gas. This finding does not support the theory. However, we suspect that the gelled foam might not be as compressible as we had hoped in the porous medium.

Another possible way to change the gel elasticity is to quench the gelation reaction at different stages of the gelation process. In this study, we chose a hydroquinone-hexamethylenetetramine-HPAM gel.[56] The gel contained 0.5445% HPAM (Alcoflood 935), 0.25% hydroquinone, 0.1% hexamethylenetetramine, and 1% $NaHCO_3$. This gelant requires high temperatures for the gelation reaction to proceed at a significant rate.[13] Based on our past experience,[13,56] we aged the gelant at 110°C, followed by quenching to 41°C. Two oil/water experiments were performed in high-permeability Berea sandstone cores. (Please refer to Tables A-2g and A-2h in Appendix A for endpoint mobilities.) In both cases, ten PV of the gelant were injected into the core at room temperature (26°C). For the first oil/water experiment, the core was shut in at 110°C for two days. After the two-day shut-in period, the temperature was lowered to 41°C to quench the gelation reaction. For the second oil/water experiment, the core was shut in at 110°C for eight days before lowering the temperature to 41°C. Results from beaker tests showed that with the gelation reaction quenched after two days at 110°C, the gel had a Sydansk gel code[105] of C (flowing gel). The gel with the gelation reaction quenched after 8 days at 110°C was less elastic with a gel code between D and E (between moderately flowing gel and barely flowing gel).

After shut-in, two cycles of oil/water injection were conducted to measure the residual resistance factors. Surprisingly, the two-day gel reduced the permeability to oil significantly more than to water (first data row of Table 17). Table 17 shows that the ratio of F_{rro}/F_{rrw} was about 4 for the two-day gel. Interestingly, the "reversed" disproportionate permeability reduction diminished in the less elastic eight-day gel (second data row of Table 17). At this moment, we don't know why this occurred. More work will be required to understand this unusual phenomenon.

Table 17. Summary of F_{rrw} and F_{rro} After Treatment
Core: High-Permeability Berea Sandstone (SSH-132, SSH-134)
Gel: 0.5445% HPAM (Alcoflood 935), 0.25% hydroquinone,
0.1% hexamethylenetetramine, and 1% $NaHCO_3$, pH=8.4

Days @ 110°C	k_w, md	Sydansk Gel Code[105]	1st F_{rro}	1st F_{rrw}	2nd F_{rro}	2nd F_{rrw}
2	467	C	20	4.7	20	4.2
8	286	D-E	13.6	10.2	14.9	$22\ u^{-0.53}$

In a different approach, we are currently exploring whether the gel elasticity can be changed by varying the system temperature. Conceptually, a gel should become more rigid (less elastic) as we lower the system temperature. Therefore, if this theory is valid, lowering the system temperature should result in a less pronounced disproportionate permeability reduction. Experiments are being performed at different system temperatures to verify this theory.

Visual Glass-Tube Experiments. To reproduce what we observed in the micromodel experiments by Dawe and Zhang,[111] we developed a simple experiment using small glass tubes to visualize the disproportionate permeability reduction. The flat-shaped glass conduits were 0.05-cm high, 0.5-cm wide, and 3 cm in length. A video camera was mounted on a microscope to monitor and record fluid movements in the glass tube. Fig. 58 shows a schematic of the experimental setup. A total of three glass-tube experiments were performed in this study. An

aqueous gel consisting of 0.5% HPAM (Alcoflood 935), 0.0417% Cr(III) acetate, 1% NaCl, and 0.1% $CaCl_2$ was used in the first two experiments. An oil-based gel containing 18% 12-hydroxystearic acid and Soltrol 130 was used in the third experiment. In all experiments, the brine composition was the same as that used for gelant preparation. We used Soltrol 130 oil.

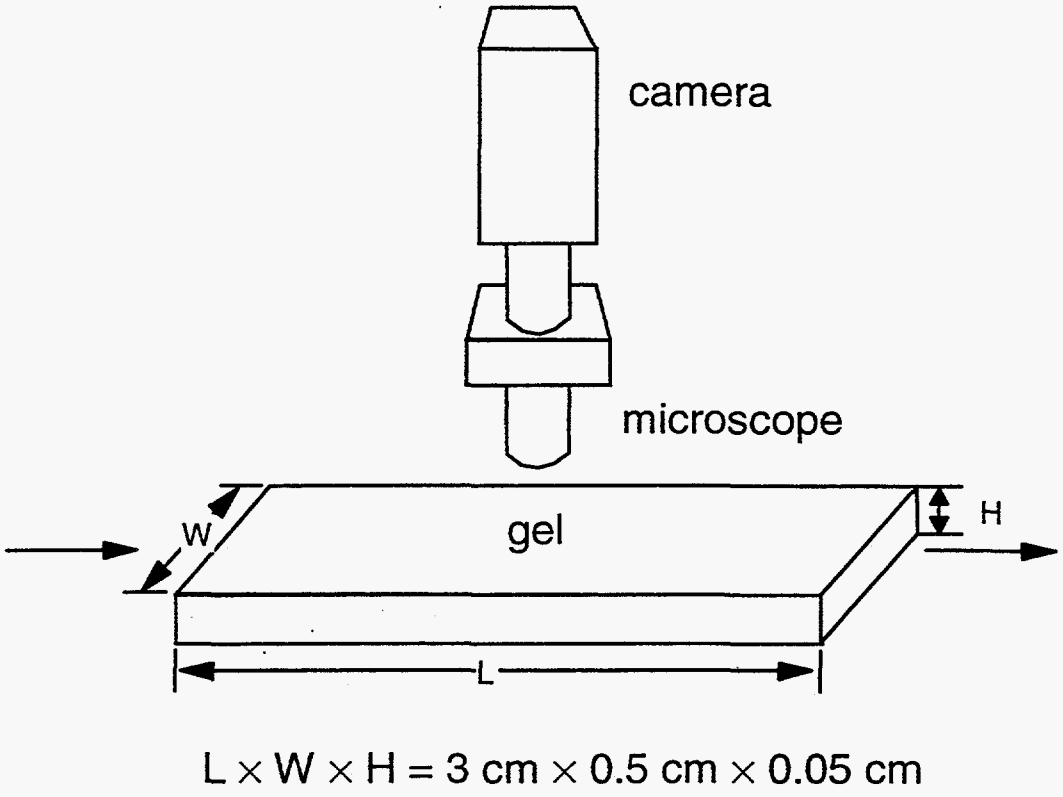

Fig. 58. Schematic of visual glass-tube experiments.

In the first experiment, an aqueous gelant was injected into an empty glass tube at room temperature (26°C). The glass tube was then shut in at 41°C for three days to promote gelation. After the shut-in period, the temperature was lowered to 26°C, and the subsequent steps were conducted at this temperature. After shut-in, a dyed oil (Soltrol 130) was injected into the glass tube at 0.5 cm^3/hr. The pressure drop across the glass tube stabilized at about 0.2 psi (first data row of Table 18). During oil injection, we observed that oil forced its way through the gel by creating a channel through the center of the tube. When oil drops forced their way through the aqueous gel, the gel acted as an elastic material, creating just enough room for the oil drops to squeeze through (as illustrated in Fig. 57). Next, a dyed brine was injected using the same flow rate (0.5 cm^3/hr). The pressure drop across the glass tube was about 3 psi (second data row of Table 18). This number was significantly higher than the 0.2-psi pressure drop during oil injection (first data row of Table 18). Also, we observed that the pathway created during oil injection closed significantly during water injection (apparently because of the elasticity of the gel). The dyed brine diffused evenly through the gel. These observations are consistent with the micromodel results reported by Dawe & Zhang.[111] After brine injection, oil was injected again at 0.5 cm^3/hr, and the pressure drop across the glass tube was 0.3 psi (third data row of Table 18).

Results in Table 18 indicate that the water-based gel reduced the permeability to water significantly more than that to oil.

Table 18. Summary of Pressure Drops After Treatment
Core ID: GTUBE-1 (Glass Tube, 3 cm × 0.5 cm × 0.05 cm)
Gel: 0.5% HPAM, 0.0417% Cr(III)-acetate, 1% NaCl, and 0.1% $CaCl_2$

Injectant	Injection rate, cm^3/hr	Pressure drop, psi
oil	0.5	0.2
brine	0.5	3
oil	0.5	0.3

A similar experiment was conducted using oil with a surfactant to visualize the effect of interfacial tension on disproportionate permeability reduction. After shut-in, we first injected a dyed oil without surfactant (Soltrol 130) into the glass tube at 5 cm^3/hr to establish a baseline for future comparison. Table 19 shows that the pressure drop stabilized at about 0.4 psi (first data row). Next, a dyed brine was injected using the same flow rate (5 cm^3/hr) and the pressure drop across the glass tube was about 1 psi (second data row of Table 19).

Table 19. Summary of Pressure Drops After Treatment
Core ID: GTUBE-2 (Glass Tube, 3 cm × 0.5 cm × 0.05 cm)
Gel: 0.5% HPAM, 0.0417% Cr(III)-acetate, 1% NaCl, and 0.1% $CaCl_2$

Injectant	Injection rate, cm^3/hr	Pressure drop, psi
oil (without surfactant)	5	0.4
brine	5	1
oil (with surfactant)	5	0.9
oil (without surfactant)	5	0.2
oil (with surfactant)	5	0.1

After brine injection, oil with surfactant was injected. The oil-soluble surfactant used in this experiment contained 0.1% Shell Neodol(R) 1-3 (a C_{11} alcohol ethoxylate). This is the same surfactant used in a previous core experiment (SSH-18). The addition of 0.1% surfactant into the oil phase (Soltrol 130) lowered the oil-water interfacial tension from 42.5 dyne/cm (0% surfactant) to 8 dyne/cm. If capillary forces and gel elasticity contribute to the disproportionate permeability reduction, lowering the interfacial tension should result in a lower permeability to oil. In other words, we expected a higher pressure drop when oil with surfactant was injected. Table 19 shows that during surfactant/oil injection, the pressure drop stabilized at about 0.9 psi (third data row). This number was significantly higher than the 0.4 psi observed during the first oil injection without surfactant (first data row of Table 19). To confirm this phenomenon, oil without surfactant was injected again. The pressure drop was indeed lower, stabilizing at about 0.2 psi (fourth data row of Table 19). These findings support the theory that capillary forces and

gel elasticity contribute to disproportionate permeability reduction. However, when oil with surfactant was injected again using the same flow rate (5 cm^3/hr), the pressure drop decreased to 0.1 psi (fifth data row of Table 19). This indicates that mechanical gel breakdown occurred during the process. Visual observations also confirmed that most of the gel washed out during the last oil injection. We intend to repeat this experiment using a stronger gel.

In a previous study,[28] we reported that an oil-based gel can reduce the permeability to oil significantly more than to water. To visualize this disproportionate permeability reduction, we conducted a glass-tube experiment using the oil-based gel, which contained 18% 12-hydroxystearic acid and Soltrol 130. After gelation, a dyed brine was injected into the glass tube at 5 cm^3/hr and the pressure drop was about 5 psi (first data row of Table 20). If capillary forces and gel elasticity contribute to disproportionate permeability reduction, we expected to see water droplets breakthrough the oil-based gel from the center of the glass tube. We also expected the gel to act as an elastic material, creating just enough room for the water droplets to squeeze through. However, during brine injection, the brine did not create a visible channel through the center of the tube. We suspect that the brine diffused through the gel-glass interface. After brine injection, oil was injected into the tube and the pressure drop stabilized at about 6 psi (second data row of Table 20). Oil channeled through the gel-glass interface, separating the gel from the glass surfaces. No further injection was attempted due to the separation of the gel from the glass surfaces. A possible solution to this problem is to increase the bonding between the gel and the glass surface by changing the glass surface to more oil wet.

Table 20. Summary of Pressure Drops After Treatment
Core ID: GTUBE-3 (Glass Tube, 3 cm × 0.5 cm × 0.05 cm)
Gel: 18% 12-hydroxystearic acid and Soltrol 130

Injectant	Injection rate, cm^3/hr	Pressure drop, psi
brine	5	5
oil	5	6

In summary, we have developed a very useful tool in visualizing disproportionate permeability reduction. Tube experiments are much easier to prepare and can be done in a much shorter period of time than micromodel experiments. In our future work, we plan to expand visualization studies in small glass tubes to complement our regular coreflood experiments.

Effects of Rock Permeability on Disproportionate Permeability Reduction

Next, we studied the effects of capillary forces as a function of rock permeability on the disproportionate permeability reduction. The gel used contained 0.5% HPAM (Alcoflood 935), 0.0417% Cr(III)-acetate, and 1% NaCl. Core experiments were performed in a 793-md Berea sandstone core, a 95-md Berea sandstone core, and a 24-md limestone core. During each core experiment, the core was first saturated with brine (1% NaCl), and permeability and porosity were determined. The core was then oil-flooded, followed by waterflooding. (Please refer to Appendix A, Tables A1b-A1d, for endpoint mobilities and residual saturations.)

Ten PV of the gelant were injected into the core at residual oil saturation. To minimize injectivity problems during placement, gelant injections for the two Berea sandstone cores were performed at room temperature (26°C). Due to its low permeability, the gelant injection for the limestone core was performed in an ice-water bath (0°C). (The remainder of the experiments were performed at 41°C.)

After gelant injection, the core was shut in at 41°C for three days. After shut-in, two cycles of oil/water injection were performed to measure the residual resistance factors. To minimize gel breakdown, residual resistance factors were measured using a single flow velocity during the first cycle of oil/water injection. During the second cycle of oil/water injection, the residual resistance factors were measured using different flow velocities. Table 21 summarizes the F_{rrw} and F_{rro} after treatment. The gel reduced permeability to water much more than that to oil in all three cores. The residual resistance factor for oil, F_{rro}, was flow-rate independent. However, the residual resistance factor for water, F_{rrw}, exhibited an apparent shear-thinning behavior that can be described by power-law equations (sixth column of Table 21).

Table 21. Summary of F_{rrw} and F_{rro} After Treatment
Gel: 0.5% HPAM (Alcoflood 935), 0.0417% Cr(III)-Acetate, and 1% NaCl
Oil: Soltrol 130

Core ID	Rock type (Initial k)	1^{st} F_{rro}	1^{st} F_{rrw}	2^{nd} F_{rro}	2^{nd} F_{rrw}
SSH-122	sandstone (793 md)	42	2,450	37	$227\ u^{-0.54}$
SSL-127	sandstone (95 md)	470	2,830	138	$276\ u^{-0.48}$
LSH-128	limestone (24 md)	12	374	12	$42\ u^{-0.51}$

For the Berea sandstone experiments, the gel reduced the permeability to water by about the same factor in 793-md sandstone as in 95-md sandstone (compare F_{rrw} values in the first and second data rows of Table 21). However, the gel reduced the permeability to oil 4 to 11 times more in the 95-md core than in the 793-md core. After two cycles of oil/water injection, the ratio, F_{rrw}/F_{rro}, (at 1 ft/d superficial velocity) was 6.1 in 793-md sandstone and 2.0 in 95-md sandstone (compare the fifth and sixth columns of Table 21). These results suggest that disproportionate permeability reduction may be more pronounced in high-permeability rock than in low-permeability rock.

In the 24-md limestone core, the water and oil residual resistance factors were significantly less than those in the 95-md core (compare the second and third data rows of Table 21). Perhaps, this result was caused by the limestone interfering with the gelation process to a greater extent than in the sandstone. Interestingly, as shown in Table 21, the disproportionate permeability reduction was more pronounced in the 24-md limestone (F_{rrw}/F_{rro}=31 during the first oil/water injection cycle) than in the 95-md sandstone (F_{rrw}/F_{rro}=6 during the first oil/water injection cycle). To eliminate the interference due to mineralogical differences, we are using artificial porous media (e.g., fused glass-bead cores) to study the effects of rock permeability.

Effects of Polymer Washout on Residual Resistance Factors

Results from our oil/water experiments revealed that many gels exhibit a shear-thinning behavior during brine injection—the residual resistance factors for water decrease with increasing fluid velocity.[27,28] In contrast, during oil injection, the residual resistance factors for oil were independent of flow rate. To date, we do not understand why this occurs. Our previous study showed that the non-Newtonian F_{rrw} values were not caused by gel breakdown.[27] Was this non-Newtonian behavior caused by polymer being leached out of the gel during brine injection? In other words, instead of just brine flowing through the porous medium, a polymer solution might flow through the porous medium. Since the polymers were hydrophilic and not soluble in oil, this might explain why we observed non-Newtonian flow behavior only during brine injection and not during oil injection.

Polymer Dissolution and Non-Newtonian Behavior During Brine Injection After Treatment. To test this theory, we performed an oil/water experiment in a high-permeability Berea sandstone core. The gel contained 0.5% HPAM, 0.0417% Cr(III)-acetate, and 1% NaCl. The oil was Soltrol 130. After shut-in, we first injected brine using different flow rates to measure F_{rrw}. In this experiment, we collected effluent samples during each brine injection, and the effluent polymer concentration was measured using a turbidity method.[112] After brine injection, oil was injected to measure F_{rro}. Multiple cycles of water/oil injection were performed.

Fig. 59 plots the effluent polymer concentration versus the cumulative brine pore volumes injected during multiple cycles of brine injection after treatment. During the first brine injection, a total of 12.7 PV of brine were injected using different fluid velocities. Fig. 59 shows that the effluent polymer concentration averaged 800 ppm during the first 0.5 PV of brine injection. It then dropped dramatically during the next pore volume and finally stabilized at about 30 ppm after injecting 5 PV of the brine.

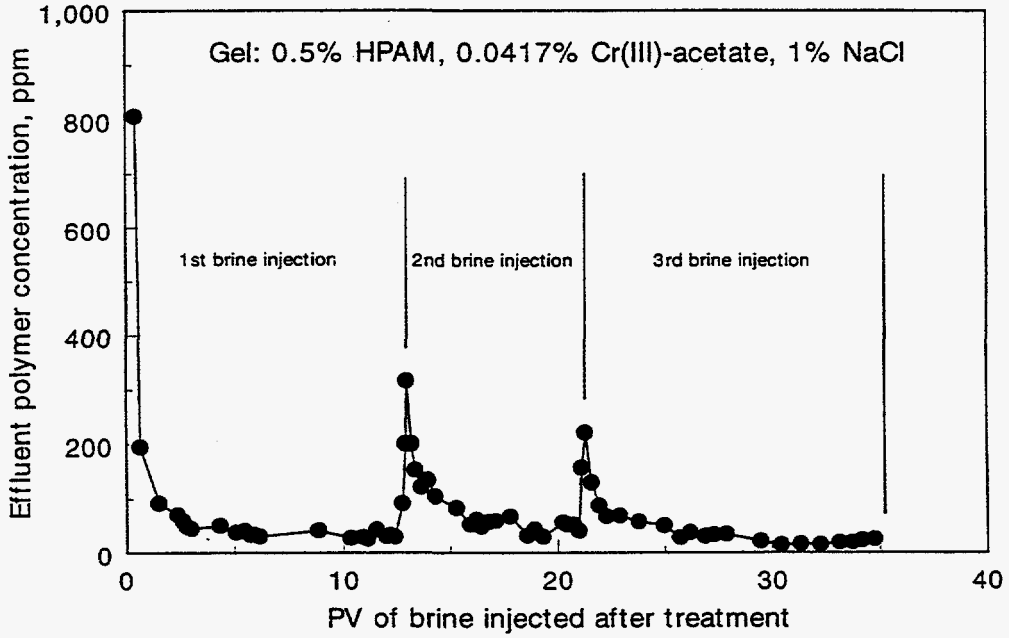

Fig. 59. Effluent polymer concentration versus PV of brine injected after treatment.

Similar behavior was observed during the subsequent brine injections. As shown in Fig. 59, the effluent polymer concentration jumped to a relatively high value each time after switching from oil to brine injection and then quickly stabilized between 20 and 50 ppm. Table 22 shows that during each cycle of brine injection, a strong shear-shinning behavior was observed that can be described by a power-law equation. (The power-law equations in Table 22 were obtained after the stabilization of effluent polymer concentration.) These findings suggest that polymer dissolution in brine is not the cause of the non-Newtonian behavior observed during brine injection after treatment. The polymer concentrations (20 to 50 ppm) were just too low to be responsible for the strong shear-shinning behavior.

Table 22. Summary of F_{rrw} and F_{rro} After Treatment
Core: 679-md Berea Sandstone (SSH-130)
Gel: 0.5% HPAM (Alcoflood 935), 0.0417% Cr(III)-Acetate, and 1% NaCl

Injectant	PV injected	Residual resistance factor
brine	12.74	$889\ u^{-0.30}$
oil	4.93	99
brine	8.35	$469\ u^{-0.38}$
oil	6.23	58
brine	13.85	$354\ u^{-0.34}$

F_{rrw} Versus Amount of Polymer Produced. Table 22 also shows that both F_{rrw} and F_{rro} were lower after each cycle of water/oil injection. We wondered if there was a correlation between the amount polymer produced and F_{rrw}. Fig. 60 plots F_{rrw} versus the fraction of polymer remaining in the porous medium during multiple cycles of brine injection. Fig. 60 shows that the most significant drop in F_{rrw} occurred after the first brine injection at 0.025 ft/d. After that, a linear correlation existed between F_{rrw} and the fraction of polymer remaining in the porous medium. As shown in Fig. 60, for a given fluid velocity, F_{rrw} decreased with decreasing amount of polymer remaining in the porous medium. Fig. 60 projects that the gel should lose its effectiveness (F_{rrw}=0) after producing more than 75% of the original polymer placed. The experiment is continuing to verify this projection.

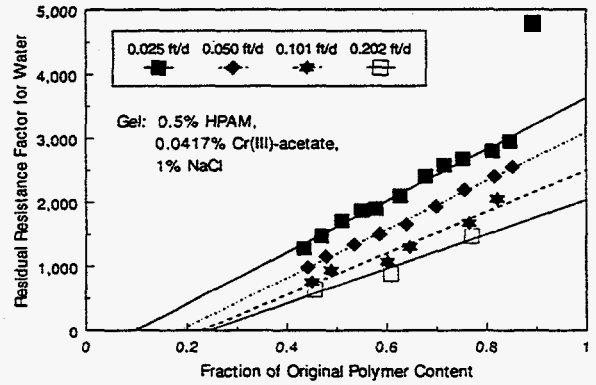

Fig. 60. Effects of polymer produced after treatment on F_{rrw}.

Segregated Oil and Water Pathways

In our previous studies,[27,28] we proposed that the disproportionate permeability reduction might be caused by water and oil following segregated pathways on a microscopic scale (Fig. 61). If (on a microscopic scale) a water-based gelant follows primarily the pathways available to water, then many of the oil pathways could remain open (relatively gel-free) after treatment while most of the water pathways would be blocked by the gel. In this way, the water-based gel could reduce permeability to water more than to oil.

Following the same logic, during high oil fractional flow, if an oil-based gel follows primarily the pathways available to oil on a microscopic scale, then many of the water pathways could remain open after treatment while most of the oil pathways would be blocked by the gel. In support of this theory, we found that an oil-based gel (12-hydroxystearic acid in Soltrol 130) reduced permeability to oil much more than to water.[27,28]

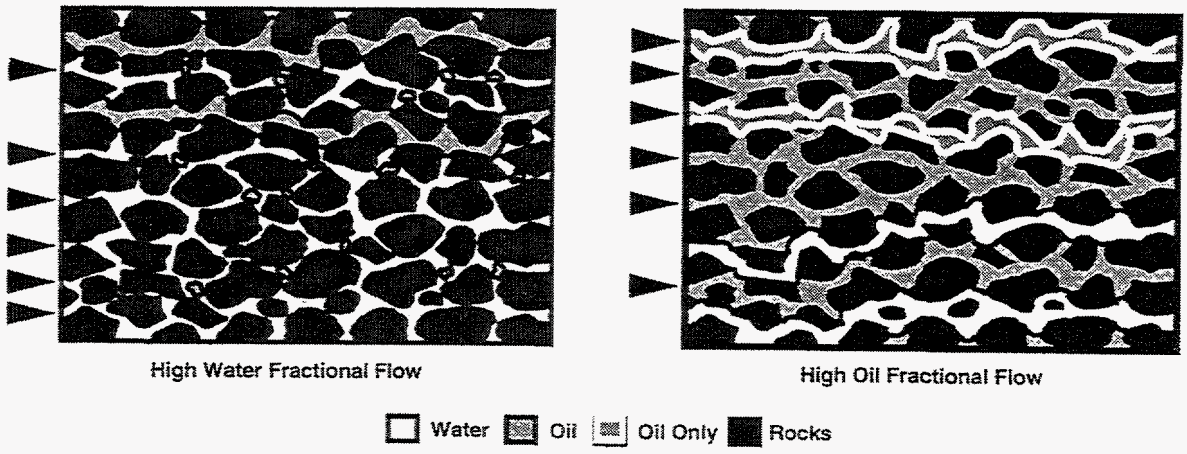

Fig. 61. Segregated oil and water pathways.

If this segregated-pathway theory is valid, we speculate that the disproportionate permeability reduction could be enhanced by simultaneously injecting oil with a water-based gelant or water with an oil-based gelant. Presumably, simultaneous injection of oil and a water-based gelant should allow a larger fraction of oil pathways to remain open than if a water-based gelant is injected by itself. Using similar logic, simultaneous injection of water and an oil-based gelant should allow a larger fraction of water pathways to remain open than if an oil-based gelant is injected by itself.

Simultaneous Injection of Water and an Oil-Based Gelant. To test this theory, we used an oil-based gel containing 18% 12-hydroxystearic acid in Soltrol 130. Two core experiments were performed using high-permeability Berea sandstone cores. (Ref. 13 contains a detailed description of the experiments.) For the base case, the oil-based gelant was injected at residual oil saturation. In the second experiment, the gelant was injected with brine using a 50/50 volume ratio. Table 23 shows that for the case where brine was injected with the gelant during placement, the water residual resistance factor (F_{rrw}=5) was much lower than that for the case where no brine was injected with the gelant (F_{rrw}=34). Interestingly, F_{rro} values were comparable

for both cases (Table 23). These results indicate that the disproportionate permeability reduction was enhanced by the simultaneous injection of water with an oil-based gelant. These findings support the segregated-pathway theory.

Table 23. Summary of F_{rrw} and F_{rro} For an Oil-Based Gel
Cores: High-Permeability Berea Sandstone
Gelant: 18% 12-hydroxystearic acid and Soltrol 130

Gelant/water volume ratio during placement	k_w, md	1st F_{rrw}	1st F_{rro}	2nd F_{rrw}
100/0	599	34	300	30
50/50	586	5	225	14

Simultaneous Injection of Oil and a Water-Based Gelant. We performed similar experiments using a water-based gel to test the validity of the segregated-pathway theory. If this theory is valid, simultaneous injection of oil and a water-based gelant should enhance the disproportionate permeability reduction. Three core experiments were conducted using different gelant/oil volume ratios during placement. These core experiments were performed in high-permeability Berea sandstone cores using a Cr(III)-acetate-HPAM gel. This water-based gel contained 0.5% HPAM (Alcoflood 935), 0.0417% Cr(III) acetate, and 1% NaCl. For the base case, the water-based gelant was injected alone at residual oil saturation. The second and third core experiments were performed using 50/50 and 30/70 gelant/oil volume ratios during placement, respectively. Table 24 shows that, in all three cases, the gel reduced permeability to water significantly more than to oil. The ratio, F_{rrw}/F_{rro}, provides a measure of the disproportionate permeability reduction. This ratio was 58 (i.e., 2,450/42), 46, and 41 for gelant/oil injection ratios of 100/0, 50/50, and 30/70, respectively. Thus, contrary to the case for oil-based gelant injected with water, simultaneous injection of oil with a water-based gelant using gelant/oil injection ratios of 50/50 and 30/70 failed to enhance the disproportionate permeability reduction. These findings do not support the segregated-pathway theory.

Table 24. Summary of F_{rrw} and F_{rro} For a Water-Based Gel
Core: High-Permeability Berea Sandstone (SSH-122, SSH-129, SSH-135)
Gelant: 0.5% HPAM, 0.0417% Cr(III) Acetate, 1% NaCl

Gelant/oil volume ratio during placement	k_w, md	1st F_{rro}	1st F_{rrw}	2nd F_{rro}	2nd F_{rrw}
100/0	793	42	2,450	37	$227\ u^{-0.54}$
50/50	520	27	1,255	16	$141\ u^{-0.31}$
30/70	622	26	1,075	20	$95\ u^{-0.39}$

We suspect that the reason why the simultaneous injection of oil and a water-based gelant failed to enhance the disproportionate permeability reduction is because the volume fraction of oil injected with the gelant was too high during placement. A higher volume fraction of oil during placement would result in more open pathways available to both oil and water flow after treatment. The purpose of the simultaneous injection of oil with an aqueous gelant is to allow a

larger fraction of oil pathways to remain open than if a water-based gelant is injected by itself. Since the gel reduced the permeability to water significantly more than to oil, a small increase in the number of open pathways after treatment could significantly increase the permeability to oil while maintaining a similar level of permeability reduction to water. However, if too many pathways remained open after treatment, the effectiveness of the gel in reducing both the permeability to water and to oil would decrease. Therefore, in our future work, we plan to use higher gelant/oil ratios (e.g., 90/10, 95/5) to study the effects of simultaneous gelant/oil injection on the disproportionate permeability reduction.

Conclusions

Results from oil/water experiments showed that lowering the oil-water interfacial tension from 42.5 dyne/cm to 8 dyne/cm did not result in a lower permeability to oil. This finding does not support the theory that capillary forces and gel elasticity contribute to disproportionate permeability reduction. However, we suspect that the addition of an oil-soluble surfactant may have changed the surface properties of both the water and the oil phases. To eliminate this complication, we are searching for a third phase with significantly different surface properties than those of Soltrol 130.

A hydroquinone-hexamethylenetetramine-HPAM gel (with gelation reaction quenched after two days at 110°C) reduced the permeability to oil more than to water in Berea sandstone. However, this "reverse" disproportionate permeability reduction diminished when a more rigid HQ/HMT-HPAM gel (with gelation reaction quenched after eight days at 110°C) was used. We do not know why this occurred. More work will be needed to understand this unusual phenomenon.

For Berea sandstone, the disproportionate permeability reduction was more pronounced in high-permeability (793-md) rock than in low-permeability (95-md) rock. However, the disproportionate permeability reduction was more pronounced in a 24-md limestone core than in a 95-md sandstone core. Also, for the limestone core, the residual resistance factors both for water and for oil were significantly lower than those in the sandstone cores. Perhaps, the limestone interfered with the gelation process to a greater extent than in the sandstone. To eliminate the interference due to mineralogical differences, we are using artificial porous media (e.g., fused glass-bead cores) to study the effect of rock permeability on the disproportionate permeability reduction.

In a small glass tube (3 cm × 0.5 cm × 0.05 cm), an aqueous gel reduced the permeability to water more than that to oil. During oil injection, we observed that oil droplets forced their way through an aqueous gel. The gel acted as an elastic material, creating just enough room for the oil droplets to squeeze through. During water injection, most of the water flowed through the pathways created by oil, except the pathways were more constricted due to the lack of capillary effects. These findings are consistent with the micromodel results of Dawe and Zhang.[111] We plan to expand our visualization studies of the disproportionate permeability reduction using these small glass tubes.

Results from a core experiment using an aqueous gel indicated that polymer was produced during multiple cycles of water/oil injection after treatment. However, the polymer concentrations in

the brine effluent were too low to be responsible for the strong non-Newtonian behavior observed during brine injection after treatment. For a given fluid velocity, F_{rrw} decreased as the amount of polymer remaining in the porous medium decreased.

Simultaneous injection of oil with an aqueous gel using gelant/oil volume ratios of 50/50, 30/70 did not enhance the disproportionate permeability reduction. These findings do not support the segregated-oil-and-water-pathway theory. However, we suspect that the volume fraction of oil used during placement might be too high. Experiments are being conducted using higher gelant/oil volume ratios.

NOMENCLATURE

A = area, ft^2 [cm^2]
a_r = gel propagation delay factor, PV
D = diffusion coefficient, cm^2/s
C = concentration, g/cm^3
C_o = initial concentration, g/cm^3
c = compressibility, psi^{-1} [Pa^{-1}]
F_r = resistance factor (brine mobility before placement of blocking agent divided by blocking-agent mobility before setting or gelation)
F_{r1} = resistance factor in Zone 1, Core 1, or Fracture 1
F_{r2} = resistance factor in Zone 2, Core 2, or Fracture 2
F_{rr} = residual resistance factor (mobility before placement of blocking agent divided by mobility after placement of blocking agent)
F_{rr1} = residual resistance factor in Zone 1, Core 1, or Fracture 1
F_{rr2} = residual resistance factor in Zone 2, Core 2, or Fracture 2
F_{rro} = oil residual resistance factor
F_{rrw} = water residual resistance factor
G = gravity number
g = acceleration of gravity, ft/s^2 [m/s^2]
h = formation thickness, ft [m]
I = injectivity, bbl/D-psi [m^3/s-Pa]
I_o = initial injectivity, bbl/D-psi [m^3/s-Pa]
k = permeability, md [μm^2]
k_f = effective fracture permeability, darcys
k_i = permeability in Zone i or direction i, md [μm^2]
k_1 = permeability in Zone 1, md [μm^2]
k_2 = permeability in Zone 2, md [μm^2]
L = length or distance of gelant or gel bank length, ft [m]
L_f = effective fracture length, ft [m]
L_m = length of the mixing zone, ft [m]
L_p = distance of blocking-agent penetration, ft [m]
L_{p1} = distance of gel penetration into Core 1, Layer 1, or Fracture 1, ft [m]
L_{p2} = distance of gel penetration into Core 2, Layer 2, or Fracture 2, ft [m]
m_H = slope from Hall plot, psi-D/B [Pa-s/m^3]
P_c = capillary pressure, psi [Pa]
PV = pore volume
p = pressure, psi, [Pa]
p_e = pressure at the external drainage radius, psi [Pa]
p_{wo} = initial pressure at the wellbore, psi [Pa]
p_{w2} = final pressure at the wellbore, psi [Pa]
Δp = pressure drop, psi [Pa]
q = volumetric injection or production rate, bbl/D [m^3/s]
r = radius, tube radius, drop radius or pore radius, ft [m]
r_e = external drainage radius, ft [m]

r_p = radius of penetration, ft [m]
r_{pi} = radius of penetration into Layer i, ft [m]
r_{p1} = radius of penetration into Layer 1, ft [m]
r_{p2} = radius of penetration into Layer 2, ft [m]
r_w = wellbore radius, ft [m]
S_{or} = residual oil saturation
S_w = water saturation
S_{wr} = residual water saturation
s = skin factor
t = time, s
t_g = gelation time, s
t_{tr} = transient time, s
u = superficial or Darcy velocity or flux, ft/d [cm/s]
u_z = vertical superficial velocity, ft/d [cm/s]
α = dispersivity, cm
μ = fluid viscosity, cp [mPa-s]
μ_o = oil viscosity, cp [mPa-s]
μ_p = gelant viscosity, cp [mPa-s]
μ_w = water viscosity, cp [mPa-s]
w = average width, inches [cm]
w_f = average fracture width, inches [cm]
σ = standard deviation, μm or interfacial tension, dyne/cm
ϕ = porosity
ϕ_i = effective aqueous-phase porosity in Zone i, Core i, or Fracture i
ϕ_1 = porosity of Zone 1, Core 1, Fracture 1
ϕ_2 = porosity of Zone 2, Core 2, Fracture 2
θ = dip angle relative to horizontal
ρ = density, g/cm^3
$\Delta\rho$ = density difference, g/cm^3

REFERENCES

1. Seright, R.S.: "Placement of Gels to Modify Injection Profiles," paper SPE/DOE 17332 presented at the 1988 SPE/DOE Enhanced Oil Recovery Symposium, Tulsa, April 17-20.

2. Seright, R.S. and Martin, F.D.: "Fluid Diversion and Sweep Improvement with Chemical Gels in Oil Recovery Processes," second annual report (DOE/BC/14447-10), Contract No. DE-FG22-89BC14447, U.S. DOE (Nov. 1991) 45-55, 56-60, 73-110.

3. Willhite, G.P.: *Waterflooding*, Textbook Series, SPE, Richardson, TX (1986) **3**, 85-115, 170-186.

4. Seright, R.S.: "Effect of Rheology on Gel Placement," *SPERE* (May 1991) 212-218; *Trans.* AIME, **291**.

5. Vela, S., Peaceman, D.W., and Sandvik, E.I.: "Evaluation of Polymer Flooding in a Layered Reservoir With Crossflow, Retention, and Degradation," *SPEJ* (April 1976) 82-96.

6. Jennings, R.R., Rogers, J.H., and West, T.J.: "Factors Influencing Mobility Control By Polymer Solutions," *JPT* (March 1971) 391-401.

7. Zaitoun, A. and Kohler, N.: "The Role of Adsorption in Polymer Propagation Through Reservoir Rocks," paper SPE 16274 presented at the 1987 SPE International Symposium on Oilfield Chemistry, San Antonio, Oct. 4-6.

8. Seright, R.S.: "Impact of Permeability and Lithology on Gel Performance," paper SPE 24190 presented at the 1992 SPE/DOE Symposium on Enhanced Oil Recovery, Tulsa, April 22-24.

9. Seright, R.S. and Martin, F.D.: "Impact of Gelation pH, Rock Permeability, and Lithology on the Performance of a Monomer-Based Gel," *SPERE* (Feb. 1993) 43-50.

10. Seright, R.S.: "Improved Techniques for Fluid Diversion in Oil Recovery Processes," first annual report (DOE/BC/14880-5), Contract No. DE-AC22-92BC14880, U.S. DOE (Dec. 1993) 1-72, 73-80, 95-100, 101-140, 166-181.

11. Seright, R.S. and Martin, F.D.: "Fluid Diversion and Sweep Improvement with Chemical Gels in Oil Recovery Processes," first annual report (DOE/BC/14447-8), Contract No. DE-FG22-89BC14447, U.S. DOE (June 1991), 34-55, 80-86.

12. Seright, R.S. and Liang, J.: "A Survey of Field Applications of Gel Treatments for Water Shutoff," paper SPE 26991 presented at the 1994 SPE III Latin American & Caribbean Petroleum Engineering Conference, Buenos Aires, April 27-29.

13. Seright, R.S.: "Improved Techniques for Fluid Diversion in Oil Recovery Processes," second annual report (DOE/BC/14880-10), Contract No. DE-AC22-92BC14880, U.S. DOE (March 1995) 1-29, 30-50, 51-64, 65-113, 114-128, 147-158.

14. Hill, A.D.: *Production Logging—Theoretical and Interpretive Elements*, Monograph Series, SPE, Richardson, TX (1990) **14**, 19-36, 37-75.

15. Buell, R.S., Kazemi, H., and Poettmann, F.H.: "Analyzing Injectivity of Polymer Solutions with the Hall Plot," *SPERE* (Feb. 1990) 41-46.

16. Seright, R.S.: "Use of Preformed Gels for Conformance Control in Fractured Systems," paper SPE 35351 presented at the 1996 SPE/DOE Symposium on Improved Oil Recovery, Tulsa, April 21-24.

17. Seright, R.S.: "Gel Placement in Fractured Systems," *SPEPF* (Nov. 1995) 241-248.

18. Liang, J., Lee, R.L., and Seright, R.S.: "Placement of Gels in Production Wells," *SPEPF* (Nov. 1993) 276-284; *Transactions* AIME **295**.

19. Needham, R.B., Threlkeld, C.B., and Gall, J.W.: "Control of Water Mobility Using Polymers and Multivalent Cations," paper SPE 4747 presented at the 1974 SPE-AIME Improved Oil Recovery Symposium, Tulsa, April 22-24.

20. Sandiford, B.B. and Graham, G.A.: "Injection of Polymer Solutions in Producing Wells," AIChE Symposium Series, (1973) **69**, No. 127, 38.

21. Schneider, F.N. and Owens, W.W.: "Steady-State Measurements of Relative Permeability for Polymer/Oil Systems," *SPEJ* (Feb. 1982) 79.

22. Sparlin, D.D.: "An Evaluation of Polyacrylamides for Reducing Water Production," *JPT* (Aug. 1976) 906-914.

23. White, J.L., Goddard, J.E., and Phillips, H.M.: "Use of Polymers To Control Water Production in Oil Wells," *JPT* (Feb. 1973) 143-150.

24. Zaitoun, A., Kohler N., and Guerrini, Y.: "Improved Polyacrylamide Treatments for Water Control in Producing Wells," *JPT* (July 1991) 862-867.

25. Seright, R.S., Liang, J., and Sun, H.: "Gel Treatments in Production Wells with Water-Coning Problems," *In Situ* (1993) **17**, No. 3, 243-72.

26. Seright, R.S.: "Reduction of Gas and Water Permeabilities Using Gels," *SPEPF* (May 1995) 103-108.

27. Liang, J., Sun, H., Seright, R.S.: "Why Do Gels Reduce Water Permeability More Than Oil Permeability?," *SPERE* (Nov. 1995) 282-286.

28. Seright, R.S.: "Improved Techniques for Fluid Diversion in Oil Recovery Processes," final report (DOE/BC/14880-15), Contract No. DE-AC22-92BC14880, U.S. DOE (Jan. 1996) 3-61, 62-89, 90-113.

29. Seright, R.S. and Martin, F.D.: "Effect of Cr^{3+} on the Rheology of Xanthan Formulations in Porous Media: Before and After Gelation," *In Situ* (1992) **16**, No.1, 1-16.

30. Hejri, S. *et al.*: "Permeability Reduction by a Xanthan/Cr(III) System in Porous Media," *SPERE* (Nov. 1993) 299-304.

31. Todd, B.J., Green, D.W., and Willhite, G.P.: "A Mathematical Model of In-Situ Gelation of Polyacrylamide by a Redox Process," *SPERE* (Feb. 1993) 51-58.

32. Zitha, P., Chauveteau, G., and Zaitoun, A.: "Permeability-Dependent Propagation of Polyacrylamides Under Near-Wellbore Flow Conditions," paper SPE 28955 presented at the 1995 SPE International Symposium on Oilfield Chemistry, San Antonio, Feb. 14-17.

33. Stavland, A. *et* al.: "Evaluation of Xanthan-Cr(III) Gels for Deep Emplacement: Retention of Cr(III) in North Sea Sandstone Reservoirs," presented at the 7th European IOR Symposium in Moscow, Oct. 27-29, 1993.

34. Kolnes, J. and Nilsson, S.: "Effect of the Core Material on Gelation of a HPAM/Chromium System at High Temperature," paper SPE/DOE 35377 presented at the 1996 SPE/DOE Symposium on Improved Oil Recovery, Tulsa, April 21-24.

35. Dovan, H.T. and Hutchins, R.D.: "New Polymer Technology for Water Control in Gas Wells," *SPEPF* (Nov. 1994) 280-286.

36. Erdey-Gruz, T.: *Transport Phenomena in Aqueous Solutions*, John Wiley, New York (1974) 151-163.

37. Southwick, J.G., Jamieson, A.M., and Blackwell, J.: "Conformation of Xanthan Dissolved in Aqueous Urea and Sodium Chloride Solutions," *Carbohydrate Research* (1982) **99**, 117-127.

38. Perkins, T.K. and Johnston, O.C.: "A Review of Diffusion and Dispersion in Porous Media,' *SPEJ* (March 1963) 70-84.

39. Prud'homme, R.K. and Uhl, J.T.: "Kinetics of Polymer/Metal-Ion Gelation," paper SPE/DOE 12640 presented at the 1984 SPE/DOE Symposium on Enhanced Oil Recovery, Tulsa, April 15-18.

40. Southard, M.Z., Green, D.W., and Willhite, G.P.: "Kinetics of the Chromium(VI)/Thiourea Reaction in the Presence of Polyacrylamide," paper SPE/DOE 12715 presented at 1984 the SPE/DOE Enhanced Oil Recovery Symposium, Tulsa, April 15-18.

41. Arya, A. et al.: "Dispersion and Reservoir Heterogeneity," *SPERE* (Feb. 1988) 139-148.

42. Seright, R.S.: "Impact of Dispersion on Gel Placement for Profile Control," *SPERE* (Aug. 1991) 343-352.

43. Daccord, G.: "Acidizing Physics" in *Reservoir Stimulation, 2nd ed.*, M.J. Economides and K.G. Nolte, eds., Prentice Hall, Houston (1989) 13-1-13.

44. Sorbie, K.S. and Seright, R.S.: "Gel Placement in Heterogeneous Systems with Crossflow," paper SPE 24192 presented at the 1992 SPE/DOE Symposium on Enhanced Oil Recovery, Tulsa, April 22-24.

45. Coats, K.H., Dempsey, J.R., and Henderson, J.H.: "The Use of Vertical Equilibrium in Two-Dimensional Simulation of Three-Dimensional Reservoir Performance," *SPEJ* (March 1971) 63-71.

46. Zapata, V.J. and Lake, L.W.: "A Theoretical Analysis of Viscous Crossflow," paper SPE 10111 presented at the 1981 SPE Annual Technical Conference and Exhibition, San Antonio, Oct. 5-7.

47. Fletcher, A.J.P. *et al.*: "Deep Diverting Gels for Very Cost-Effective Waterflood Control," *J. Polym. Sci. & Eng.* (April 1992) 7(1-2) 33-43.

48. Kvanvik, B.A. *et al.*: "An Evaluation of Stable Gel Systems for Deep Injector Treatments and High-Temperature Producer Treatments," presented at the 8th European IOR Symposium, Vienna, Austria, May 15-17, 1995

49. Lockhart, T.P.: "Chemical Properties of Chromium/Polyacrylamide Gels," *SPE Adv. Technology Series* (April 1994) **2**, No. 2, 199-205.

50. Lockhart, T.P. and Albonico, P.: "New Chemistry for the Placement of Chromium(III)/Polymer Gels in High-Temperature Reservoirs," *SPEPF* (Nov. 1994) 273-279.

51. Albonico, P. and Lockhart, T.P.: "Divalent Ion-Resistant Polymer Gels for High-Temperature Applications: Syneresis Inhibiting Additives," paper SPE 25220 presented at the 1993 SPE International Symposium on Oilfield Chemistry, New Orleans, March 2-5.

52. Albonico, P. *et al.*: "Effective Gelation-Delaying Additives for Cr^{+3}/Polymer Gels," paper SPE 25221 presented at the 1993 SPE International Symposium on Oilfield Chemistry, New Orleans, March 2-5.

53. Albonico, P. *et al.*: "Studies on Phenol-Formaldehyde Crosslinked Polymer Gels in Bulk and in Porous Media," paper SPE 25221 presented at the 1995 SPE International Symposium on Oilfield Chemistry, New Orleans, Feb. 14-17.

54. Moradi-Araghi, A., Bjornson, G., and Doe, P.H.: "Thermally Stable Gels for Near-Wellbore Permeability Contrast Corrections," *SPE Advanced Technology Series* (June 1993) **1**, No. 1, 140-145.

55. Moradi-Araghi, A.: "Application of Low-Toxity Crosslinking Systems in Production of Thermally Stable Gels," paper SPE 27826 presented at the 1994 SPE/DOE Symposium on Improved Oil Recovery, Tulsa, April 17-20.

56. Whitney, D.D., Montgomery, D.W., and Hutchins, R.D.: "Water Shutoff in the North Sea: Testing a New Polymer Gel System in the Heather Field, UKCS Block 2/5," *SPEPF* (May 1996) 108-112.

57. Midha, V. *et al.*: "Modeling the Effect of Filtration of Pre-Gel Aggregates on Gel Placement in Layered Reservoirs with Crossflow," presented at the 1996 SPE/DOE Symposium on Improved Oil Recovery, Tulsa, April 21-24.

58. Breston, J.N.: "Selective Plugging of Waterflood Input Wells Theory, Methods and Results," *JPT* (March 1957) 26-31.

59. Matthews, C.S. and Russell, D.G.: *Pressure Buildup and Flow Tests in Wells*, Monograph Series, SPE, Richardson, TX (1967) **1**, 48.

60. Lake, L.W.: "The Origins of Anisotropy," *JPT* (April 1988) 395-396.

61. Elkins, L.F. and Skov, A.M.: "Determination of Fracture Orientation from Pressure Interference," *JPT* (Dec. 1960) 301-304; *Trans.*, AIME, **219.**

62. Ramey, H.J.: "Interference Analysis for Anisotropic Formations—A Case History," *JPT* (Oct. 1975) 1290-1298; *Trans.*, AIME, **259**.

63. Ye, M. and Seright, R.S.: "Gel Placement in Anisostropic Flow Systems," *In Situ* (1996) **20**, No.2, 115-135.

64. Dake, L.P.: *Fund. of Reservoir Engineering*, Elsevier Scientific Publishing Co., New York (1982) **110**, 343-430.

65. Williams, B.B., Gidley, J.L., and Schechter, R.S.: *Acidizing Fundamentals*, Monograph Series, SPE, Richardson, TX (1979) **6**, 99-100.

66. Davidson, D.H.: "Invasion and Impairment of Formations by Particulates," paper SPE 8210 presented at the 1979 SPE Annual Technical Conference and Exhibition, Las Vegas, Sept. 23-26.

67. Baghdikian, S.Y., Sharma, M.M., and Handy, L.L.: "Flow of Clay Suspensions Through Porous Media," *SPERE* (May 1989) 213-220.

68. Eleri, O.O. and Ursin, J-R.: "Physical Aspects of Formation Damage in Linear Flooding Experiments," paper SPE 23784 presented at the 1992 International Symposium on Formation Damage Control, Lafayette, Feb. 26-27.

69. Tien, C. and Payatakes, A.C.: "Advances in Deep Bed Filtration," *AIChE Journal* (1979) **25**, No. 5, 737-759.

70. Vetter, O.J., Kandarpa, V., Stratton, M., and Veith, E.: "Particle Invasion Into Porous Medium and Related Injectivity Problems," paper SPE 16255 presented at the 1987 International Symposium on Oilfield Chemistry, San Antonio, Feb. 4-6.

71. van Oort, E., van Velzen, J.F.G., and Leerlooijer, K.: "Impairment by Suspended Solids Invasion: Testing and Prediction," *SPEPF* (Aug. 1993) 178-184.

72. Houchin, L.R. *et al.*: "Evaluation of Oil-Soluble Resin as an Acid-Diverting Agent," paper SPE 15574 presented at the 1986 SPE Annual Technical Conference and Exhibition, New Orleans, Oct. 5-8.

73. Thompson, K.E. and Fogler, H.S.: "A Study of Diversion Mechanisms by Reactive Water-Diverting Agents," paper SPE 25222 presented at the 1993 SPE International Symposium on Oilfield Chemistry, New Orleans, March 2-5.

74. Llave F.M. and Dobson, R.E.: "Field Application of Surfactant-Alcohol Blends for Conformance Control," paper SPE 28618 presented at the 1994 SPE Annual Technical Conference and Exhibition, New Orleans, Sept. 25-28.

75. Bae, J.H., Chambers, K.T., and Lee, H.O.: "Microbial Profile Modification Using Spores," paper SPE 28617 presented at the 1994 SPE Annual Technical Conference and Exhibition, New Orleans, Sept. 25-28.

76. Friedmann, F. *et al.*: "Steam Foam Mechanistic Field Trial in the Midway-Sunset Field," paper SPE 21780 presented at the 1991 SPE Western Regional Meeting, Long Beach, March 20-22.

77. Gauglitz, P.A. *et al.*: "Field Optimization of Steam/Foam for Profile Control," paper SPE 25781 presented at the 1993 International Thermal Operations Symposium, Bakersfield, Feb. 8-10.

78. Stevens, J.E. and Martin, F.D: "CO_2 Foam Field Verification Pilot Test at EVGSAU: Phase IIIB—Project Operations and Performance Review," paper SPE 27786 presented at the 1994 SPE/DOE Symposium on Improved Oil Recovery, Tulsa, April 17-20.

79. Harpole, K.J., Siemers, W.T., and Gerard, M.G.: "CO_2 Foam Field Verification Pilot Test at EVGSAU: Phase IIIC—Reservoir Characterization and Response to Foam Injection," paper SPE 27798 presented at the 1994 SPE/DOE Symposium on Improved Oil Recovery, Tulsa, April 17-20.

80. Hoefner, M.L. *et al.*: "CO_2 Foam: Results From Four Developmental Field Trials," paper SPE 27787 presented at the 1994 SPE/DOE Symposium on Improved Oil Recovery, Tulsa, April 17-20.

81. Kuehne, D.L. *et al.*: "Design and Evaluation of a Nitrogen-Foam Field Trial," *JPT* (April 1990) 504-512.

82. Nimir, H.B. and Seright, R.S.: "Placement Properties of Foams Versus Gelants When Used as Blocking Agents," paper SPE 35172 presented at the 1996 SPE Permian Basin Oil & Gas Recovery Conference, Midland, March 27-29.

83. Khatib, Z.I., Hirasaki, G.J., and Falls, A.H.: "Effects of Capillary Pressure on Coalescence and Phase Mobilities in Foams Flowing Through Porous Media," *SPERE* (Aug. 1988) 919-926.

84. Zhou, Z.H. and Rossen, W.R.: "Applying Fractional-Flow Theory to Foam Processes at the Limiting Capillary Pressure," paper SPE 24180 presented at the 1992 SPE/DOE Symposium on Enhanced Oil Recovery, Tulsa, April 22-24.

85. Kovscek, A.R., Patzek, T.W., and Radke, C.J.: "Mechanistic Prediction of Foam Displacement in Multidimensions: A Population Balance Approach," paper SPE 27789 presented at the 1994 SPE/DOE Symposium on Improved Oil Recovery, Tulsa, April 17-20.

86. Eson, R.L. and Cooke, R.W.: "A Successful High-Temperature Gel System to Reduce Steam Channeling," paper SPE 24665 presented at the 1992 SPE Annual Technical Conference and Exhibition, Washington, D.C., Oct. 4-7.

87. Craighead, M.S., Hossaini, M., and Freeman, E.R.: "Foam Fracturing Utilizing Delayed Crosslinked Gels," paper SPE 14437 presented at the 1985 SPE Annual Technical Conference and Exhibition, Las Vegas, Sept. 22-25.

88. Bernard, G.G. and Holm, L.W.: "Effect of Foam on Permeability of Porous Media to Gas," *SPEJ* (Sept. 1964) 267-274.

89. Bernard, G.G., Holm, L.W., and Jacobs, W.L.: "Effect of Foam on Trapped Gas Saturation and on Permeability of Porous Media to Water," *SPEJ* (Dec. 1965) 295-300.

90. Miller, M.J. and Fogler, H.S.: "A Mechanistic Investigation of Waterflood Diversion Using Foamed Gels," paper SPE 24662 presented at the 1992 SPE Annual Technical Conference and Exhibition, Washington, D.C., Oct. 4-7.

91. Sydansk, R.D.: "Polymer-Enhanced Foams," *SPE Advanced Technology Series* (April 1994) **2**, No. 2, 150-166.

92. Alvarado, D.A. and Marsden, S.S.: "Flow of Oil-in-Water Emulsions Through Tubes and Porous Media," *SPEJ* (Dec. 1979) 369-377.

93. Gogarty, W.B.: "Rheological Properties of Pseudoplastic Fluids in Porous Media," *SPEJ* (June 1967) 149-160.

94. Soo, H. and Radke, C.J.: "The Flow Mechanism of Dilute, Stable Emulsions in Porous Media," *I&EC Fundamentals* (1984) **23**, 342-347.

95. Soo, H. and Radke, C.J.: "A Filtration Model for the Flow of Dilute, Stable Emulsions in Porous Media," *Chemical Engineering Science* (1986) **41**, No. 2, 263-281.

96. McAuliffe, C.D.: "Oil-in-Water Emulsions and Their Flow Properties in Porous Media," *JPT* (June 1973) 727-733.

97. Lane, R.H. and Sanders, G.S.: "Water Shutoff Through Fullbore Placement of Polymer Gel in Faulted and in Hydraulically Fractured Producers of the Prudhoe Bay Field," paper SPE 29475 presented at the 1995 SPE Production Operations Symposium, Oklahoma City, April 2-4.

98. Sanders, G.S., Chambers, M.J., and Lane, R.H.: "Successful Gas Shutoff With Polymer Gel Using Temperature Modeling and Selective Placement in the Prudhoe Bay Field," paper SPE 28502 presented at the 1994 SPE Annual Technical Conference and Exhibition, New Orleans, September 25-28.

99. Dalrymple, D., Takington, J.T., and Hallock, J.: "A Gelation System for Conformance Technology," paper SPE 28503 presented at the 1994 SPE Annual Technical Conference and Exhibition, New Orleans, September 25-28.

100. Sydansk, R.D. and Moore, P.E.: "Gel Conformance Treatments Increase Oil Production in Wyoming," *Oil & Gas J.* (Jan. 20, 1992) 40-45.

101. Moffitt, P.D.: "Long-Term Production Results of Polymer Treatments on Producing Wells in Western Kansas," *JPT* (April 1993) 356-362.

102. Borling, D.C.: "Injection Conformance Control Case Histories Using Gels at the Wertz Field CO_2 Teriary Flood in Wyoming, USA," paper SPE 27825 presented at the 1994 SPE/DOE Symposium on Improved Oil Recovery, April 17-20.

103. Odorisio, V.G. and Curtis, S.C.: "Operational Advances from Field Application of Short-Radius Horizontal Drilling in the Yates Field Unit," paper SPE 24612 presented at the 1992 SPE Annual Technical Conference and Exhibition, Washington, D.C., Oct. 4-7.

104. Bird, R.B., Stewart, W.E., and Lightfoot, E.N.: *Transport Phenomena*, John Wiley & Sons, New York (1960) 46, 62.

105. Sydansk, R.D.: "A Newly Developed Chromium(III) Gel Technology," *SPERE* (Aug. 1990) 346-352.

106. Penny, G.S. and Conway, M.W.: "Fluid Leakoff," *Recent Advances in Hydraulic Fracturing*, Monograph Series, SPE, Richardson, TX, (1989) **12**, 147.

107. Liang, J., Sun, H., and Seright, R.S.: "Reduction of Oil and Water Permeabilities Using Gels," paper SPE 24195 presented at the 1992 SPE/DOE Symposium on Enhanced Oil Recovery, Tulsa, April 22-24.

108. Avery, M.R. and Wells, T.A.: "Field Evaluation of a New Gelant for Water Control in Production Wells," paper SPE 18201 presented at the 1988 SPE Annual Technical Conference and Exhibition, Houston, Oct. 2-5.

109. Zaitoun, A. and Kohler N.: "Two-Phase Flow Through Porous Media: Effect of an Adsorbed Polymer Layer," paper SPE 18085 presented at the 1988 SPE Annual Technical Conference and Exhibition, Houston, Oct. 2-5.

110. Zaitoun, A. and Kohler N.: "Thin Polyacrylamide Gels for Water Control in High-Permeability Production Wells," paper SPE 22785 presented at the 1991 SPE Annual Technical Conference and Exhibition, Dallas, Oct. 6-9.

111. Dawe, R.A. and Zhang, Y.: "Mechanistic study of the selective action of oil and water penetrating into a gel emplaced in a porous medium," *Journal of Petroleum Science and Engineering* (1994) 12, 113-125.

112. Foshee, W.C., Jennings, R.R., and West, T.J.: "Preparation and Testing of Partially Hydrolyzed Polyacrylamide Solutions," paper SPE 6202 presented at the 1976 SPE Annual Technical Conference and Exhibition, New Orleans, Oct. 3-6.

APPENDIX A: Data Supplement for Chapter 6

Table A-1a. Summary of Water and Oil Mobilities Before Gel Treatment
(Core SSH-118, High-Permeability Berea Sandstone, Strongly Water-Wet, 41°C)

$(k/\mu)_w$, md/cp @ $S_w = 1.0$	$(k/\mu)_o$, md/cp @ $S_{wr} = 0.3$	$(k/\mu)_w$, md/cp @ $S_{or} = 0.34$
700	432	104

Table A-1b. Summary of Water and Oil Mobilities Before Gel Treatment
(Core SSH-122, High-Permeability Berea Sandstone, Strongly Water-Wet, 41°C)

$(k/\mu)_w$, md/cp @ $S_w = 1.0$	$(k/\mu)_o$, md/cp @ $S_{wr} = 0.27$	$(k/\mu)_w$, md/cp @ $S_{or} = 0.36$
793	737	154

Table A-1c. Summary of Water and Oil Mobilities Before Gel Treatment
(Core SSL-127, Low-Permeability Berea Sandstone, Strongly Water-Wet, 41°C)

$(k/\mu)_w$, md/cp @ $S_w = 1.0$	$(k/\mu)_o$, md/cp @ $S_{wr} = 0.33$	$(k/\mu)_w$, md/cp @ $S_{or} = 0.35$
158	91	154

Table A-1d. Summary of Water and Oil Mobilities Before Gel Treatment
(Core LSH-128, Limestone, 41°C)

$(k/\mu)_w$, md/cp @ $S_w = 1.0$	$(k/\mu)_o$, md/cp @ $S_{wr} = 0.38$	$(k/\mu)_w$, md/cp @ $S_{or} = 0.29$
40	22	17

Table A-1e. Summary of Water and Oil Mobilities Before Gel Treatment
(Core SSH-129, High-Permeability Berea Sandstone, Strongly Water-Wet, 41°C)

$(k/\mu)_w$, md/cp @ $S_w = 1.0$	$(k/\mu)_o$, md/cp @ $S_{wr} = 0.29$	$(k/\mu)_w$, md/cp @ $S_{or} = 0.34$
866	531	148

Table A-1f. Summary of Water and Oil Mobilities Before Gel Treatment
(Core SSH-130, High-Permeability Berea Sandstone, Strongly Water-Wet, 41°C)

$(k/\mu)_w$, md/cp @ $S_w = 1.0$	$(k/\mu)_o$, md/cp @ $S_{wr} = 0.27$	$(k/\mu)_w$, md/cp @ $S_{or} = 0.37$
1132	653	259

Table A-1g. Summary of Water and Oil Mobilities Before Gel Treatment
(Core SSH-132, High-Permeability Berea Sandstone, Strongly Water-Wet, 41°C)

$(k/\mu)_w$, md/cp @ $S_w = 1.0$	$(k/\mu)_o$, md/cp @ $S_{wr} = 0.36$	$(k/\mu)_w$, md/cp @ $S_{or} = 0.25$
778	518	131

Table A-1h. Summary of Water and Oil Mobilities Before Gel Treatment
(Core SSH-134, High-Permeability Berea Sandstone, Strongly Water-Wet, 41°C)

$(k/\mu)_w$, md/cp @ $S_w = 1.0$	$(k/\mu)_o$, md/cp @ $S_{wr} = 0.31$	$(k/\mu)_w$, md/cp @ $S_{or} = 0.29$
476	323	96

Table A-1i. Summary of Water and Oil Mobilities Before Gel Treatment
(Core SSH-135, High-Permeability Berea Sandstone, Strongly Water-Wet, 41°C)

$(k/\mu)_w$, md/cp @ $S_w = 1.0$	$(k/\mu)_o$, md/cp @ $S_{wr} = 0.29$	$(k/\mu)_w$, md/cp @ $S_{or} = 0.31$
1036	573	200

Table A-2a. Summary of Residual Resistance Factors-Core SSH-118
Core: 420-md Berea Sandstone
Gel: 0.5% HPAM (Alcoflood 935), 0.1667% Cr(III)-Acetate, 1% NaCl
Surfactant: 0.1% Shell NEODOL® 1-3 (a C_{11} Alcohol Ethoxylate)

1^{st} waterflood		
Flux, ft/d	F_{rrw} (1^{st} short core segment)	F_{rrw} (Center core segment)
0.013	2,015	6,350
1^{st} oilflood without surfactant		
Flux, ft/d	F_{rro} (1^{st} short core segment)	F_{rro} (Center core segment)
3.937	53	77
1.969	32	80
2.756	27	74
Average F_{rro} (across center segment) = 77		
1^{st} oilflood with surfactant		
Flux, ft/d	F_{rro} (1^{st} short core segment)	F_{rro} (Center core segment)
2.756	27	50
1.969	30	51
Average F_{rro} (across center segment) = 50.5		
2^{nd} oilflood without surfactant		
Flux, ft/d	F_{rro} (1^{st} short core segment)	F_{rro} (Center core segment)
2.756	22	52
1.969	24	43
Average F_{rro} (across center segment) = 47.5		

Table A-2a. Summary of Residual Resistance Factors-Core SSH-118 (Cont'd)
Core: 420-md Berea Sandstone
Gel: 0.5% HPAM (Alcoflood 935), 0.1667% Cr(III)-Acetate, 1% NaCl
Surfactant: 0.1% Shell NEODOL® 1-3 (a C_{11} Alcohol Ethoxylate)

2^{nd} waterflood		
Flux, ft/d	F_{rrw} (1^{st} short core segment)	F_{rrw} (Center core segment)
0.025	96	1,040
0.50	160	750
0.101	102	545
0.05	166	800
0.202	80	380
0.101	115	505
0.05	144	640
0.394	66	225
0.202	94	340
0.101	108	440
0.05	160	670
0.394	70	228
F_{rrw} (across center segment, last five data points) = 143 $u^{-0.54}$, r=0.9858		
3^{rd} oilflood without surfactant		
Flux, ft/d	F_{rro} (1^{st} short core segment)	F_{rro} (Center core segment)
25.2	2	9
12.6	5	8
25.2	4	7
Average F_{rro} (across center segment) = 8		

Table A-2b. Summary of Residual Resistance Factors-Core SSH-122
Core: 793-md Berea Sandstone
Gel: 0.5% HPAM (Alcoflood 935), 0.0417% Cr(III)-Acetate, 1% NaCl

1^{st} oilflood		
Flux, ft/d	F_{rro} (1^{st} short core segment)	F_{rro} (Center core segment)
3.15	20	42
1^{st} waterflood		
Flux, ft/d	F_{rrw} (1^{st} short core segment)	F_{rrw} (Center core segment)
0.025	130	2,450
2^{nd} oilflood		
Flux, ft/d	F_{rro} (1^{st} short core segment)	F_{rro} (Center core segment)
3.15	22	37
2^{nd} waterflood		
Flux, ft/d	F_{rrw} (1^{st} short core segment)	F_{rrw} (Center core segment)
0.025	130	1,800
0.050	100	1,275
0.025	130	1,735
0.101	82	822
0.050	97	1,114
0.025	140	1,575
0.197	68	544
0.101	92	769
0.050	105	1,105
0.025	140	1,520
0.394	51	338
0.197	63	484
0.101	62	606
0.050	90	861
0.394	41	343
F_{rrw} (across center segment, last five data points) = $227\ u^{-0.54}$, r=0.9978		
3^{rd} oilflood		
Flux, ft/d	F_{rro} (1^{st} short core segment)	F_{rro} (Center core segment)
25.2	3	9
12.6	3	8
Average F_{rro} (across center segment) = 8.5		

Table A-2c. Summary of Residual Resistance Factors-Core SSL-127
Core: 95-md Berea Sandstone
Gel: 0.5% HPAM (Alcoflood 935), 0.0417% Cr(III)-Acetate, 1% NaCl

1^{st} oilflood		
Flux, ft/d	F_{rro} (1^{st} short core segment)	F_{rro} (Center core segment)
0.025	440	470
1^{st} waterflood		
Flux, ft/d	F_{rrw} (1^{st} short core segment)	F_{rrw} (Center core segment)
0.013	1,365	2,830
2^{nd} oilflood		
Flux, ft/d	F_{rro} (1^{st} short core segment)	F_{rro} (Center core segment)
0.101	48	138
2^{nd} waterflood		
Flux, ft/d	F_{rrw} (1^{st} short core segment)	F_{rrw} (Center core segment)
0.013	392	2,860
0.025	265	2,090
0.013	310	2,580
0.050	123	1,170
0.025	162	1,580
0.013	222	2,280
0.050	128	1,190
F_{rrw} (across center segment, last five data points) = $276\ u^{-0.48}$, r=0.997		
3^{rd} oilflood		
Flux, ft/d	F_{rro} (1^{st} short core segment)	F_{rro} (Center core segment)
0.101	20	139
0.202	18	120
Average F_{rro} (across center segment) = 129.5		

Table A-2d. Summary of Residual Resistance Factors-Core LSH-128
Core: 24-md Indiana Limestone
Gel: 0.5% HPAM (Alcoflood 935), 0.0417% Cr(III)-Acetate, 1% NaCl

1st oilflood		
Flux, ft/d	F_{rro} (1st short core segment)	F_{rro} (Center core segment)
0.394	20	12
1st waterflood		
Flux, ft/d	F_{rrw} (1st short core segment)	F_{rrw} (Center core segment)
0.025	117	374
2nd oilflood		
Flux, ft/d	F_{rro} (1st short core segment)	F_{rro} (Center core segment)
0.394	3	12
2nd waterflood		
Flux, ft/d	F_{rrw} (1st short core segment)	F_{rrw} (Center core segment)
0.025	290	295
0.050	164	210
0.025	120	290
0.101	58	132
0.050	135	176
0.025	175	229
0.101	60	59
F_{rrw} (across center segment, first six data points) = $42\ u^{-0.51}$, r=0.9388		
3rd oilflood		
Flux, ft/d	F_{rro} (1st short core segment)	F_{rro} (Center core segment)
0.394	6	6
1.575	1	7
0.787	1	10
0.394	9	5
Average F_{rro} (across center segment) = 7		

Table A-2e. Summary of Residual Resistance Factors-Core SSH-129
Core: 520-md Berea Sandstone
Gel: 0.5% HPAM (Alcoflood 935), 0.0417% Cr(III)-Acetate, 1% NaCl
Gelant/Oil Volume Ratio During Placement: 50/50

1st oilflood		
Flux, ft/d	F_{rro} (1st short core segment)	F_{rro} (Center core segment)
3.15	25	27
1st waterflood		
Flux, ft/d	F_{rrw} (1st short core segment)	F_{rrw} (Center core segment)
0.025	540	1,255
2nd oilflood		
Flux, ft/d	F_{rro} (1st short core segment)	F_{rro} (Center core segment)
6.3	18	16
2nd waterflood		
Flux, ft/d	F_{rrw} (1st short core segment)	F_{rrw} (Center core segment)
0.025	380	820
0.050	275	643
0.101	165	430
0.050	220	566
0.202	103	282
0.101	135	351
0.050	180	456
0.394	74	190
0.202	80	220
0.101	85	285
0.050	137	370
0.394	100	196
F_{rrw} (across center segment, first six data points) = 141 $u^{-0.31}$, r=0.9913		
3rd oilflood		
Flux, ft/d	F_{rro} (1st short core segment)	F_{rro} (Center core segment)
50.4	5	7
25.2	6	7
12.6	5	7
6.3	2	7
Average F_{rro} (across center segment) = 7		

Table A-2f. Summary of Residual Resistance Factors-Core SSH-130
Core: 679-md Berea Sandstone
Gel: 0.5% HPAM (Alcoflood 935), 0.0417% Cr(III)-Acetate, 1% NaCl

1st waterflood		
Flux, ft/d	F_{rrw} (1st short core segment)	F_{rrw} (Center core segment)
0.025	4,800	4,800
0.050	2,550	2,550
0.025	2,950	2,950
0.101	2,050	2,050
0.050	2,400	2,400
0.025	2,800	2,800
0.202	1,470	1,470
0.101	1,670	1,670
0.050	2,190	2,190
0.025	2,675	2,675
F_{rrw} (across center segment, last four data points) = 889 $u^{-0.30}$, r=0.9919		
1st oilflood without surfactant		
Flux, ft/d	F_{rro} (1st short core segment)	F_{rro} (Center core segment)
0.787	40	99
2nd waterflood		
Flux, ft/d	F_{rrw} (1st short core segment)	F_{rrw} (Center core segment)
0.025	950	2,850
0.050	770	1,930
0.025	1,060	2,400
0.101	550	1,300
0.050	830	1,655
0.025	940	2,100
0.202	435	880
0.101	630	1,070
0.050	840	1,500
0.025	1,050	1,900
F_{rrw} (across center segment, last four data points) =469 $u^{-0.38}$, r=0.9955		
2nd oilflood without surfactant		
Flux, ft/d	F_{rro} (1st short core segment)	F_{rro} (Center core segment)
1.575	20	58

Table A-2f. Summary of Residual Resistance Factors-Core SSH-130 (Cont'd)
Core: 679-md Berea Sandstone
Gel: 0.5% HPAM (Alcoflood 935), 0.0417% Cr(III)-Acetate, 1% NaCl

3^{rd} waterflood		
Flux, ft/d	F_{rrw} (1^{st} short core segment)	F_{rrw} (Center core segment)
0.025	500	1,870
0.050	360	1,340
0.025	450	1,710
0.101	250	936
0.050	310	1,150
0.025	410	1,475
0.202	160	630
0.101	200	750
0.050	265	985
0.025	350	1,280
F_{rrw} (across center segment, last four data points) = 354 $u^{-0.34}$, r=0.9958		
3^{rd} oilflood without surfactant		
Flux, ft/d	F_{rro} (1^{st} short core segment)	F_{rro} (Center core segment)
6.3	7	21

Table A-2g. Summary of Residual Resistance Factors-Core SSH-132
Core: 467-md Berea Sandstone
Gel: 0.5445% HPAM (Alcoflood 935), 0.25% hydroquinone, 0.1% hexamethylenetetramine, and 1% $NaHCO_3$, pH=8.4. Aged two days at 110°C.

1^{st} oilflood		
Flux, ft/d	F_{rro} (1^{st} short core segment)	F_{rro} (Center core segment)
3.15	13	20
1^{st} waterflood		
Flux, ft/d	F_{rrw} (1^{st} short core segment)	F_{rrw} (Center core segment)
6.3	7.5	4.7
2^{nd} oilflood		
Flux, ft/d	F_{rro} (1^{st} short core segment)	F_{rro} (Center core segment)
6.3	13	20
2^{nd} waterflood		
Flux, ft/d	F_{rrw} (1^{st} short core segment)	F_{rrw} (Center core segment)
6.3	6	4.2
50.4	1.8	2.7
25.2	3.0	2.5
12.6	3.3	2.3
6.3	3.5	2.3
Final F_{rrw} (across center segment) = 2.5		

Table A-2h. Summary of Residual Resistance Factors-Core SSH-134
Core: 286-md Berea Sandstone
Gel: 0.5445% HPAM (Alcoflood 935), 0.25% hydroquinone, 0.1% hexamethylenetetramine, and 1% $NaHCO_3$, pH=8.4. Aged two days at 110°C.

1^{st} oilflood		
Flux, ft/d	F_{rro} (1^{st} short core segment)	F_{rro} (Center core segment)
6.3	14	13.6
1^{st} waterflood		
Flux, ft/d	F_{rrw} (1^{st} short core segment)	F_{rrw} (Center core segment)
6.3	11.4	10.2
2^{nd} oilflood		
Flux, ft/d	F_{rro} (1^{st} short core segment)	F_{rro} (Center core segment)
6.3	12.4	14.6
3.15	10.7	15.1
Average F_{rro} (across center segment) = 14.9		
2^{nd} waterflood		
Flux, ft/d	F_{rrw} (1^{st} short core segment)	F_{rrw} (Center core segment)
6.3	8.2	7.7
3.15	12.3	13
6.3	8.7	8.7
12.6	6	5.8
6.3	7.3	7.6
3.15	10.2	11
1.575	15.4	17
F_{rrw} (across center segment) = $22\ u^{-0.53}$, r=0.9827		

Table A-2i. Summary of Residual Resistance Factors-Core SSH-135
Core: 622-md Berea Sandstone
Gel: 0.5% HPAM (Alcoflood 935), 0.0417% Cr(III)-Acetate, 1% NaCl
Gelant/Oil Volume Ratio During Placement: 30/70

1^{st} oilflood		
Flux, ft/d	F_{rro} (1^{st} short core segment)	F_{rro} (Center core segment)
6.3	22	26
1^{st} waterflood		
Flux, ft/d	F_{rrw} (1^{st} short core segment)	F_{rrw} (Center core segment)
0.025	820	1,075
2^{nd} oilflood		
Flux, ft/d	F_{rro} (1^{st} short core segment)	F_{rro} (Center core segment)
6.3	7.6	20
2^{nd} waterflood		
Flux, ft/d	F_{rrw} (1^{st} short core segment)	F_{rrw} (Center core segment)
0.025	125	394
0.050	110	310
0.101	50	233
0.050	65	302
0.025	177	410
F_{rrw} (across center segment) $=95\ u^{-0.39}$, r=0.9973		
3^{rd} oilflood		
Flux, ft/d	F_{rro} (1^{st} short core segment)	F_{rro} (Center core segment)
6.3	15	10

APPENDIX B: Technology Transfer

On June 4 and 5, we held a project review in Socorro, NM. The review was attended by 27 people (not including New Mexico Tech personnel) representing 18 different organizations.

On August 19, we presented the paper, "What Gels Can and Cannot Do," at the 2nd International Conference on Reservoir Conformance, Profile Control, and Water and Gas Shutoff that was held in Houston, Texas.

On September 24, we presented the talk, "Issues Involved with Sizing Gel Treatments," at the 2nd Annual Subsurface Fluid Control Symposium and Exhibition that was held in Houston, Texas.